

Molecular Preorganization Unlocks Reversible Solid-State Photoconversion in Dianthrylnaphthalene-Based Molecular Solar Thermal Systems

Downloaded from: https://research.chalmers.se, 2026-11-04 11:46 UTC

Citation for the original published paper (version of record):

Baggi, N., Muhammad, L., Hölzel, H. et al (2026). Molecular Preorganization Unlocks Reversible Solid-State Photoconversion in
Dianthrylnaphthalene-Based Molecular Solar Thermal Systems. Angewandte Chemie, In Press.
http://dx.doi.org/10.1002/anie.1015605

N.B. When citing this work, cite the original published paper.

research.chalmers.se offers the possibility of retrieving research publications produced at Chalmers University of Technology. It covers all kind of research output: articles, dissertations, conference papers, reports etc. since 2004. research.chalmers.se is administrated and maintained by Chalmers Library

(article starts on next page)

International Journal of Solids and Structures 343 (2027) 114358

Contents lists available at ScienceDirect

International Journal of Solids and Structures

journal homepage: www.elsevier.com/locate/ijsolstr

On the electro-chemo-thermo-mechanical couplings in solids with interfaces

Ali Javili [a,*], Fredrik Larsson [b], Kenneth Runesson [b], Paul Steinmann [c,d]

[a] Department of Mechanical Engineering, Bilkent University, 06800 Ankara, Türkiye
[b] Department of Mechanical Engineering, Chalmers University of Technology, 412 96 Gothenburg, Sweden
[c] Institute of Applied Mechanics, Friedrich-Alexander-Universität, Erlangen, Germany
[d] Glasgow Computational Engineering Centre, School of Engineering, University of Glasgow, Glasgow G12 8QQ, United Kingdom

ARTICLE INFO

Keywords:
Canonical interface modeling
Multiphysics in solids
Electro-chemo-thermo-mechanical interactions
Thermodynamically consistent framework

ABSTRACT

Electro-chemo-thermo-mechanical couplings, wherein electro-chemo-thermal processes interact with mechanical deformation, govern the behavior of a wide class of multi-functional materials and devices. Typical examples are batteries and shape-morphing devices that comprise electrodes separated by (liquid or solid) electrolyte. In these systems, ionic transport, electrochemical reactions, and electric fields are intrinsically coupled with deformation, both in the bulk material and, not the least, at interfaces. In this paper we consider, at the outset, the generic situation when ions and electrons coexist (at the considered scale of continuum). To retain maximal generality, we then consider the interface as an "energetic" surface that is equipped with its own balance and constitutive equations. It is thereby tacitly assumed that the interface is "imperfect" in the sense that kinematic as well as flux variables are discontinuous across the interface. We develop a generic thermodynamically consistent framework, while restricting to small strain kinematics, that provides constraints on constitutive relations for the bulk material, as well as for the interface, from mechanical, electric, chemical and thermal viewpoints. A particular challenge is offered by extending Ampere's and Faraday's laws, as well as establishing the proper definition of the Poynting vector (representing the electro-magnetic power), to interfaces. As illustrations of the canonical framework, under isothermal conditions, we consider three specific systems: (a) An electronic conductor of dissimilar material with electronic interface, (b) an ionic conductor of dissimilar material with ionic interface, (c) electrode/electrolyte with electronic interface. The latter may represent a halfcell, wafering a Solid Electrolyte Interphase (SEI), in a battery or in a shape-morphing device. The electro-chemical activity in the interface is modeled by classical and non-classical models of Butler–Volmer type, which are shown to be thermodynamically consistent.

1. Introduction

A large class of engineering materials are designed such that regions with dissimilar material properties are separated by *interphase* regions, that are thin although of finite width. Typically, this is the case on the macroscale when the manufacturing involves some type of joining procedure, e.g. gluing, welding, etc. It may also be a characteristic feature of micro-heterogeneous materials (composites). Two examples, out of many, are thin heat affected zones (HAZ) between inclusions and the matrix in composites, and grain boundaries in polycrystalline solids. In this case, the ultimate goal of modeling and analysis is to determine effective (macroscopic) properties through some sort of homogenization procedure, whereby the influence of interphases must be accounted for properly. For the purpose of modeling, it is common to replace a finite-thickness interphase zone by a zero-thickness *interface* model, see Fig. 1, which is a two-dimensional manifold that is embedded in the three-dimensional space.

The objective of this contribution is to extend our recently introduced canonical interface model (Javili et al., 2025) to account for electro-chemo-thermo-mechanical couplings that are relevant to multifunctional materials. Thus, the two main ingredients of this contribution are (i) interface modeling and (ii) electro-chemo-thermo-mechanical couplings. A brief review of these topics is given subsequently in Sections 1.1 and 1.2.

1.1. Classification and overview of interface modeling

As a point of departure, we consider the solid mechanics problem. In *mechanical systems*, interface models are commonly classified with respect to presumed (dis)continuity of the displacement and the normal stress across the interface. Fig. 2 (left column) summarizes the various conceptual "prototypes" of interface models in mechanical systems. If

* Corresponding author.
E-mail address: ajavili@bilkent.edu.tr (A. Javili).

https://doi.org/10.1016/j.ijsolstr.2026.114358
Received 12 August 2026; Accepted 26 September 2026
Available online 15 October 2026
0020-7683/© 2026 The Authors. Published by Elsevier Ltd. This is an open access article under the CC BY-NC license (http://creativecommons.org/licenses/by-nc/4.0/).

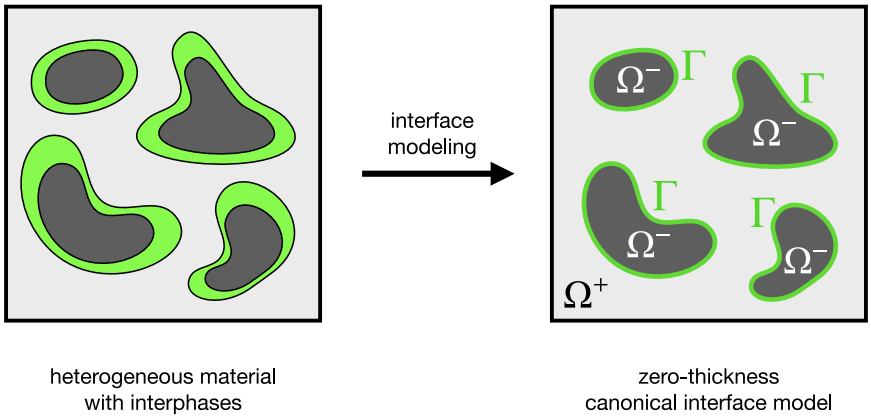


Fig. 1. Schematic illustration of a material with its underlying microstructure. The finite-thickness interphase zone between the constituents at the microscale is replaced by a zero-thickness interface model.

the displacement is continuous across the interface, this is referred to as kinematically coherent, while kinematically non-coherent interfaces allow for a displacement jump. In a similar fashion, kinetically coherent interfaces are characterized by a normal stress that is continuous across the interface, while kinetically non-coherent interfaces allow for a jump of the normal stress. Therefore, four interface categories emerge naturally: (i) the *perfect* interface model, also referred to as a free singular surface, (ii) the *membrane* (elastic) interface model, also referred to as a thermodynamic singular surface with its roots in surface elasticity theory, (iii) the *cohesive* interface model, also referred to as the spring-type interface model, and (iv) the *canonical* (general) interface model. The latter fills the gap between the two extremes of the elastic interface model and the cohesive interface model, allowing for jumps in both the displacement and normal stress fields. If the interface is both kinematically and kinetically coherent, then it is said to be perfect; otherwise, it is imperfect.

Remark 1. Consider the situation when the membrane interface model is employed for composites, whereby the interface model is associated with its own energy per unit surface area. It then appears that the interface effect on the effective response is more pronounced at smaller scales. The obvious reason is that, since the ratio of interface to volume energy is proportional to the area-to-volume ratio, this ratio scales inversely with the characteristic problem dimension. □

It is not our aim here to provide a comprehensive review of interface modeling and its influence on the effective mechanical properties of composites; indeed, such reviews have been given elsewhere, e.g. Firooz et al. (2022). We shall merely note that interface modeling has a long history in solid mechanics that dates back to the early works of Hashin (2001), Sanchez-Palencia (1974), see also Gu et al. (2011). Seminal contributions to membrane modeling or, rather, surface/interface elasticity, are those of Gurtin and Murdoch (1975), Murdoch (1976), Moeckel (1975), Daher and Maugin (1986), Dell'Isola and Romano (1987), Steigmann and Ogden (1999), and Javili et al. (2014). Cohesive interface modeling is the most commonly used interface model concept, dating back to the early works of Barenblatt (1959), Dugdale (1960), and with a very rich literature, see e.g. Xu and Needleman (1994), Fagerström and Larsson (2006), van den Bosch et al. (2006), Brassart et al. (2009), Park and Paulino (2011), among others. The general interface model (Javili et al., 2017; Javili, 2018) has been introduced to bridge the membrane and cohesive interface models, which itself is a subclass of the canonical interface model.

Recently, the authors presented the so-called canonical interface model (Javili et al., 2025, 2026), wherein the fundamental novelty and generalization, compared to previous works, Saeb et al. (2021), is that the "interface displacement" is introduced as a kinematically independent field, which is resolved through a variationally consistent approach. In fact, the present contribution should be viewed as the generalization of Javili et al. (2025) to a significantly more complex problem setting. We recall that interface models for *mechanical systems* are classified in regard to the continuity of the kinematic (displacement) and the kinetic (stress) fields.

A similar classification can also be applied to ECTM systems. Fig. 2 shows, in addition to the mechanical problem, the basic balance equations in the bulk and the appropriate coherence situations on the interface for the other physical fields involved in the ECTM system. However, this is done without accounting for possible couplings between the fields. We thus consider the thermal problem (θ is the temperature and $\boldsymbol{q}$ is the heat flux), the chemical problem (μ is the chemical potential and $\boldsymbol{j}$ is the diffusive flux/density for a single species), and the electrostatic problem (φ is the electric potential and $\boldsymbol{i}$ is the current flux/density). To a varying degree, the complexity of interface relations has been considered in the literature for the single (or "uncoupled") physical fields. The main thrust of this paper is the synthesis of the various couplings, in particular with respect to mechanics.

Remark 2. The present classification of interfaces applies essentially to small deformation kinematics, in particular regarding the concept of cohesive interface. Moreover, it is restricted to non-sliding interface motions (in general). Indeed, models for sliding contact (dry or with lubrication) must be based on the finite deformation setting, e.g. Vakis (Vakis et al., 2018), see also Bigoni (Bigoni et al., 2018). Furthermore, we note that a common way of entirely circumventing the concept of a (lower-dimensional) interface is to use phase-field formulation(s). The literature is abundant; here, we merely mention examples from void nucleation and growth, Zhao (Zhao et al., 2022), intergranular and transgranular fracture in polycrystalline cathodes, Chen et al. (2024), and defect evolution in solid-state battery interfaces, Kamikawa et al. (2024). □

1.2. ECTM systems with interfaces

ECTM couplings, wherein electro-chemical and (possibly) thermal processes interact with mechanical deformation, govern the behavior of a wide class of materials and engineering devices. In these systems, ionic transport, electro-chemical reactions, and electric fields are intrinsically coupled with deformation and stress, both in the bulk material and, not the least, at interfaces. The resulting interplay gives rise to complex phenomena such as stress-assisted diffusion and migration, phase separation (Cahn and Hilliard, 1958, Anand, 2012; Di Leo et al., 2014, Kaessmair and Steinmann, 2016) and transformation, interfacial delamination (decohesion) and various other degradation phenomena. The thermodynamic foundations of coupled diffusion and mechanics

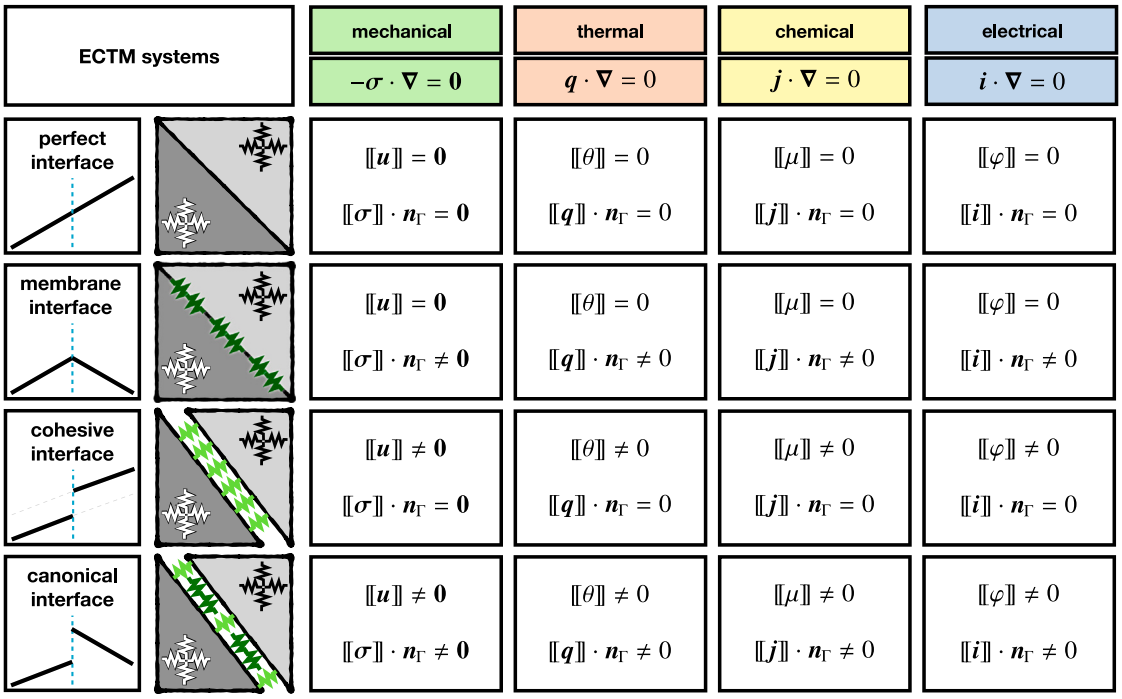


Fig. 2. Classification of interface models in electro-chemo-thermo-mechanical (ECTM) systems. Each column corresponds to a single-field problem, and a complete ECTM coupling is pursued in this contribution. Furthermore, the time derivatives are omitted in this classification, in that the columns from left to right correspond to mechanostatic, thermostatic, chemostatic, and electrostatic problems, respectively. The perfect interface model enforces continuity of all generalized kinematic and kinetic fields, whereas the imperfect interface models allow for discontinuity of one or more fields.

were established in the classical works of Larché and Cahn (1973, 1978). In particular, they introduced the dependence of mechanical stress on the chemical potential. McBride et al. (2011) considered mechanics coupled to diffusion on external surfaces, and Wilmers et al. (2017) extended the framework to interfaces.

These concepts extend naturally to electro-chemical systems, whereby the electro-chemical potential incorporates the electric potential. Electro-mechanical couplings based on electronic current, rather than ionic transport, represent a subclass that may include interface actions, cf. Kaiser et al. (2024). More specifically, electro-mechanically coupled cohesive zone modeling was discussed recently by Güzel et al. (2023).

A major motivation for studying ECTM couplings arises from electro-chemical energy storage systems, particularly batteries, and electro-chemically activated shape-forming devices, Carlstedt et al. (2023). In these systems, ion transport in electrode materials induces significant volumetric (intercalation) strains, while complex electro-chemical (redox) reactions occur at/in electrode–electrolyte interfaces. The strong coupling between volume diffusion, interfacial kinetics, and mechanical deformation leads to critical degradation mechanisms such as particle fracture, void formation and delamination. Early continuum models of electro-chemo-mechanical couplings in electrode and electrolyte materials are those of Christensen and Newman (2006), Zhang et al. (2010). Whereas a wealth of literature is devoted to the volume response, the modeling of interface phenomena has attracted less attention. A significant exception is the classical Butler–Volmer relation, e.g., in Dickinson and Wain (2020), which describes redox reactions at the electrode/electrolyte interface. The contribution on the chemo-mechanical coupling in membranes by Serpelloni et al. (2022) is noteworthy.

Electro-chemo-mechanical effects are also central to a variety of phenomena in structural materials, such as stress corrosion cracking and hydrogen embrittlement. In these cases, electro-chemical reactions at surfaces or crack tips interact with stress-driven diffusion of species, leading to localized damage and failure.

In geomaterials and porous media, electro-chemo-mechanical coupling governs processes such as reactive transport, mineral dissolution and precipitation, and electrokinetic phenomena. These processes are relevant for a variety of applications, including CO_2 sequestration, geothermal energy, and subsurface engineering. On the one hand, the interaction between electro-chemistry and mechanical stress may lead to dissolution-induced instabilities and fracture, Tang (Tang and Hu, 2024). On the other hand, however, electro-osmosis driven consolidation and dewatering of fine-grained soil are known to lead to improved bearing capacity of foundations, (Ge et al., 2023).

Despite these advances, significant challenges remain in the mathematical modeling and numerical simulation of electro-chemo-thermo-mechanically coupled systems. In particular, the thermodynamically consistent treatment of energy and dissipation, which provides constraints on constitutive relations for volume and interface, poses a challenge. A particular challenge is offered by extending Ampere's and Faraday's laws, as well as defining the proper definition of the Poynting vector (representing the electro-magnetic power), to interfaces. These issues will be addressed thoroughly in this paper.

In order to fix ideas, we shall henceforth consider an *ECTM model system* consisting of several chemically and electrically active species. In this paper, we consider the generic setup when it is assumed that ions and electrons can coexist (at the continuum scale, which is considered here). Ions from several species, e.g. Li^+ and a companion anion, are transported in the bulk material and across interfaces by (stress-assisted) diffusion and migration. In a more general setup, e.g. a liquid-filled porous medium, one should also take convection into account. The interface is equipped with its own balance and constitutive equations of different physical origins. It is thereby tacitly assumed that the interface is "imperfect" in the sense that kinematic as well as flux variables are discontinuous across the interface. We develop a generic thermodynamically consistent framework, while restricting to small

Table 1
Nomenclature: notation and operators. Generic placeholder fields are denoted $\{\bullet\}$, $\{\circ\}$.

Notation	Description
$[\![\{\bullet\}]\!]$	Jump operator
$\{\!\{\bullet\}\!\}$	Mean operator
$\boldsymbol{\nabla}$, $\boldsymbol{\nabla}_\Gamma$, $\boldsymbol{\nabla}_\Gamma^\parallel$, $\boldsymbol{\nabla}_\Gamma^\perp$	Nabla operator and interface counterparts
$\{\bullet\}\otimes\boldsymbol{\nabla}$, $\{\bullet\}\cdot\boldsymbol{\nabla}$, $\{\bullet\}\times\boldsymbol{\nabla}$	Gradient, divergence and (negative) curl
$\{\bullet\}_\Gamma$	Quantity associated with the interface Γ
$\{\bullet\}^+$, $\{\bullet\}^-$	Limit from the Ω^+ and the Ω^- side
$\{\bullet\}^{\mathrm{C}}$	Transmitted (C=cohesion-associated) interface flux through Γ
$\{\bullet\}^{\mathrm{D}}$	Emitted (D=deviation-associated) interface flux from Γ
$\{\bullet\}^\parallel$, $\{\bullet\}^\perp$	In-plane (superficial) and out-of-plane part
$\{\bullet\}'$	Electro-chemical (charge-augmented) counterpart
$\{\bullet\}_{\mathrm{el}}$, $\{\bullet\}_{\mathrm{ion}}$	Electronic and ionic contribution
$\{\bullet\}_\alpha$, $\{\bullet\}_{\Gamma,\alpha}$	Pertaining to species α in Ω and on Γ
$\{\bullet\}_{\mathrm{me}}$, $\{\bullet\}_{\mathrm{th}}$, $\{\bullet\}_{\mathrm{el\text{-}ch}}$, $\{\bullet\}_{\mathrm{en}}$	Mechanical, thermal, electro-chemical, energetic
$\{\bullet\}_{\mathrm{Max}}$	Maxwell (current)

strain kinematics, that provides constraints on constitutive relations for the bulk material, as well as for the interface, from mechanical, electric, chemical, and thermal viewpoints.

1.3. Organization of this manuscript

The remainder of the manuscript is organized as follows. Section 2 provides the mathematical preliminaries and introduces notation, definitions, and terminologies. Section 3 presents the balance equations pertinent to the ECTM model system with an imperfect interface. The core of this section is the energy balance, including contributions to the power input of mechanical, thermal, electro-magnetic, and chemical nature. Section 4 elaborates on the entropy inequality and presents general constraints on constitutive relations of energetic and dissipative type. Section 5 summarizes the weak forms. Further, it contains a discussion of specific and noteworthy characteristics of the modeling framework. The generic framework is elucidated in Section 6 by application to a few specific ECTM systems: The electronic conductor, the ionic conductor, and the so-called half-cell (of a battery or shape-morphing device). Finally, Section 7 presents conclusions and suggests an outlook to possible extensions. Appendices contain supplementary material. Appendix A summarizes differential geometry related to surfaces, and Appendix B details derivations of electro-magnetic relations for systems with an imperfect interface.

2. Preliminaries

This section collects the mathematical prerequisites underlying the subsequent developments. We first introduce the geometrical setting of two subdomains joined along an interface, together with their boundaries, normal vectors, and the associated jump and mean operators across the interface. The differential operators and the corresponding integral theorems are summarized, and the notion of "superficial" fields is introduced in preparation for the interface fluxes employed throughout the manuscript. The generic notation and the operators used in the sequel are collected in Table 1.

2.1. Domains and boundaries

We denote the global solution domain as $\Omega=\Omega^+\cup\Omega^-$, where $\Omega^\pm$ are smooth subdomains. The subdomains are "joined" along an interface Γ, which is equipped with its own ECTM properties. Geometrically, the interface Γ is a two-dimensional smooth manifold, that is, a curved surface, embedded in the three-dimensional Ω. To establish balance laws for the smooth domains and for the interface, we consider the arbitrarily chosen subdomain $\mathcal{B}\subset\Omega$ with external boundary $\partial\mathcal{B}:=\mathcal{S}^-\cup\mathcal{S}^+$, as shown in Fig. 3, and identify $\mathcal{B}^{-/+}\subset\Omega^{-/+}$. The restriction $\mathcal{I}$ of the interface Γ to $\mathcal{B}$ is, therefore, $\mathcal{I}=\partial\mathcal{B}^-\cap\Gamma=\partial\mathcal{B}^+\cap\Gamma$. We then have $\partial\mathcal{B}^-=\mathcal{S}^-\cup\mathcal{I}$ and $\partial\mathcal{B}^+=\mathcal{S}^+\cup\mathcal{I}$. Finally, we introduce the boundary of the interface $\mathcal{I}$ as $\partial\mathcal{I}$. The outwards-pointing normal to $\partial\mathcal{B}$ is $\boldsymbol{n}$. The normal to the interface $\mathcal{I}$ is denoted $\boldsymbol{n}^-=\boldsymbol{n}_\Gamma$, pointing out from $\mathcal{B}^-$ and into $\mathcal{B}^+$, while $\boldsymbol{n}^+=-\boldsymbol{n}_\Gamma$, pointing out from $\mathcal{B}^+$ and into $\mathcal{B}^-$. The normal to the interface boundary $\partial\mathcal{I}$, a closed curve, is tangential to the curved surface $\mathcal{I}$ and is denoted $\tilde{\boldsymbol{n}}_\Gamma$. Note that $\tilde{\boldsymbol{n}}_\Gamma$ is in general not normal to $\partial\mathcal{B}$, as shown in Fig. 3, and thus does not necessarily coincide with $\boldsymbol{n}$.

2.2. Jumps and averages

We assume that all solution fields $\{\bullet\}$ are smooth in the (open) domain $\Omega=\Omega^-\cup\Omega^+$, however, they may be discontinuous across the interface Γ. Thus, a generic field $\{\bullet\}$ is smooth away from Γ on either side, taking the values $\{\bullet\}^\pm=\lim_{\epsilon\to0}\{\bullet\}(\boldsymbol{x}|_{\mathcal{I}}\pm\epsilon\,\boldsymbol{n}_\Gamma)$ with $\epsilon>0$. We shall frequently consider the strength of these discontinuities and therefore introduce the difference (operator) $[\![\{\bullet\}]\!]:=\{\bullet\}^+-\{\bullet\}^-$ and the mean (operator) $\{\!\{\bullet\}\!\}:=\frac{1}{2}[\{\bullet\}^++\{\bullet\}^-]$. We then establish that

$$\{\bullet\}^+=\{\!\{\bullet\}\!\}+\frac{1}{2}[\![\{\bullet\}]\!],\quad \{\bullet\}^-=\{\!\{\bullet\}\!\}-\frac{1}{2}[\![\{\bullet\}]\!]. \tag{1}$$

Furthermore, for two fields $\{\bullet\}$ and $\{\circ\}$, and multiplication $\star$, we have the helpful relations

$$\begin{aligned}[\![\{\bullet\}\star\{\circ\}]\!]&=\{\!\{\bullet\}\!\}\star[\![\{\circ\}]\!]+[\![\{\bullet\}]\!]\star\{\!\{\circ\}\!\},\\ \{\!\{\{\bullet\}\star\{\circ\}\}\!\}&=\{\!\{\bullet\}\!\}\star\{\!\{\circ\}\!\}+\frac{1}{4}[\![\{\bullet\}]\!]\star[\![\{\circ\}]\!].\end{aligned} \tag{2}$$

2.3. Differential operators and integral theorems in a volume

In a volume, we define the tensor-valued gradient, scalar-valued divergence, and vector-valued (negative) curl operators of vector fields $\{\bullet\}$ as $\{\bullet\}\otimes\boldsymbol{\nabla}$, $\{\bullet\}\cdot\boldsymbol{\nabla}$ and $\{\bullet\}\times\boldsymbol{\nabla}$, respectively,[1] where $\boldsymbol{\nabla}$ denotes the gradient operator. As an important consequence of the above definitions, differential identities of "divergence-curl"-type for vector fields $\{\bullet\}$ and "curl-gradient"-type for scalar fields $\{\circ\}$ hold

$$[\{\bullet\}\times\boldsymbol{\nabla}]\cdot\boldsymbol{\nabla}=0\quad\text{and}\quad[\boldsymbol{\nabla}\{\circ\}]\times\boldsymbol{\nabla}=\boldsymbol{0}. \tag{3}$$

With a and $\boldsymbol{a}$ scalar and vector fields, respectively, these motivate the unique Helmholtz decomposition of any vector field $\boldsymbol{v}$ into a curl-free contribution $\boldsymbol{\nabla}a$ and a divergence-free contribution $\boldsymbol{\nabla}\times\boldsymbol{a}$, that is, $\boldsymbol{v}=\boldsymbol{\nabla}a+\boldsymbol{\nabla}\times\boldsymbol{a}$.

For a quantity within $\mathcal{B}=\mathcal{B}^-\cup\mathcal{B}^+$, with closed boundary $\partial\mathcal{B}$, and that is discontinuous across an interface $\mathcal{I}$, Gauss' theorem reads

$$\int_{\partial\mathcal{B}}\{\bullet\}\cdot\boldsymbol{n}\,\mathrm{d}S=\int_{\mathcal{B}}\{\bullet\}\cdot\boldsymbol{\nabla}\,\mathrm{d}V+\int_{\mathcal{I}}[\![\{\bullet\}]\!]\cdot\boldsymbol{n}_\Gamma\,\mathrm{d}S. \tag{4}$$

[1] Note the definition of the (negative) curl operator when expressed with $\boldsymbol{\nabla}$ operating "from the right"; a fully equivalent version, more established in classical electro-magneto-dynamics, with $\boldsymbol{\nabla}$ operating "from the left" reads $\boldsymbol{\nabla}\times\{\bullet\}=-\{\bullet\}\times\boldsymbol{\nabla}$.

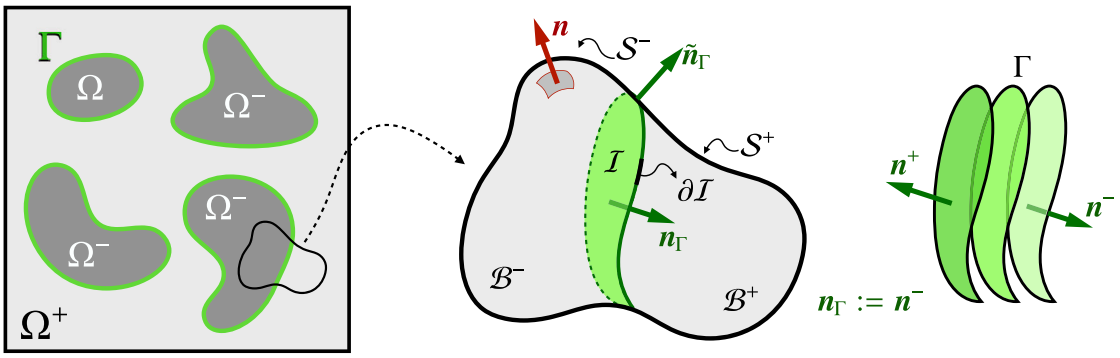


Fig. 3. Schematic illustration of the subdomains Ω^- and Ω^+ occupied by inclusion (e.g. battery electrode) and matrix (e.g. battery electrolyte) with the interface Γ at their intersection.

2.4. Differential operators and integral theorems on a surface

On a surface, we abbreviate the tensor-valued surface gradient, scalar-valued surface divergence, and vector-valued (negative) surface curl operators of vector fields $\{\bullet\}$ by $\{\bullet\}\otimes\boldsymbol{\nabla}_\Gamma$, $\{\bullet\}\cdot\boldsymbol{\nabla}_\Gamma$, and $\{\bullet\}\times\boldsymbol{\nabla}_\Gamma$, respectively.[2] Here, $\boldsymbol{\nabla}_\Gamma$ denotes the surface gradient operator, defined as $\boldsymbol{\nabla}_\Gamma := \boldsymbol{\nabla}\cdot\boldsymbol{I}_\Gamma$, where $\boldsymbol{I}_\Gamma = \boldsymbol{I} - \boldsymbol{n}_\Gamma\otimes\boldsymbol{n}_\Gamma$ is the surface identity tensor; when operating on a scalar field $\{\circ\}$ the surface gradient $\boldsymbol{\nabla}_\Gamma\{\circ\}$ renders a superficial vector field, that is, $[\boldsymbol{\nabla}_\Gamma\{\circ\}]\cdot\boldsymbol{n}_\Gamma = 0$. Applied to the surface normal $\boldsymbol{n}_\Gamma$, the negative surface gradient and surface divergence render the symmetric and superficial surface curvature tensor $\boldsymbol{K}_\Gamma := -\boldsymbol{n}_\Gamma\otimes\boldsymbol{\nabla}_\Gamma$ (with $\boldsymbol{K}_\Gamma\cdot\boldsymbol{n}_\Gamma = \boldsymbol{n}_\Gamma\cdot\boldsymbol{K}_\Gamma = \boldsymbol{0}$) and twice the mean curvature $K_\Gamma := -\boldsymbol{n}_\Gamma\cdot\boldsymbol{\nabla}_\Gamma$ (surface trace $\boldsymbol{K}_\Gamma : \boldsymbol{I}_\Gamma$ of $\boldsymbol{K}_\Gamma$), respectively. It may be noted that $\boldsymbol{n}_\Gamma\times\boldsymbol{\nabla}_\Gamma$ is proportional to the axial vector of $\boldsymbol{K}_\Gamma$ and thus vanishes due the symmetry of $\boldsymbol{K}_\Gamma$. We denote the superficial part of the tensor-valued surface gradient of a vector field $\{\bullet\}$ as $\{\bullet\}\otimes\boldsymbol{\nabla}_\Gamma^{\parallel}$ and the normal part of the vector-valued surface curl of a vector field $\{\bullet\}$ as $\{\bullet\}\times\boldsymbol{\nabla}_\Gamma^{\perp}$, see Appendix A for more details. Differential identities of "divergence-curl"-type for vector fields $\{\bullet\}$ and "curl-gradient"-type for scalar fields $\{\circ\}$ hold also on surfaces

$$[\{\bullet\}\times\boldsymbol{\nabla}_\Gamma^{\perp}]\cdot\boldsymbol{\nabla}_\Gamma = 0 \quad\text{and}\quad [\boldsymbol{\nabla}_\Gamma\{\circ\}]\times\boldsymbol{\nabla}_\Gamma^{\perp} = \boldsymbol{0}\,. \tag{5}$$

With a and $\boldsymbol{a}$ scalar and vector fields, respectively, these motivate the surface Helmholtz decomposition of any vector field $\boldsymbol{v}$ into a normal surface curl-free contribution $\boldsymbol{\nabla}_\Gamma a$ and a surface divergence-free contribution $\boldsymbol{\nabla}_\Gamma^{\perp}\times\boldsymbol{a}$, that is, $\boldsymbol{v} = \boldsymbol{\nabla}_\Gamma a + \boldsymbol{\nabla}_\Gamma^{\perp}\times\boldsymbol{a}$. For a surface that occupies the configuration $\mathcal{I}$ with a closed boundary $\partial\mathcal{I}$, Gauss' theorem reads

$$\int_{\partial\mathcal{I}}\{\bullet\}\cdot\tilde{\boldsymbol{n}}_\Gamma\,\mathrm{d}L = \int_{\mathcal{I}}\{\bullet\}\cdot\boldsymbol{\nabla}_\Gamma\,\mathrm{d}S + \int_{\mathcal{I}}K_\Gamma\,\{\bullet\}\cdot\boldsymbol{n}_\Gamma\,\mathrm{d}S\,. \tag{6}$$

2.5. Superficial fluxes on the interface

For the subsequent derivations, we define variables on the interface equivalent to those in the volume, e.g. the surface stress $\boldsymbol{\sigma}_\Gamma$, the surface heat flux $\boldsymbol{q}_\Gamma$, and the like. We will generically denote these by a subscript Γ, that is, $\{\bullet\}_\Gamma$ denotes a quantity associated with the interface. Specifically, the surface stress $\boldsymbol{\sigma}_\Gamma$ is entirely superficial, that is, $\boldsymbol{\sigma}_\Gamma = \boldsymbol{I}_\Gamma\cdot\boldsymbol{\sigma}_\Gamma\cdot\boldsymbol{I}_\Gamma$, thus $\boldsymbol{\sigma}_\Gamma\cdot\boldsymbol{n}_\Gamma = \boldsymbol{n}_\Gamma\cdot\boldsymbol{\sigma}_\Gamma = \boldsymbol{0}$, and the surface heat flux is superficial, that is, $\boldsymbol{q}_\Gamma = \boldsymbol{q}_\Gamma\cdot\boldsymbol{I}_\Gamma$, thus $\boldsymbol{q}_\Gamma\cdot\boldsymbol{n}_\Gamma = 0$. In the sequel, we will introduce further fluxes either normal to the interface or as superficial surface fields.

[2] Here we shall only state relations of importance for the subsequent derivations; more details are found in Appendix A.

3. Governing field equations of the ECTM model system with an interface

The governing field equations of the ECTM model system are established in this section, in the volume as well as on the interface, whereby the balance laws are localized in the presence of the discontinuities introduced in Section 2. The interface is thereby equipped with its own fields and fluxes, which supplement the limiting values of the volume fields from either side.

3.1. Preliminaries

The governing field equations comprise balance equations (momentum, mass, and energy) together with Gauss' law for electric charge and circulation laws (Ampere's and Faraday's laws), as well as the entropy inequality. At the outset, we shall presume that electrons and ionic species can coexist in a continuum setting, producing charge and current in a distinctly different fashion. This situation may be visualized as the result of homogenization of separate physical activity on the microscale, e.g., within a positive electrode composite with electronic activity in carbon black and ionic activity in the active particles. Clearly, when pursued consistently, such an approach would require the introduction of separate electric potentials. However, in practice (when applied to electro-chemical systems as those considered in the present paper), the subdomains Ω^+ and Ω^- will be associated with either ionic or electronic activity. When "stitching" these domains together along the common interface Γ, it then appears that the advantage of the unified analysis is twofold: (i) The nature of the interface condition becomes transparent, (ii) The dimensionality (in space and time) of strong and weak forms becomes transparent.

The relevant fields in the bulk material are the displacement field $\boldsymbol{u}$, the (molar) concentrations $\{c_\alpha\}_{\alpha=1}^{M}$, the chemical potentials $\{\mu_\alpha\}_{\alpha=1}^{M}$, the electric potential φ, and the temperature θ. Most importantly, the corresponding separate fields associated with the interface, considered as an arbitrarily curved surface in 3D, will be introduced.

3.2. Balance of momentum

In the absence of dynamic effects and body forces, the global force balance on $\mathcal{B}$ reads:

$$\int_{\partial\mathcal{B}}\boldsymbol{\sigma}\cdot\boldsymbol{n}\,\mathrm{d}S + \int_{\partial\mathcal{I}}\boldsymbol{\sigma}_\Gamma\cdot\tilde{\boldsymbol{n}}_\Gamma\,\mathrm{d}L = \boldsymbol{0}\,, \tag{7}$$

where $\boldsymbol{\sigma}$ is the (symmetric) stress tensor in the volume ($\boldsymbol{t} := \boldsymbol{\sigma}\cdot\boldsymbol{n}$ denotes the traction on $\partial\mathcal{B}$). Further, $\boldsymbol{\sigma}_\Gamma$ is the superficial (symmetric) stress tensor in the interface, i.e. $\boldsymbol{\sigma}_\Gamma\cdot\boldsymbol{n}_\Gamma = \boldsymbol{0}$. Now, using the generic results in (4) and (6), we may localize the result in (7) to the volume and interface, respectively. We then obtain

$$-\boldsymbol{\sigma}\cdot\boldsymbol{\nabla} = \boldsymbol{0} \quad\text{in } \Omega^-\cup\Omega^+\,, \tag{8}$$

and

$$-\boldsymbol{\sigma}_\Gamma \cdot \boldsymbol{\nabla}_\Gamma - [\![\boldsymbol{\sigma}]\!] \cdot \boldsymbol{n}_\Gamma = \boldsymbol{0} \quad \text{on } \Gamma\,. \tag{9}$$

3.3. Balance of mass

The global mass balance of ions reads:

$$\int_{\mathcal{B}} \partial_t c_\alpha \,\mathrm{d}V + \int_{\mathcal{I}} \partial_t c_{\Gamma,\alpha} \,\mathrm{d}S = -\int_{\partial\mathcal{B}} \boldsymbol{j}_\alpha \cdot \boldsymbol{n} \,\mathrm{d}S - \int_{\partial\mathcal{I}} \boldsymbol{j}_{\Gamma,\alpha} \cdot \tilde{\boldsymbol{n}}_\Gamma \,\mathrm{d}L + \int_{\mathcal{B}} r_\alpha \,\mathrm{d}V + \int_{\mathcal{I}} r_{\Gamma,\alpha} \,\mathrm{d}S\,, \tag{10}$$

for $\alpha = 1, 2, \dots, M$. Here, c_α is the volume-specific "diffusive chemical substance" concentration in the bulk of species α, and $\boldsymbol{j}_\alpha$ is the mass flux vector in the volume. Further, $c_{\Gamma,\alpha}$ is the surface-specific concentration in the surface, and $\boldsymbol{j}_{\Gamma,\alpha}$ is the (superficial) flux vector in the surface, i.e. $\boldsymbol{j}_{\Gamma,\alpha} \cdot \boldsymbol{n}_\Gamma = 0$ on Γ. Note that the mass is reduced when the mass flux at the boundary makes an acute angle with the outwards-pointing surface normal, thus the negative signs for the first two integrals on the right-hand side of (10). The source term r_α is the (rate of) net increase of mass due to reactive exchange with the other species $\beta \neq \alpha$ in the system. We thereby note the constraints $\sum_\alpha r_\alpha = 0$ and $\sum_\alpha r_{\Gamma,\alpha} = 0$. Again, using the generic results in (4) and (6), respectively, we may localize (10) to the bulk and interface, respectively, and thus obtain

$$\partial_t c_\alpha + \boldsymbol{j}_\alpha \cdot \boldsymbol{\nabla} - r_\alpha = 0 \quad \text{in } \Omega^- \cup \Omega^+\,, \tag{11}$$

and

$$\partial_t c_{\Gamma,\alpha} + \boldsymbol{j}_{\Gamma,\alpha} \cdot \boldsymbol{\nabla}_\Gamma + [\![\boldsymbol{j}_\alpha]\!] \cdot \boldsymbol{n}_\Gamma - r_{\Gamma,\alpha} = 0 \quad \text{on } \Gamma\,, \tag{12}$$

with $\alpha \in \{1, 2, \dots, M\}$, while initial values are required on $c_\alpha(0)$ and $c_{\Gamma,\alpha}(0)$.

3.4. Gauss' law for electric charge

Following the balances of momentum and mass, we now turn to the electro-magnetic field equations, commencing with Gauss' law for electric charge. We first establish the basic format, whereby the interface is equipped with a surface-specific free charge and a superficial electric flux density. Subsequently, this format is applied to an electro-chemical system, whereby the free charge is additively split into its electronic and ionic contributions.

3.4.1. Basic format

The global format of Gauss' law for electric charge in $\mathcal{B}$ reads:

$$-\int_{\mathcal{B}} \zeta \,\mathrm{d}V - \int_{\mathcal{I}} \zeta_\Gamma \,\mathrm{d}S = -\int_{\partial\mathcal{B}} \boldsymbol{d} \cdot \boldsymbol{n} \,\mathrm{d}S - \int_{\partial\mathcal{I}} \boldsymbol{d}_\Gamma \cdot \tilde{\boldsymbol{n}}_\Gamma \,\mathrm{d}L\,, \tag{13}$$

where $\boldsymbol{d}$ is the electric flux density (dielectric displacement) vector, and ζ is the volume-specific free charge. Further, ζ_Γ is the surface-specific free charge in the interface, and $\boldsymbol{d}_\Gamma$ is the superficial electric surface flux density vector in the interface. Again, using the generic results in (4) and (6), we may localize the resulting expression to the volume and interface, respectively, so as to obtain

$$-\zeta + \boldsymbol{d} \cdot \boldsymbol{\nabla} = 0 \quad \text{in } \Omega^- \cup \Omega^+\,, \tag{14}$$

and

$$-\zeta_\Gamma + \boldsymbol{d}_\Gamma \cdot \boldsymbol{\nabla}_\Gamma + [\![\boldsymbol{d}]\!] \cdot \boldsymbol{n}_\Gamma = 0 \quad \text{on } \Gamma\,. \tag{15}$$

3.4.2. Gauss' law applied to an electro-chemical system

We shall now introduce the split of ζ into electronic and ionic parts, ζ_{el} and ζ_{ion}, respectively, i.e.

$$\zeta = \zeta_{\text{el}} + \sum_\alpha z'_\alpha c_\alpha\,, \tag{16}$$

where $z'_\alpha = F z_\alpha$ is the specific charge (z_α is the valence number and F is Faraday's constant). For example, $z'_{\text{Li}} = +F$ for Lithium. Likewise, we may introduce the split of ζ_Γ as

$$\zeta_\Gamma = \zeta_{\Gamma,\text{el}} + \sum_\alpha z'_{\Gamma,\alpha} c_{\Gamma,\alpha}\,. \tag{17}$$

Note that this relation has to be understood in the sense of mixture (continuum) theory. Now, upon inserting (16) and (17) into (14) and (15), respectively, we rephrase these equations as Gauss' law in the strong format

$$-\zeta_{\text{el}} + \boldsymbol{d} \cdot \boldsymbol{\nabla} - \sum_\alpha z'_\alpha c_\alpha = 0 \quad \text{in } \Omega^- \cup \Omega^+\,, \tag{18}$$

and

$$-\zeta_{\Gamma,\text{el}} + \boldsymbol{d}_\Gamma \cdot \boldsymbol{\nabla}_\Gamma + [\![\boldsymbol{d}]\!] \cdot \boldsymbol{n}_\Gamma - \sum_\alpha z'_{\Gamma,\alpha} c_{\Gamma,\alpha} = 0 \quad \text{on } \Gamma\,. \tag{19}$$

3.5. Ampere's law

Whereas Gauss' law admits a rather direct extension to an interface, the situation is more subtle for Ampere's law, which is formulated in terms of circulations along closed loops rather than fluxes across closed surfaces. We first establish the basic format by evaluating the circulation law for loops that either cross the interface or are embedded within it, thereby identifying the interfacial Maxwell current. Subsequently, this format is applied to an electro-chemical system, whereby the electric current is additively split into its electronic and ionic contributions.

3.5.1. Basic format

Ampere's law for the volume is well established as one of the two circulation laws expressed by Maxwell's equations. However, this is not the case for the counterpart on an interface. Here, we present a summary of the pertinent derivations.[3] Ampere's law relates the magnetic field $\boldsymbol{h}$ along an arbitrary closed space-curved loop γ in $\mathbb{R}^3$ to the so-called Maxwell current, defined as $\boldsymbol{i}_{\text{Max}} := \boldsymbol{i} + \partial_t \boldsymbol{d}$, through the (curved) surface ω (with surface normal $\boldsymbol{n}$) that is enclosed by γ.

Firstly, we consider the case that the loop γ intersects the interface, as illustrated in Fig. 4, creating two open curves γ^- and γ^+ on either side of the interface. Note that, since we consider the limit case of an interface with thickness $w \to 0$, all paths through the thickness of the resolved interphase must be parallel to $\boldsymbol{n}_\Gamma$. Consequently, we may decompose ω into ω^- and ω^+, as illustrated in Fig. 4. The intersection between the surface and the interface is denoted $\mathcal{L} = \omega \cap \Gamma$ with endpoints A and B. Along γ^+ and γ^-, the unit tangent vector $\boldsymbol{t}$ is defined in accordance with a positive circulation about the surface normal $\boldsymbol{n}$. Along $\mathcal{L}$ we define the tangent vectors $\boldsymbol{t}^- = -\boldsymbol{t}^+$ on opposite sides to maintain a positive circulation along $\partial\omega^- = \gamma^- \cup \mathcal{L}$ and $\omega^+ = \gamma^+ \cup \mathcal{L}$, respectively.

It is noted that all flux vectors $(\boldsymbol{i}, \boldsymbol{d}, \boldsymbol{h})$ are generally discontinuous across the interface Γ, i.e. $[\![\boldsymbol{i}]\!] \neq \boldsymbol{0}$, $[\![\boldsymbol{d}]\!] \neq \boldsymbol{0}$, $[\![\boldsymbol{h}]\!] \neq \boldsymbol{0}$. We now state Ampere's law in integral form as

$$\int_{\omega^-} \boldsymbol{i}_{\text{Max}} \cdot \boldsymbol{n} \,\mathrm{d}S + \int_{\mathcal{L}} \boldsymbol{i}^{\parallel}_{\text{Max},\Gamma} \cdot \boldsymbol{n}_{\text{L}} \,\mathrm{d}L + \int_{\omega^+} \boldsymbol{i}_{\text{Max}} \cdot \boldsymbol{n} \,\mathrm{d}S = \int_{\gamma^-} \boldsymbol{h} \cdot \boldsymbol{t} \,\mathrm{d}L + h^{\perp}_\Gamma\Big|_A + \int_{\gamma^+} \boldsymbol{h} \cdot \boldsymbol{t} \,\mathrm{d}L - h^{\perp}_\Gamma\Big|_B\,, \tag{20}$$

where we introduced (the superficial vector field) $\boldsymbol{i}^{\parallel}_{\text{Max},\Gamma} := \boldsymbol{i}^{\parallel}_\Gamma + \partial_t \boldsymbol{d}^{\parallel}_\Gamma$, and where $h^{\perp}_\Gamma := \boldsymbol{h}_\Gamma \cdot \boldsymbol{n}_\Gamma$ is the normal component of the interface magnetic field $\boldsymbol{h}_\Gamma$. Further, we used that the tangent of the loop through the interface is $\boldsymbol{n}_\Gamma$ and $-\boldsymbol{n}_\Gamma$ at A and B, respectively. It is noteworthy that it is only the *in-plane* part of $\boldsymbol{i}_{\text{Max},\Gamma}$ and the *normal* component of $\boldsymbol{h}_\Gamma$ that appear in (20). By identifying the loops around ω^+ and ω^-,

[3] Details of the derivation, which includes the use of Stokes' theorem, are given in Appendix B.

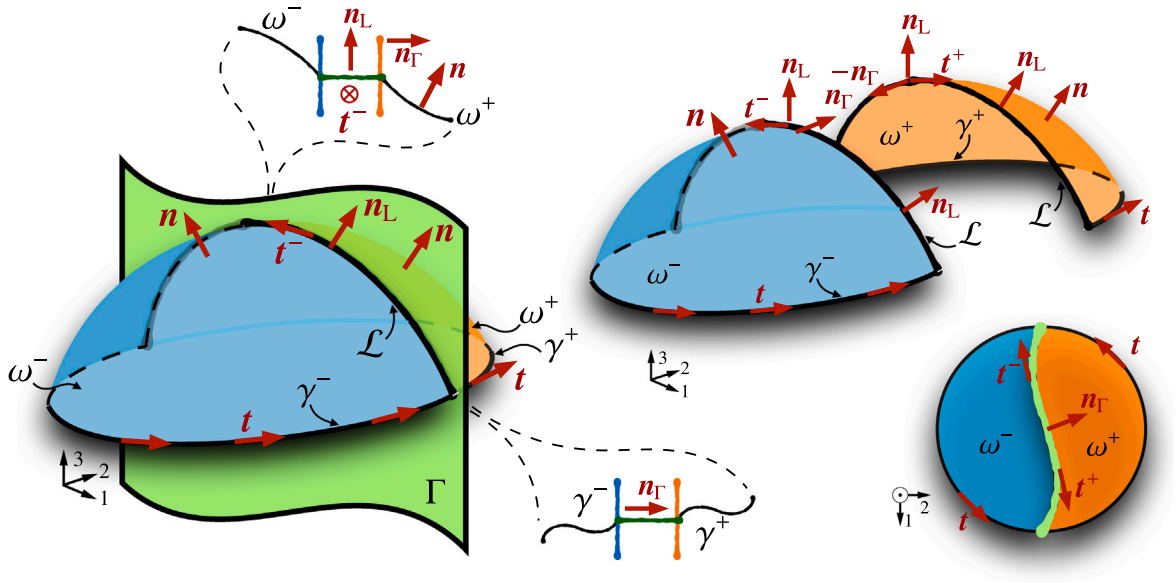


Fig. 4. Illustration for the derivation of circulation laws of Ampere and Faraday. The surface ω, bounded by the closed loop γ, crosses the interface Γ. Since the effective interface is very thin, all paths through the resolved layers must be parallel to the interface normal $\boldsymbol{n}_\Gamma$.

we may restate this equation in a format from which it is possible to deduce the local Ampere's (standard) law in the volume

$$\boldsymbol{i}_\mathrm{Max} + \boldsymbol{h} \times \boldsymbol{\nabla} = \boldsymbol{0} \quad \text{in } \Omega^- \cup \Omega^+ , \tag{21}$$

and on the interface

$$\boldsymbol{i}^{\parallel}_{\mathrm{Max},\Gamma} + [h^{\perp}_{\Gamma} \boldsymbol{n}_\Gamma] \times \boldsymbol{\nabla}_\Gamma + [\![\boldsymbol{h}]\!] \times \boldsymbol{n}_\Gamma = \boldsymbol{0} \quad \text{on } \Gamma . \tag{22}$$

Further, we may derive the following (Ampere's) identities

$$\boldsymbol{i}_\mathrm{Max} \cdot \boldsymbol{\nabla} = 0 \quad \text{in } \Omega^- \cup \Omega^+ , \tag{23}$$

and

$$\boldsymbol{i}^{\parallel}_{\mathrm{Max},\Gamma} \cdot \boldsymbol{\nabla}_\Gamma + [\![\boldsymbol{i}_\mathrm{Max}]\!] \cdot \boldsymbol{n}_\Gamma = 0 \quad \text{on } \Gamma . \tag{24}$$

Remark 3. An extreme situation is at hand when the circulation loop is embedded "entirely within the interface" with its normal $\boldsymbol{n} = \boldsymbol{n}_\Gamma$, cf. Fig. 5. The corresponding analysis[4] leads to the conclusion that the out-of-plane component of $\boldsymbol{i}_{\mathrm{Max},\Gamma}$ vanishes, i.e. $\boldsymbol{i}^{\parallel}_{\mathrm{Max},\Gamma} = \boldsymbol{i}_{\mathrm{Max},\Gamma}$ (which is used henceforth in the main text). □

Remark 4. The interfacial Ampere's law (22) agrees with its surface counterpart proposed by Chatzigeorgiou et al. (2015). In particular, equation (32) of Chatzigeorgiou et al. (2015) defines the surface magnetic field (in the notation of Chatzigeorgiou et al. (2015)) as $\hat{\boldsymbol{h}} := h^{\perp}_{\Gamma} \boldsymbol{n}_\Gamma$, and expresses $[h^{\perp}_{\Gamma} \boldsymbol{n}_\Gamma] \times \boldsymbol{\nabla}_\Gamma$ as the negative of $\widehat{\mathrm{curl}}\, \hat{\boldsymbol{h}}$ (the notation for the surface curl of $\hat{\boldsymbol{h}}$ in Chatzigeorgiou et al. (2015)). Furthermore, $\hat{\boldsymbol{j}}^{f} := \boldsymbol{i}^{\parallel}_{\mathrm{Max},\Gamma}$ for the special case of $\partial_t \boldsymbol{d}_\Gamma = \boldsymbol{0}$ is defined as a vector tangent to the boundary surface. With these identifications, the equivalence follows directly. □

3.5.2. Ampere's law applied to an electro-chemical system

Similarly to ζ, we shall now introduce the split of $\boldsymbol{i}$ into electronic and ionic parts, $\boldsymbol{i}_\mathrm{el}$ and $\boldsymbol{i}_\mathrm{ions}$, respectively. Using Faraday's law of electrolysis, we thus have

$$\boldsymbol{i} = \boldsymbol{i}_\mathrm{el} + \boldsymbol{i}_\mathrm{ion} \quad \text{with} \quad \boldsymbol{i}_\mathrm{ion} = \sum_\alpha z'_\alpha \boldsymbol{j}_\alpha . \tag{25}$$

[4] Details of the derivation are given in Appendix B.

Likewise, we may introduce the split of $\boldsymbol{i}_\Gamma$ as

$$\boldsymbol{i}_\Gamma = \boldsymbol{i}_{\Gamma,\mathrm{el}} + \boldsymbol{i}_{\Gamma,\mathrm{ion}} \quad \text{with} \quad \boldsymbol{i}_{\Gamma,\mathrm{ion}} = \sum_\alpha z'_{\Gamma,\alpha} \boldsymbol{j}_{\Gamma,\alpha} . \tag{26}$$

Now, upon inserting (25) and (26) into (23) and (24), respectively, while also using the mass balance equations (11) and (12), we rephrase (23) and (24) as follows:

$$\big[\partial_t \boldsymbol{d} + \boldsymbol{i}_\mathrm{el}\big] \cdot \boldsymbol{\nabla} - \sum_\alpha z'_\alpha [\partial_t c_\alpha - r_\alpha] = 0 \quad \text{in } \Omega^- \cup \Omega^+ , \tag{27}$$

and

$$\big[\partial_t \boldsymbol{d}_\Gamma + \boldsymbol{i}_{\Gamma,\mathrm{el}}\big] \cdot \boldsymbol{\nabla}_\Gamma + [\![\partial_t \boldsymbol{d} + \boldsymbol{i}_\mathrm{el}]\!] \cdot \boldsymbol{n}_\Gamma - \sum_\alpha z'_{\Gamma,\alpha} [\partial_t c_{\Gamma,\alpha} - r_{\Gamma,\alpha}] + \sum_\alpha [\![\Delta z'_\alpha \boldsymbol{j}_\alpha]\!] \cdot \boldsymbol{n}_\Gamma = 0 \quad \text{on } \Gamma , \tag{28}$$

where we introduced the notation $\Delta z'_\alpha := z'_\alpha - z'_{\Gamma,\alpha}$. Note that z'_α has different values in Ω^- and Ω^+, whereas $z'_{\Gamma,\alpha}$ is the (single) value on the interface Γ, thus $[\![\Delta z'_\alpha]\!] = [\![z'_\alpha]\!]$. Although z'_α and $z'_{\Gamma,\alpha}$ refer to the same species for any given α, it may be independently electrically active ($z' \neq 0$) or neutral ($z' = 0$) in the volume and the interface, respectively. Rearranging terms, we obtain the alternative formulations

$$\partial_t \left[\boldsymbol{d} \cdot \boldsymbol{\nabla} - \sum_\alpha z'_\alpha c_\alpha \right] + \boldsymbol{i}_\mathrm{el} \cdot \boldsymbol{\nabla} + \sum_\alpha z'_\alpha r_\alpha = 0 \quad \text{in } \Omega^- \cup \Omega^+ , \tag{29}$$

and

$$\partial_t \left[\boldsymbol{d}_\Gamma \cdot \boldsymbol{\nabla}_\Gamma + [\![\boldsymbol{d}]\!] \cdot \boldsymbol{n}_\Gamma - \sum_\alpha z'_{\Gamma,\alpha} c_{\Gamma,\alpha} \right] + \boldsymbol{i}_{\Gamma,\mathrm{el}} \cdot \boldsymbol{\nabla}_\Gamma + [\![\boldsymbol{i}_\mathrm{el}]\!] \cdot \boldsymbol{n}_\Gamma + \sum_\alpha [\![\Delta z'_\alpha \boldsymbol{j}_\alpha]\!] \cdot \boldsymbol{n}_\Gamma + \sum_\alpha z'_{\Gamma,\alpha} r_{\Gamma,\alpha} = 0 \quad \text{on } \Gamma , \tag{30}$$

whereby we note the more explicit expression $[\![\Delta z'_\alpha \boldsymbol{j}_\alpha]\!] \cdot \boldsymbol{n}_\Gamma = [\![z'_\alpha]\!] \{\!\{\boldsymbol{j}_\alpha\}\!\} \cdot \boldsymbol{n}_\Gamma + \left[\{\!\{z'_\alpha\}\!\} - z'_{\Gamma,\alpha} \right] [\![\boldsymbol{j}_\alpha]\!] \cdot \boldsymbol{n}_\Gamma$. However, we may invoke Gauss' laws, as expressed in (18) and (19), to rewrite (29) and (30) in the alternative fashion as

$$\partial_t \zeta_\mathrm{el} + \boldsymbol{i}_\mathrm{el} \cdot \boldsymbol{\nabla} + \sum_\alpha z'_\alpha r_\alpha = 0 \quad \text{in } \Omega^- \cup \Omega^+ , \tag{31}$$

and

$$\partial_t \zeta_{\Gamma,\mathrm{el}} + \boldsymbol{i}_{\Gamma,\mathrm{el}} \cdot \boldsymbol{\nabla}_\Gamma + [\![\boldsymbol{i}_\mathrm{el}]\!] \cdot \boldsymbol{n}_\Gamma + \sum_\alpha [\![\Delta z'_\alpha \boldsymbol{j}_\alpha]\!] \cdot \boldsymbol{n}_\Gamma + \sum_\alpha z'_{\Gamma,\alpha} r_{\Gamma,\alpha} = 0 \quad \text{on } \Gamma . \tag{32}$$

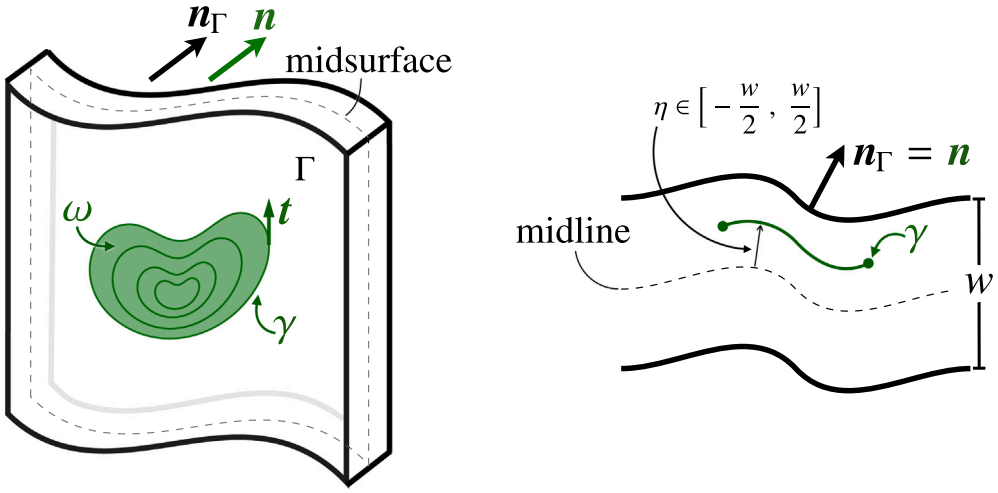


Fig. 5. Illustration for the derivation of circulation laws of Ampere and Faraday. The surface ω bounded by the closed loop γ lies perfectly within the interface Γ. Within the resolved layer, the circulation law can be established at an arbitrary through-thickness coordinate η, and the normal to ω is always identical to the interface normal, i.e. $\boldsymbol{n} \equiv \boldsymbol{n}_\Gamma$.

Eqs. (29) and (30) must be subjected to initial conditions on $(\boldsymbol{d} \cdot \boldsymbol{\nabla})(0)$, which also gives $[\![\boldsymbol{d}]\!] \cdot \boldsymbol{n}_\Gamma(0)$, and $(\boldsymbol{d}_\Gamma \cdot \boldsymbol{\nabla}_\Gamma)(0)$ in addition to conditions on $c_\alpha(0)$ and $c_{\Gamma,\alpha}(0)$.

3.6. Faraday's law — Condition for electro-statics

Faraday's law of induction is the second of the two circulation laws represented by Maxwell's equations. It relates the electric field $\boldsymbol{e}$ along an arbitrary closed loop γ in the three-dimensional space to the rate of magnetic flux density $\boldsymbol{b}$, i.e. the induction rate, through the surface enclosed by the loop. It is then possible to derive the local forms of Faraday's law in complete analogy with Ampere's law.[5] Here, we shall merely state the main result that follows from the particular assumption of stationarity, i.e. $\partial_t \boldsymbol{b} = \boldsymbol{0}$, corresponding to electro-statics. Upon denoting $\boldsymbol{e}$ the electric field in the volume, and $\boldsymbol{e}_\Gamma^{\parallel}$ the tangential electric field on the interface, we arrive at the conditions:

$$\boldsymbol{e} \times \boldsymbol{\nabla} = \boldsymbol{0} \quad \Rightarrow \quad \exists \varphi \ : \ \boldsymbol{e} = -\boldsymbol{\nabla}\varphi \,, \tag{33a}$$

$$\boldsymbol{e}_\Gamma^{\parallel} \times \boldsymbol{\nabla}_\Gamma^{\perp} = \boldsymbol{0} \ \hat{=} \ \left[\boldsymbol{e}_\Gamma^{\parallel} \times \boldsymbol{\nabla}_\Gamma\right] \cdot \boldsymbol{n}_\Gamma = 0 \quad \Rightarrow \quad \exists \varphi_\Gamma \ : \ \boldsymbol{e}_\Gamma^{\parallel} = -\boldsymbol{\nabla}_\Gamma \varphi_\Gamma \,, \tag{33b}$$

where φ and φ_Γ are the electric potentials in the volume and the interface, respectively. We note that, despite the fact that the out-of-plane component of $\boldsymbol{e}_\Gamma$ does not vanish in general, we use the simplified notation $\boldsymbol{e}_\Gamma := -\boldsymbol{\nabla}_\Gamma \varphi_\Gamma$ (instead of $\boldsymbol{e}_\Gamma^{\parallel}$) henceforth in the main text. In fact, the out-of-plane component of the electric field vanishes only for the case of perfect continuity, i.e., when $\varphi^+ = \varphi^- = \varphi_\Gamma$. Under such continuity, the notion of a purely tangential surface electro-static field is in line with the hypothesis in Chatzigeorgiou et al. (2014).

3.7. Balance of energy

The global format of the energy balance reads

$$\int_{\mathcal{B}} \partial_t e \, \mathrm{d}V + \int_{\mathcal{I}} \partial_t e_\Gamma \, \mathrm{d}S = \mathcal{P}_{\mathrm{me}} + \mathcal{P}_{\mathrm{th}} + \mathcal{P}_{\mathrm{el}} + \sum_\alpha \mathcal{P}_{\mathrm{ch},\alpha} \,, \tag{34}$$

where e is the volume-specific internal energy density in $\mathcal{B}$, whereas e_Γ is the surface-specific internal energy density on $\mathcal{I}$. (The parametrization of these densities is discussed later.) Referring to Fig. 6, we define the power supply to the body of mechanical, thermal, electromagnetic, and chemical nature as follows:

$$\mathcal{P}_{\mathrm{me}} = \int_{\partial\mathcal{B}} [\boldsymbol{\sigma} \cdot \boldsymbol{n}] \cdot \partial_t \boldsymbol{u} \, \mathrm{d}S + \int_{\partial\mathcal{I}} [\boldsymbol{\sigma}_\Gamma \cdot \tilde{\boldsymbol{n}}_\Gamma] \cdot \partial_t \boldsymbol{u}_\Gamma \, \mathrm{d}L \,, \tag{35a}$$

$$\mathcal{P}_{\mathrm{th}} = -\int_{\partial\mathcal{B}} \boldsymbol{q} \cdot \boldsymbol{n} \, \mathrm{d}S - \int_{\partial\mathcal{I}} \boldsymbol{q}_\Gamma \cdot \tilde{\boldsymbol{n}}_\Gamma \, \mathrm{d}L \,, \tag{35b}$$

$$\mathcal{P}_{\mathrm{el}} = -\int_{\partial\mathcal{B}} \boldsymbol{s} \cdot \boldsymbol{n} \, \mathrm{d}S - \int_{\partial\mathcal{I}} \boldsymbol{s}_\Gamma \cdot \tilde{\boldsymbol{n}}_\Gamma \, \mathrm{d}L \,, \tag{35c}$$

$$\mathcal{P}_{\mathrm{ch},\alpha} = -\int_{\partial\mathcal{B}} [e_\alpha^{\mathrm{ch}} \boldsymbol{j}_\alpha] \cdot \boldsymbol{n} \, \mathrm{d}S - \int_{\partial\mathcal{I}} [e_{\Gamma,\alpha}^{\mathrm{ch}} \boldsymbol{j}_{\Gamma,\alpha}] \cdot \tilde{\boldsymbol{n}}_\Gamma \, \mathrm{d}L \,, \quad \alpha = 1, 2, \ldots, M \,, \tag{35d}$$

where we introduced the following variables/notation: $\boldsymbol{u}$ and $\boldsymbol{u}_\Gamma$ are the displacement (fields) in the bulk material and the interface, respectively; $\boldsymbol{q}$ and $\boldsymbol{q}_\Gamma$ are the heat flux vectors in the bulk material and the interface, respectively; $\boldsymbol{s}$ and $\boldsymbol{s}_\Gamma$ are the electromagnetic energy flux vectors (Poynting vectors) in the bulk material and the interface, and they are defined as

$$\boldsymbol{s} := \boldsymbol{e} \times \boldsymbol{h} \,, \tag{36a}$$

$$\boldsymbol{s}_\Gamma := \boldsymbol{e}_\Gamma \times [h_\Gamma^{\perp} \boldsymbol{n}_\Gamma] + \{\!\{\boldsymbol{h}\}\!\} \times \boldsymbol{n}_\Gamma [\![\varphi]\!] + [\![\boldsymbol{h}]\!] \times \boldsymbol{n}_\Gamma [\{\!\{\varphi\}\!\} - \varphi_\Gamma] \,. \tag{36b}$$

Further, e_α^{ch} and $e_{\Gamma,\alpha}^{\mathrm{ch}}$ are the volume- and surface-specific internal energy carried by the diffusing species in the bulk material and the interface, respectively. We note that the expression for $\boldsymbol{s}$ in (36a) is classical; however, the expression for $\boldsymbol{s}_\Gamma$ in (36b) is non-classical and cannot be found in the literature. The detailed derivation is given in Appendix B.5.1.

Integrating by parts, while using the identities (1) and (2), and using the (appropriate) balance equations, we obtain

$$\begin{aligned} \mathcal{P}_{\mathrm{me}} = &\int_{\mathcal{B}^- \cup \mathcal{B}^+} \boldsymbol{\sigma} : \partial_t \boldsymbol{\epsilon} \, \mathrm{d}V \\ &+ \int_{\mathcal{I}} \Big[\boldsymbol{\sigma}_\Gamma : \partial_t \boldsymbol{\epsilon}_\Gamma + [\{\!\{\boldsymbol{\sigma}\}\!\} \cdot \boldsymbol{n}_\Gamma] \cdot \partial_t [\![\boldsymbol{u}]\!] \\ &\quad + [[\![\boldsymbol{\sigma}]\!] \cdot \boldsymbol{n}_\Gamma] \cdot \partial_t \left[\{\!\{\boldsymbol{u}\}\!\} - \boldsymbol{u}_\Gamma\right] \Big] \, \mathrm{d}S \,, \end{aligned} \tag{37a}$$

$$\begin{aligned} \mathcal{P}_{\mathrm{th}} = &\int_{\mathcal{B}^- \cup \mathcal{B}^+} [-\boldsymbol{q} \cdot \boldsymbol{\nabla}] \, \mathrm{d}V \\ &+ \int_{\mathcal{I}} \left[-\boldsymbol{q}_\Gamma \cdot \boldsymbol{\nabla}_\Gamma - [\![\boldsymbol{q}]\!] \cdot \boldsymbol{n}_\Gamma \right] \, \mathrm{d}S \,, \end{aligned} \tag{37b}$$

$$\begin{aligned} \mathcal{P}_{\mathrm{el}} = &\int_{\mathcal{B}^- \cup \mathcal{B}^+} \boldsymbol{i}_{\mathrm{Max}} \cdot \boldsymbol{e} \, \mathrm{d}V \\ &+ \int_{\mathcal{I}} \left[\boldsymbol{i}_{\mathrm{Max},\Gamma} \cdot \boldsymbol{e}_\Gamma - \{\!\{\boldsymbol{i}_{\mathrm{Max}}\}\!\} \cdot \boldsymbol{n}_\Gamma [\![\varphi]\!] \right. \end{aligned}$$

[5] Details of the derivation, which are somewhat elaborate, are given in Appendix B.

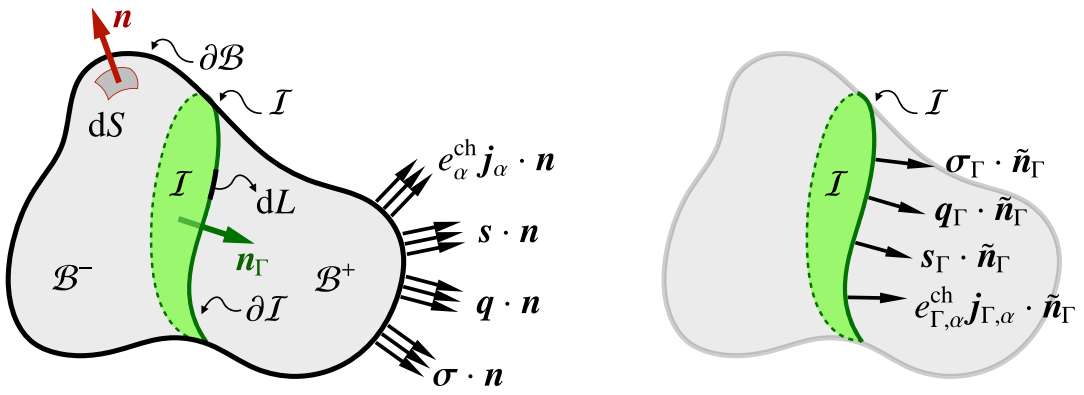


Fig. 6. Body exchanging energy (and entropy) of electro-magneto-chemo-thermo-mechanical nature with the surrounding material.

$$- [\![\boldsymbol{i}_{\text{Max}}]\!] \cdot \boldsymbol{n}_\Gamma \left[\{\!\{\varphi\}\!\} - \varphi_\Gamma \right] \big] \, \mathrm{d}S \,, \tag{37c}$$

$$\begin{aligned}\mathcal{P}_{\text{ch},\alpha} = &\int_{\mathcal{B}^- \cup \mathcal{B}^+} \left[e^{\text{ch}}_\alpha [\partial_t c_\alpha - r_\alpha] - \boldsymbol{j}_\alpha \cdot [\boldsymbol{\nabla} e^{\text{ch}}_\alpha] \right] \mathrm{d}V \\ &+ \int_{\mathcal{I}} \Big[e^{\text{ch}}_{\Gamma,\alpha} [\partial_t c_{\Gamma,\alpha} - r_{\Gamma,\alpha}] - \boldsymbol{j}_{\Gamma,\alpha} \cdot [\boldsymbol{\nabla}_\Gamma e^{\text{ch}}_{\Gamma,\alpha}] - [\![\{\!\{\boldsymbol{j}_\alpha\}\!\}]\!] \cdot \boldsymbol{n}_\Gamma [\![e^{\text{ch}}_\alpha]\!] \\ &- [\![\boldsymbol{j}_\alpha]\!] \cdot \boldsymbol{n}_\Gamma \left[\{\!\{e^{\text{ch}}_\alpha\}\!\} - e^{\text{ch}}_{\Gamma,\alpha} \right] \Big] \, \mathrm{d}S \,, \end{aligned} \tag{37d}$$

where $\boldsymbol{\epsilon}$ and $\boldsymbol{\epsilon}_\Gamma$ are the strain tensors in the volume and in the interface, respectively. Further, the superficial Maxwell current is $\boldsymbol{i}_{\text{Max},\Gamma} := \boldsymbol{i}_\Gamma + \partial_t \boldsymbol{d}_\Gamma$.

To be more specific regarding the derivation of (37), we note the following: In order to derive (37a), we used the equilibrium Eqs. (8) and (9). How to arrive at (37c) is not entirely trivial and is, therefore, shown in some detail in Appendix B.5.2, ending up with (B.41). In particular, we note the definition $\boldsymbol{e}_\Gamma := -\boldsymbol{\nabla}_\Gamma \varphi_\Gamma$. Finally, to derive (37d) we used the continuity Eqs. (11) and (12).

Remark 5. Subject to the condition of electro-statics, it is possible to rewrite $\mathcal{P}_{\text{el}}$, expressed in (37c), as

$$\begin{aligned}\mathcal{P}_{\text{el}} = &- \int_{\mathcal{B}^- \cup \mathcal{B}^+} \boldsymbol{i}_{\text{Max}} \cdot \boldsymbol{\nabla} \varphi \, \mathrm{d}V \\ &+ \int_{\mathcal{I}} \left[-\boldsymbol{i}_{\text{Max},\Gamma} \cdot \boldsymbol{\nabla}_\Gamma \varphi_\Gamma - [\![\boldsymbol{i}_{\text{Max}} \varphi]\!] \cdot \boldsymbol{n}_\Gamma + [\![\boldsymbol{i}_{\text{Max}} \varphi_\Gamma]\!] \cdot \boldsymbol{n}_\Gamma \right] \mathrm{d}S \,. \end{aligned} \tag{38}$$

Upon integration by parts and using Gauss' theorems for the volume and interface, we obtain

$$\mathcal{P}_{\text{el}} = - \int_{\partial(\mathcal{B}^- \cup \mathcal{B}^+)} [\boldsymbol{i}_{\text{Max}} \, \varphi] \cdot \boldsymbol{n} \, \mathrm{d}S - \int_{\partial \mathcal{I}} [\boldsymbol{i}_{\text{Max},\Gamma} \, \varphi_\Gamma] \cdot \tilde{\boldsymbol{n}}_\Gamma \, \mathrm{d}L \,. \tag{39}$$

It thus appears that the "structure" of the expression for electromagnetic power entering into the interface is consistent with the power entering into the volume. □

In order to obtain an operational expression for $\mathcal{P}_{\text{el}}$, we may introduce the constitutive split of $\boldsymbol{i}$ and $\boldsymbol{i}_\Gamma$, given in (25) and (26), respectively. We then obtain

$$\begin{aligned}\mathcal{P}_{\text{el}} = &\int_{\mathcal{B}^- \cup \mathcal{B}^+} \left[\partial_t \boldsymbol{d} \cdot \boldsymbol{e} + \boldsymbol{i}_{\text{el}} \cdot \boldsymbol{e} + \sum_\alpha z'_\alpha \boldsymbol{j}_\alpha \cdot \boldsymbol{e} \right] \mathrm{d}V \\ &+ \int_{\mathcal{I}} \left[\partial_t \boldsymbol{d}_\Gamma \cdot \boldsymbol{e}_\Gamma + \boldsymbol{i}_{\Gamma\text{el}} \cdot \boldsymbol{e}_\Gamma + \sum_\alpha z'_{\Gamma,\alpha} \boldsymbol{j}_{\Gamma,\alpha} \cdot \boldsymbol{e}_\Gamma \right] \mathrm{d}S \\ &- \int_{\mathcal{I}} \left[\partial_t \{\!\{\boldsymbol{d}\}\!\} \cdot \boldsymbol{n}_\Gamma + \{\!\{\boldsymbol{i}_{\text{el}}\}\!\} \cdot \boldsymbol{n}_\Gamma + \sum_\alpha \{\!\{z'_\alpha \boldsymbol{j}_\alpha\}\!\} \cdot \boldsymbol{n}_\Gamma \right] [\![\varphi]\!] \, \mathrm{d}S \\ &- \int_{\mathcal{I}} \left[\partial_t [\![\boldsymbol{d}]\!] \cdot \boldsymbol{n}_\Gamma + [\![\boldsymbol{i}_{\text{el}}]\!] \cdot \boldsymbol{n}_\Gamma + \sum_\alpha [\![z'_\alpha \boldsymbol{j}_\alpha]\!] \cdot \boldsymbol{n}_\Gamma \right] [\{\!\{\varphi\}\!\} - \varphi_\Gamma] \, \mathrm{d}S \,. \end{aligned} \tag{40}$$

Once again, we note that the interfacial current $\boldsymbol{i}_{\Gamma\text{el}}$ is assumed to represent *electronic activity*.

As a matter of convenience (and brevity of notation), we now introduce the constitutive "normal flux" variables, cf. Table 1:

$$\begin{aligned} t^{\text{C}}_\Gamma &:= \{\!\{\boldsymbol{\sigma}\}\!\} \cdot \boldsymbol{n}_\Gamma \,, & t^{\text{D}}_\Gamma &:= [\![\boldsymbol{\sigma}]\!] \cdot \boldsymbol{n}_\Gamma \\ j^{\text{C}}_{\Gamma,\alpha} &:= \{\!\{\boldsymbol{j}_\alpha\}\!\} \cdot \boldsymbol{n}_\Gamma \,, & j^{\text{D}}_{\Gamma,\alpha} &:= [\![\boldsymbol{j}_\alpha]\!] \cdot \boldsymbol{n}_\Gamma \\ q^{\text{C}}_\Gamma &:= \{\!\{\boldsymbol{q}\}\!\} \cdot \boldsymbol{n}_\Gamma \,, & q^{\text{D}}_\Gamma &:= [\![\boldsymbol{q}]\!] \cdot \boldsymbol{n}_\Gamma \\ d^{\text{C}}_\Gamma &:= \{\!\{\boldsymbol{d}\}\!\} \cdot \boldsymbol{n}_\Gamma \,, & d^{\text{D}}_\Gamma &:= [\![\boldsymbol{d}]\!] \cdot \boldsymbol{n}_\Gamma \\ i^{\text{C}}_{\Gamma,\text{el}} &:= \{\!\{\boldsymbol{i}_{\text{el}}\}\!\} \cdot \boldsymbol{n}_\Gamma \,, & i^{\text{D}}_{\Gamma,\text{el}} &:= [\![\boldsymbol{i}_{\text{el}}]\!] \cdot \boldsymbol{n}_\Gamma \,. \end{aligned} \tag{41}$$

We may now localize (34) as follows:

$$\begin{aligned}&\partial_t e - \boldsymbol{\sigma} : \partial_t \boldsymbol{\epsilon} - \sum_\alpha e^{\text{ch}}_\alpha \partial_t c_\alpha - \boldsymbol{e} \cdot \partial_t \boldsymbol{d} + \sum_\alpha \boldsymbol{j}_\alpha \cdot \left[\boldsymbol{\nabla} [e^{\text{ch}}_\alpha + z'_\alpha \varphi] \right] \\ &\quad + \sum_\alpha r_\alpha e^{\text{ch}}_\alpha - \boldsymbol{i}_{\text{el}} \cdot \boldsymbol{e} + \boldsymbol{q} \cdot \boldsymbol{\nabla} = 0 \,, \quad \text{in } \Omega^- \cup \Omega^+ \,, \end{aligned} \tag{42}$$

and

$$\begin{aligned}&\partial_t e_\Gamma - \boldsymbol{\sigma}_\Gamma : \partial_t \boldsymbol{\epsilon}_\Gamma - \sum_\alpha e^{\text{ch}}_{\Gamma,\alpha} \partial_t c_{\Gamma,\alpha} - \boldsymbol{e}_\Gamma \cdot \partial_t \boldsymbol{d}_\Gamma \\ &\quad - \boldsymbol{t}^{\text{C}}_\Gamma \cdot \partial_t [\![\boldsymbol{u}]\!] - \boldsymbol{t}^{\text{D}}_\Gamma \cdot \partial_t \left[\{\!\{\boldsymbol{u}\}\!\} - \boldsymbol{u}_\Gamma \right] + [\![\varphi]\!] \partial_t d^{\text{C}}_\Gamma + \left[\{\!\{\varphi\}\!\} - \varphi_\Gamma \right] \partial_t d^{\text{D}}_\Gamma \\ &\quad + \sum_\alpha \boldsymbol{j}_{\Gamma,\alpha} \cdot \left[\boldsymbol{\nabla}_\Gamma [e^{\text{ch}}_{\Gamma,\alpha} + z'_{\Gamma,\alpha} \varphi_\Gamma] \right] + \sum_\alpha r_{\Gamma,\alpha} e^{\text{ch}}_{\Gamma,\alpha} \\ &\quad + \sum_\alpha j^{\text{C}}_{\Gamma,\alpha} \left[[\![e^{\text{ch}}_\alpha]\!] + [\![z'_\alpha \varphi]\!] - [\![z'_\alpha]\!] \varphi_\Gamma \right] \\ &\quad + \sum_\alpha j^{\text{D}}_{\Gamma,\alpha} \left[\{\!\{e^{\text{ch}}_\alpha\}\!\} - e^{\text{ch}}_{\Gamma,\alpha} + \{\!\{z'_\alpha \varphi\}\!\} - \{\!\{z'_\alpha\}\!\} \varphi_\Gamma \right] \\ &\quad - \boldsymbol{i}_{\Gamma,\text{el}} \cdot \boldsymbol{e}_\Gamma + i^{\text{C}}_{\Gamma,\text{el}} [\![\varphi]\!] + i^{\text{D}}_{\Gamma,\text{el}} \left[\{\!\{\varphi\}\!\} - \varphi_\Gamma \right] \\ &\quad + \boldsymbol{q}_\Gamma \cdot \boldsymbol{\nabla}_\Gamma + q^{\text{D}}_\Gamma = 0 \,, \quad \text{on } \Gamma \,. \end{aligned} \tag{43}$$

In order to obtain this result, we used (in particular) the identity

$$\begin{aligned}&\{\!\{z'_\alpha \boldsymbol{j}_\alpha\}\!\} \cdot \boldsymbol{n}_\Gamma [\![\varphi]\!] + [\![z'_\alpha \boldsymbol{j}_\alpha]\!] \cdot \boldsymbol{n}_\Gamma [\{\!\{\varphi\}\!\} - \varphi_\Gamma] \\ &\quad = [\![z'_\alpha \boldsymbol{j}_\alpha [\varphi - \varphi_\Gamma]]\!] \cdot \boldsymbol{n}_\Gamma \\ &\quad = \{\!\{\boldsymbol{j}_\alpha\}\!\} \cdot \boldsymbol{n}_\Gamma [\![z'_\alpha [\varphi - \varphi_\Gamma]]\!] + [\![\boldsymbol{j}_\alpha]\!] \cdot \boldsymbol{n}_\Gamma \{\!\{z'_\alpha [\varphi - \varphi_\Gamma]\}\!\} \\ &\quad = j^{\text{C}}_{\Gamma,\alpha} \left[[\![z'_\alpha \varphi]\!] - [\![z'_\alpha]\!] \varphi_\Gamma \right] + j^{\text{D}}_{\Gamma,\alpha} \left[\{\!\{z'_\alpha \varphi\}\!\} - \{\!\{z'_\alpha\}\!\} \varphi_\Gamma \right] \,. \end{aligned} \tag{44}$$

Further, in order to obtain (42), we used that $\boldsymbol{e} = -\boldsymbol{\nabla}\varphi$, whereby $\boldsymbol{\nabla} e^{\text{ch}}_\alpha - z'_\alpha \boldsymbol{e} = \boldsymbol{\nabla} \left[e^{\text{ch}}_\alpha + z'_\alpha \varphi \right]$. Similarly, in order to obtain (43), we used that $\boldsymbol{e}_\Gamma = -\boldsymbol{\nabla}_\Gamma \varphi_\Gamma$, whereby $\boldsymbol{\nabla}_\Gamma e^{\text{ch}}_{\Gamma,\alpha} - z'_{\Gamma,\alpha} \boldsymbol{e}_\Gamma = \boldsymbol{\nabla}_\Gamma \left[e^{\text{ch}}_{\Gamma,\alpha} + z'_{\Gamma,\alpha} \varphi_\Gamma \right]$.

4. General constraints on constitutive relations — Entropy inequality

The balance equations established in Section 3 must be supplemented by constitutive relations, in the volume as well as on the interface, in order to close the ECTM model system. Such relations cannot be chosen arbitrarily, but are restricted by the entropy inequality, which is exploited here to identify the energetic (state) relations and to

establish the constraints imposed on the dissipative fluxes. To this end, the entropy inequality is first localized and elaborated in terms of the internal energy density, thereafter it is rephrased in terms of the free energy density via a Legendre transformation.

4.1. Basic format of entropy inequality in terms of internal energy density

The global format of the entropy inequality for a system with an interface reads

$$\int_{\mathcal{B}} \partial_t s \,\mathrm{d}V + \int_{\mathcal{I}} \partial_t s_\Gamma \,\mathrm{d}S \geq \mathcal{R}\,, \tag{45}$$

where s is the volume-specific entropy in $\mathcal{B}$, s_Γ is the surface-specific entropy on $\mathcal{I}$ and $\mathcal{R}$ is the external entropy supply that is given as

$$\mathcal{R} := -\int_{\partial\mathcal{B}} \boldsymbol{\eta}\cdot\boldsymbol{n}_\Gamma \,\mathrm{d}S - \int_{\partial\mathcal{I}} \boldsymbol{\eta}_\Gamma\cdot\tilde{\boldsymbol{n}}_\Gamma \,\mathrm{d}L\,, \tag{46}$$

where we introduced the entropy flux in the volume and in the interface, respectively, as follows

$$\boldsymbol{\eta} := \theta^{-1}\boldsymbol{q} + \sum_\alpha \boldsymbol{j}_\alpha s^{\mathrm{ch}}_\alpha\,, \quad \boldsymbol{\eta}_\Gamma := [\theta_\Gamma]^{-1}\boldsymbol{q}_\Gamma + \sum_\alpha \boldsymbol{j}_{\Gamma,\alpha} s^{\mathrm{ch}}_{\Gamma,\alpha}\,, \tag{47}$$

where $\theta > 0$ and $\theta_\Gamma > 0$ are the absolute temperature in the volume and the interface, respectively. Further, we introduced the volume-specific and surface-specific entropy carried by the ionic species in the volume and the interface, denoted s^{ch}_α and $s^{\mathrm{ch}}_{\Gamma,\alpha}$, respectively.

Using Gauss' theorems in (4) and (6), respectively, we may localize (45) to obtain

$$\theta\partial_t s + \theta[\boldsymbol{\eta}\cdot\boldsymbol{\nabla}] \geq 0\,, \quad \text{in } \Omega\,, \tag{48}$$

and

$$\theta_\Gamma\partial_t s_\Gamma + \theta_\Gamma[\![\boldsymbol{\eta}]\!]\cdot\boldsymbol{n}_\Gamma + \theta_\Gamma[\boldsymbol{\eta}_\Gamma\cdot\boldsymbol{\nabla}_\Gamma] \geq 0\,, \quad \text{on } \Gamma\,. \tag{49}$$

Upon introducing the effective heat flux $\boldsymbol{q}^{\mathrm{eff}}$ and $\boldsymbol{q}^{\mathrm{eff}}_\Gamma$ in the volume and on the interface, respectively, defined as

$$\boldsymbol{q}^{\mathrm{eff}} := \theta\boldsymbol{\eta} = \boldsymbol{q} + \theta\sum_\alpha s^{\mathrm{ch}}_\alpha \boldsymbol{j}_\alpha\,, \quad \boldsymbol{q}^{\mathrm{eff}}_\Gamma := \theta_\Gamma\boldsymbol{\eta}_\Gamma = \boldsymbol{q}_\Gamma + \theta_\Gamma\sum_\alpha s^{\mathrm{ch}}_{\Gamma,\alpha}\boldsymbol{j}_{\Gamma,\alpha}\,, \tag{50}$$

we may reformulate the entropy inequality expressions (48) and (49) as

$$\theta\partial_t s - \frac{1}{\theta}\boldsymbol{q}^{\mathrm{eff}}\cdot[\boldsymbol{\nabla}\theta] + \boldsymbol{q}^{\mathrm{eff}}\cdot\boldsymbol{\nabla} \geq 0\,, \quad \text{in } \Omega\,, \tag{51}$$

and

$$\theta_\Gamma\partial_t s_\Gamma - \frac{1}{\theta_\Gamma}\boldsymbol{q}^{\mathrm{eff}}_\Gamma\cdot[\boldsymbol{\nabla}_\Gamma\theta_\Gamma] + \boldsymbol{q}^{\mathrm{eff}}_\Gamma\cdot\boldsymbol{\nabla}_\Gamma + q^{\mathrm{eff,C}}_\Gamma\theta_\Gamma[\![\theta^{-1}]\!] + q^{\mathrm{eff,D}}_\Gamma\theta_\Gamma\{\!\{\theta^{-1}\}\!\} \geq 0\,, \quad \text{on } \Gamma\,, \tag{52}$$

where we also introduced the notation

$$\begin{aligned} q^{\mathrm{eff,C}}_\Gamma &:= \{\!\{\boldsymbol{q}^{\mathrm{eff}}\}\!\}\cdot\boldsymbol{n}_\Gamma = q^{\mathrm{C}}_\Gamma + \sum_\alpha \{\!\{\theta s^{\mathrm{ch}}_\alpha \boldsymbol{j}_\alpha\}\!\}\cdot\boldsymbol{n}_\Gamma\,,\\ q^{\mathrm{eff,D}}_\Gamma &:= [\![\boldsymbol{q}^{\mathrm{eff}}]\!]\cdot\boldsymbol{n}_\Gamma = q^{\mathrm{D}}_\Gamma + \sum_\alpha [\![\theta s^{\mathrm{ch}}_\alpha \boldsymbol{j}_\alpha]\!]\cdot\boldsymbol{n}_\Gamma\,. \end{aligned} \tag{53}$$

It also turns out to be convenient to use the definitions of $\boldsymbol{q}^{\mathrm{eff}}$ and $\boldsymbol{q}^{\mathrm{eff}}_\Gamma$ in (50) in order to rephrase the localized energy balance in (42) (for the bulk) and in (43) (for the interface). We then obtain the following expressions:

$$\begin{aligned} &\partial_t e - \boldsymbol{\sigma} : \partial_t\boldsymbol{\epsilon} - \sum_\alpha \mu_\alpha\partial_t c_\alpha - \boldsymbol{e}\cdot\partial_t\boldsymbol{d}\\ &\quad + \sum_\alpha \boldsymbol{j}_\alpha\cdot\boldsymbol{\nabla}\mu'_\alpha + \sum_\alpha r_\alpha\mu_\alpha - \boldsymbol{i}_{\mathrm{el}}\cdot\boldsymbol{e} + \boldsymbol{q}^{\mathrm{eff}}\cdot\boldsymbol{\nabla} = 0\,, \quad \text{in } \Omega^-\cup\Omega^+\,, \end{aligned} \tag{54}$$

and

$$\begin{aligned} &\partial_t e_\Gamma - \boldsymbol{\sigma}_\Gamma : \partial_t\boldsymbol{\epsilon}_\Gamma - \sum_\alpha \mu_{\Gamma,\alpha}\partial_t c_{\Gamma,\alpha} - \boldsymbol{e}_\Gamma\cdot\partial_t\boldsymbol{d}_\Gamma\\ &\quad - \boldsymbol{t}^{\mathrm{C}}_\Gamma\cdot\partial_t[\![\boldsymbol{u}]\!] - \boldsymbol{t}^{\mathrm{D}}_\Gamma\cdot\partial_t\left[\{\!\{\boldsymbol{u}\}\!\} - \boldsymbol{u}_\Gamma\right] + [\![\varphi]\!]\partial_t d^{\mathrm{C}}_\Gamma + \left[\{\!\{\varphi\}\!\} - \varphi_\Gamma\right]\partial_t d^{\mathrm{D}}_\Gamma\\ &\quad + \sum_\alpha \boldsymbol{j}_{\Gamma,\alpha}\cdot\left[\boldsymbol{\nabla}_\Gamma\mu'_{\Gamma,\alpha}\right] + \sum_\alpha r_{\Gamma,\alpha}\mu_{\Gamma,\alpha}\\ &\quad + \sum_\alpha j^{\mathrm{C}}_{\Gamma,\alpha}\left[[\![\mu'_\alpha]\!] - [\![z'_\alpha]\!]\varphi_\Gamma\right] + \sum_\alpha j^{\mathrm{D}}_{\Gamma,\alpha}\left[\{\!\{\mu'_\alpha\}\!\} - \mu'_{\Gamma,\alpha} - [\{\!\{z'_\alpha\}\!\} - z'_{\Gamma,\alpha}]\varphi_\Gamma\right]\\ &\quad - \boldsymbol{i}_{\Gamma,\mathrm{el}}\cdot\boldsymbol{e}_\Gamma + i^{\mathrm{C}}_{\Gamma,\mathrm{el}}[\![\varphi]\!] + i^{\mathrm{D}}_{\Gamma,\mathrm{el}}\left[\{\!\{\varphi\}\!\} - \varphi_\Gamma\right]\\ &\quad + \boldsymbol{q}^{\mathrm{eff}}_\Gamma\cdot\boldsymbol{\nabla}_\Gamma + q^{\mathrm{eff,D}}_\Gamma = 0\,, \quad \text{on } \Gamma\,. \end{aligned} \tag{55}$$

Here, we introduced the (standard) volume-specific chemical potential and the corresponding electro-chemical potential μ'_α

$$\mu_\alpha := e^{\mathrm{ch}}_\alpha - \theta s^{\mathrm{ch}}_\alpha\,, \quad \mu'_\alpha := \mu_\alpha + z'_\alpha\varphi\,. \tag{56}$$

We also introduced the surface-specific chemical and electro-chemical potentials for the interface

$$\mu_{\Gamma,\alpha} := e^{\mathrm{ch}}_{\Gamma,\alpha} - \theta_\Gamma s^{\mathrm{ch}}_{\Gamma,\alpha}\,, \quad \mu'_{\Gamma,\alpha} = \mu_{\Gamma,\alpha} + z'_{\Gamma,\alpha}\varphi_\Gamma\,. \tag{57}$$

Remark 6. Introducing the "effective" heat flux vectors $\boldsymbol{q}^{\mathrm{eff}}$ and $\boldsymbol{q}^{\mathrm{eff}}_\Gamma$ apparently infers the following consequences:

- It is sufficient to devise constitutive models for the chemical potentials $\mu_\alpha, \mu_{\Gamma,\alpha}$; there will be no need to compute the quantities $e^{\mathrm{ch}}_\alpha, s^{\mathrm{ch}}_\alpha$ in the volume and $e^{\mathrm{ch}}_{\Gamma,\alpha}, s^{\mathrm{ch}}_{\Gamma,\alpha}$ in the interface (even if it would be possible theoretically, cf. (Salvadori et al., 2018)).
- It is necessary to assign exterior boundary conditions on $q^{\mathrm{eff}}_n := \boldsymbol{q}^{\mathrm{eff}}\cdot\boldsymbol{n}$ (rather than on the standard heat flux $q_n := \boldsymbol{q}\cdot\boldsymbol{n}$). However, in view of the identity $q^{\mathrm{eff}}_n = q_n + \theta\sum_\alpha s^{\mathrm{ch}}_\alpha j_{\alpha,n}$, and the common assumption that $j_{\alpha,n} = 0$ on the Neumann boundary, the standard expression $q^{\mathrm{eff}}_n = q_n$ is retrieved.

Now, it is possible to invoke the localized energy balance (54) in order to eliminate $\boldsymbol{q}^{\mathrm{eff}}\cdot\boldsymbol{\nabla}$ in (51). As a result, we rewrite the entropy inequality as follows:

$$\mathcal{D} := \mathcal{D}_{\mathrm{en}} + \mathcal{D}_{\mathrm{el-ch}} + \mathcal{D}_{\mathrm{th}} \geq 0 \quad \text{in } \Omega^-\cup\Omega^+\,, \tag{58}$$

where the different terms are defined as

$$\mathcal{D}_{\mathrm{en}} := -\partial_t e + \boldsymbol{\sigma} : \partial_t\boldsymbol{\epsilon} + \theta\partial_t s + \sum_\alpha \mu_\alpha\partial_t c_\alpha + \boldsymbol{e}\cdot\partial_t\boldsymbol{d}\,, \tag{59a}$$

$$\mathcal{D}_{\mathrm{el-ch}} := -\sum_\alpha \boldsymbol{j}_\alpha\cdot\boldsymbol{\nabla}\mu'_\alpha - \sum_\alpha r_\alpha\mu_\alpha + \boldsymbol{i}_{\mathrm{el}}\cdot\boldsymbol{e}\,, \tag{59b}$$

$$\mathcal{D}_{\mathrm{th}} := -\frac{1}{\theta}\boldsymbol{q}^{\mathrm{eff}}\cdot\boldsymbol{\nabla}\theta\,. \tag{59c}$$

Similarly, we invoke the localized energy balance pertinent to the interface, (55), in order to eliminate $\boldsymbol{q}^{\mathrm{eff}}_\Gamma\cdot\boldsymbol{\nabla}_\Gamma$ in (52), whereby the dissipation inequality for the interface is expressed as

$$\mathcal{D}_\Gamma := \mathcal{D}_{\Gamma,\mathrm{en}} + \mathcal{D}_{\Gamma,\mathrm{el\text{-}ch}} + \mathcal{D}_{\Gamma,\mathrm{th}} \geq 0 \quad \text{on } \Gamma\,, \tag{60}$$

where the terms in (60) become

$$\begin{aligned} \mathcal{D}_{\Gamma,\mathrm{en}} =& -\partial_t e_\Gamma + \boldsymbol{\sigma}_\Gamma : \partial_t\boldsymbol{\epsilon}_\Gamma + \theta_\Gamma\partial_t s_\Gamma + \sum_\alpha \mu_{\Gamma,\alpha}\partial_t c_{\Gamma,\alpha} + \boldsymbol{e}_\Gamma\cdot\partial_t\boldsymbol{d}_\Gamma\\ &+ \boldsymbol{t}^{\mathrm{C}}_\Gamma\cdot\partial_t\boldsymbol{u}^{\mathrm{C}}_\Gamma + \boldsymbol{t}^{\mathrm{D}}_\Gamma\cdot\partial_t\boldsymbol{u}^{\mathrm{D}}_\Gamma - \varphi^{\mathrm{C}}_\Gamma\partial_t d^{\mathrm{C}}_\Gamma - \varphi^{\mathrm{D}}_\Gamma\partial_t d^{\mathrm{D}}_\Gamma \end{aligned} \tag{61a}$$

$$\begin{aligned} \mathcal{D}_{\Gamma,\text{el-ch}} =& -\sum_\alpha \boldsymbol{j}_{\Gamma,\alpha}\cdot\left[\boldsymbol{\nabla}_\Gamma\mu'_{\Gamma,\alpha}\right] + \boldsymbol{i}_{\Gamma,\mathrm{el}}\cdot\boldsymbol{e}_\Gamma - \sum_\alpha r_{\Gamma,\alpha}\mu_{\Gamma,\alpha}\\ &- i^{\mathrm{C}}_{\Gamma,\mathrm{el}}\varphi^{\mathrm{C}}_\Gamma - i^{\mathrm{D}}_{\Gamma,\mathrm{el}}\varphi^{\mathrm{D}}_\Gamma - \sum_\alpha j^{\mathrm{C}}_{\Gamma,\alpha}\mu^{\mathrm{C}}_{\Gamma,\alpha} - \sum_\alpha j^{\mathrm{D}}_{\Gamma,\alpha}\mu^{\mathrm{D}}_{\Gamma,\alpha} \end{aligned} \tag{61b}$$

$$\mathcal{D}_{\Gamma,\mathrm{th}} = -\frac{1}{\theta_\Gamma}\boldsymbol{q}^{\mathrm{eff}}_\Gamma\cdot\boldsymbol{\nabla}_\Gamma\theta_\Gamma + \frac{1}{\theta_\Gamma}q^{\mathrm{eff,C}}_\Gamma\theta^{\mathrm{C}}_\Gamma + \frac{1}{\theta_\Gamma}q^{\mathrm{eff,D}}_\Gamma\theta^{\mathrm{D}}_\Gamma \tag{61c}$$

Here, we introduced the following kinematic quantities that are energetically conjugate to the kinetic quantities introduced in (41):

$$\begin{aligned}
&\boldsymbol{u}_\Gamma^{\mathrm{C}} := [\![\boldsymbol{u}]\!], && \boldsymbol{u}_\Gamma^{\mathrm{D}} := \{\!\{\boldsymbol{u}\}\!\} - \boldsymbol{u}_\Gamma, \\
&\varphi_\Gamma^{\mathrm{C}} := [\![\varphi]\!], && \varphi_\Gamma^{\mathrm{D}} := \{\!\{\varphi\}\!\} - \varphi_\Gamma, \\
&\mu_{\Gamma,\alpha}^{\mathrm{C}} := [\![\mu'_\alpha]\!] - [\![z'_\alpha]\!]\varphi_\Gamma, && \mu_{\Gamma,\alpha}^{\mathrm{D}} := \{\!\{\mu'_\alpha\}\!\} - \mu'_{\Gamma,\alpha} - [\{\!\{z'_\alpha\}\!\} - z'_{\Gamma,\alpha}]\varphi_\Gamma, \\
&\theta_\Gamma^{\mathrm{C}} := [\theta_\Gamma]^2[\![\theta^{-1}]\!], && \theta_\Gamma^{\mathrm{D}} := [\theta_\Gamma]^2\left[\{\!\{\theta^{-1}\}\!\} - [\theta_\Gamma]^{-1}\right].
\end{aligned} \tag{62}$$

In standard fashion, we adopt a strong version of the dissipation inequality for the volume as well as for the interface:

- Clausius–Planck Inequality (CPI): $\mathcal{D}_{\mathrm{en}} \geq 0$, $\mathcal{D}_{\Gamma,\mathrm{en}} \geq 0$,
- Fick-Ohm Inequality: $\mathcal{D}_{\mathrm{el-ch}} \geq 0$, $\mathcal{D}_{\Gamma,\mathrm{el\text{-}ch}} \geq 0$,
- Fourier Inequality (FI): $\mathcal{D}_{\mathrm{th}} \geq 0$, $\mathcal{D}_{\Gamma,\mathrm{th}} \geq 0$

which are henceforth assumed to be the valid constraints for the formulation of explicit constitutive models.

4.2. Entropy inequality in terms of free energy density

We first note that the natural and simplest parametrization of the volume-specific internal energy for the bulk material is $e(\epsilon, s, \boldsymbol{d}, \underline{c}, \underline{z})$, where $\underline{z}$ represents a set of internal variables. The next step is to introduce the volume-specific free energy density $\psi(\epsilon, \theta, \boldsymbol{e}, \underline{c}, \underline{z})$ by replacing s with θ and $\boldsymbol{d}$ with $\boldsymbol{e}$ via the double Legendre transformation

$$\psi(\epsilon, \theta, \boldsymbol{e}, \underline{c}, \underline{z}) = \operatorname*{stat}_{\hat{s},\hat{\boldsymbol{d}}} \left[-\theta\hat{s} - \boldsymbol{e}\cdot\hat{\boldsymbol{d}} + e(\epsilon, \hat{s}, \hat{\boldsymbol{d}}, \underline{c}, \underline{z})\right]. \tag{63}$$

Upon evaluating the stationarity in (63), we obtain the corresponding conditions $\theta - \partial_s e = 0$ and $\boldsymbol{e} - \partial_{\boldsymbol{d}} e = \boldsymbol{0}$, from which it is assumed that it is possible to solve for $s, \boldsymbol{d}$ in terms of $\epsilon, \theta, \boldsymbol{e}, \underline{c}, \underline{z}$. Upon inserting into (59a), we may rephrase $\mathcal{D}_{\mathrm{en}}$ as

$$\mathcal{D}_{\mathrm{en}} = -\partial_t\psi + \boldsymbol{\sigma} : \partial_t\boldsymbol{\epsilon} - s\partial_t\theta - \boldsymbol{d}\cdot\partial_t\boldsymbol{e} + \sum_\alpha \mu_\alpha\partial_t c_\alpha. \tag{64}$$

In analogy with the modeling of the volume behavior, the natural parametrization of the surface-specific internal energy for the interface is $e_\Gamma(\boldsymbol{\epsilon}_\Gamma, s_\Gamma, \boldsymbol{d}_\Gamma, \underline{c}_\Gamma, \boldsymbol{u}_\Gamma^{\mathrm{C}}, \boldsymbol{u}_\Gamma^{\mathrm{D}}, d_\Gamma^{\mathrm{C}}, d_\Gamma^{\mathrm{D}}, \underline{z}_\Gamma)$. We thus introduce the interfacial free energy density $\psi_\Gamma(\boldsymbol{\epsilon}_\Gamma, \theta_\Gamma, \boldsymbol{e}_\Gamma, \underline{c}_\Gamma, \boldsymbol{u}_\Gamma^{\mathrm{C}}, \boldsymbol{u}_\Gamma^{\mathrm{D}}, \varphi_\Gamma^{\mathrm{C}}, \varphi_\Gamma^{\mathrm{D}}, \underline{z}_\Gamma)$ via the following Legendre transformation

$$\begin{aligned}
&\psi_\Gamma(\boldsymbol{\epsilon}_\Gamma, \theta_\Gamma, \boldsymbol{e}_\Gamma, \underline{c}_\Gamma, \boldsymbol{u}_\Gamma^{\mathrm{C}}, \boldsymbol{u}_\Gamma^{\mathrm{D}}, \varphi_\Gamma^{\mathrm{C}}, \varphi_\Gamma^{\mathrm{D}}, \underline{z}_\Gamma) = \\
&\operatorname*{stat}_{\hat{s}_\Gamma,\hat{\boldsymbol{d}}_\Gamma,\hat{d}_\Gamma^{\mathrm{C}},\hat{d}_\Gamma^{\mathrm{D}}} \left[-\theta_\Gamma\hat{s_\Gamma} - \boldsymbol{e}_\Gamma\cdot\hat{\boldsymbol{d}}_\Gamma + \varphi_\Gamma^{\mathrm{C}}\hat{d}_\Gamma^{\mathrm{C}} + \varphi_\Gamma^{\mathrm{D}}\hat{d}_\Gamma^{\mathrm{D}} + e_\Gamma(\boldsymbol{\epsilon}_\Gamma, \hat{s}_\Gamma, \hat{\boldsymbol{d}}_\Gamma, \underline{c}_\Gamma, \boldsymbol{u}_\Gamma^{\mathrm{C}}, \boldsymbol{u}_\Gamma^{\mathrm{D}}, \hat{d}_\Gamma^{\mathrm{C}}, \hat{d}_\Gamma^{\mathrm{D}}, \underline{z}_\Gamma)\right].
\end{aligned} \tag{65}$$

Upon evaluating the stationarity in (65), we rephrase $\mathcal{D}_{\Gamma,\mathrm{en}}$ as

$$\begin{aligned}
\mathcal{D}_{\Gamma,\mathrm{en}} = &-\partial_t\psi_\Gamma + \boldsymbol{\sigma}_\Gamma : \partial_t\boldsymbol{\epsilon}_\Gamma - s_\Gamma\partial_t\theta_\Gamma \\
&+ \sum_\alpha \mu_{\Gamma,\alpha}\partial_t c_{\Gamma,\alpha} - \boldsymbol{d}_\Gamma\cdot\partial_t\boldsymbol{e}_\Gamma + \boldsymbol{t}_\Gamma^{\mathrm{C}}\cdot\partial_t\boldsymbol{u}_\Gamma^{\mathrm{C}} + \boldsymbol{t}_\Gamma^{\mathrm{D}}\cdot\partial_t\boldsymbol{u}_\Gamma^{\mathrm{D}} + d_\Gamma^{\mathrm{C}}\partial_t\varphi_\Gamma^{\mathrm{C}} + d_\Gamma^{\mathrm{D}}\partial_t\varphi_\Gamma^{\mathrm{D}}.
\end{aligned} \tag{66}$$

Next, we introduce some simplifying restrictions that affect $\mathcal{D}_{\Gamma,\mathrm{th}}$. Firstly, for the bulk material, upon observing the parametrization $\psi(\epsilon, \theta, \boldsymbol{e}, \underline{c}, \underline{z})$, we note that the CPI can be rewritten as

$$\begin{aligned}
\mathcal{D}_{\mathrm{en}} = &\left[\boldsymbol{\sigma} - \partial_{\boldsymbol{\epsilon}}\psi\right] : \partial_t\boldsymbol{\epsilon} + \left[-s - \partial_\theta\psi\right]\partial_t\theta + \left[-\boldsymbol{d} - \partial_{\boldsymbol{e}}\psi\right]\cdot\partial_t\boldsymbol{e} \\
&+ \sum_\alpha \left[\mu_\alpha - \partial_{c_\alpha}\psi\right]\partial_t c_\alpha + \left[-\partial_{\underline{z}}\psi\right] \star \partial_t\underline{z} \geq 0.
\end{aligned} \tag{67}$$

Now, since our focus is on interface behavior in this paper, it will be assumed that $\boldsymbol{\sigma}, s, \boldsymbol{d}, \underline{\mu}$ are of purely energetic character.[6] In other words,

$$\boldsymbol{\sigma} = \partial_{\boldsymbol{\epsilon}}\psi, \quad s = -\partial_\theta\psi, \quad \boldsymbol{d} = -\partial_{\boldsymbol{e}}\psi, \quad \mu_\alpha = \partial_{c_\alpha}\psi, \quad \alpha = 1, 2, \ldots, M, \tag{68}$$

together with the condition

$$\mathcal{D}_{\mathrm{en}} = -\underline{Z} \star \partial_t\underline{z} \geq 0, \quad \text{with} \quad \underline{Z} := \partial_{\underline{z}}\psi, \tag{69}$$

where we (formally) introduced the energetic "stress" $\underline{Z}$ that is energetically conjugated to $\underline{z}$.

Next, as to the CPI for the interface, it is rewritten similarly as follows:

$$\begin{aligned}
\mathcal{D}_{\Gamma,\mathrm{en}} = &\left[\boldsymbol{\sigma}_\Gamma - \partial_{\boldsymbol{e}_\Gamma}\psi_\Gamma\right] : \partial_t\boldsymbol{\epsilon}_\Gamma + \left[-s_\Gamma - \partial_{\theta_\Gamma}\psi_\Gamma\right]\partial_t\theta_\Gamma \\
&+ \sum_\alpha \left[\mu_{\Gamma,\alpha} - \partial_{c_{\Gamma,\alpha}}\psi_\Gamma\right]\partial_t c_{\Gamma,\alpha} + \left[-\boldsymbol{d}_\Gamma - \partial_{\boldsymbol{e}_\Gamma}\psi_\Gamma\right]\partial_t\boldsymbol{e}_\Gamma \\
&+ \left[\boldsymbol{t}_\Gamma^{\mathrm{C}} - \partial_{\boldsymbol{u}_\Gamma^{\mathrm{C}}}\psi_\Gamma\right]\cdot\partial_t\boldsymbol{u}_\Gamma^{\mathrm{C}} + \left[\boldsymbol{t}_\Gamma^{\mathrm{D}} - \partial_{\boldsymbol{u}_\Gamma^{\mathrm{D}}}\psi_\Gamma\right]\cdot\partial_t\boldsymbol{u}_\Gamma^{\mathrm{D}} \\
&+ \left[d_\Gamma^{\mathrm{C}} - \partial_{\varphi_\Gamma^{\mathrm{C}}}\psi_\Gamma\right]\cdot\partial_t\varphi_\Gamma^{\mathrm{C}} + \left[d_\Gamma^{\mathrm{D}} - \partial_{\varphi_\Gamma^{\mathrm{D}}}\psi_\Gamma\right]\cdot\partial_t\varphi_\Gamma^{\mathrm{D}} \\
&+ \left[-\partial_{\underline{z}_\Gamma}\psi_\Gamma\right] \star \partial_t\underline{z}_\Gamma \geq 0.
\end{aligned} \tag{70}$$

Like for the bulk material, we assume that $\boldsymbol{\sigma}_\Gamma, s_\Gamma, \boldsymbol{d}_\Gamma, \underline{\mu}_\Gamma, \boldsymbol{t}_\Gamma^{\mathrm{C}}, \boldsymbol{t}_\Gamma^{\mathrm{D}}, d_\Gamma^{\mathrm{C}}, d_\Gamma^{\mathrm{D}}$ are purely energetic quantities. In standard fashion, the generic constitutive relations then become

$$\begin{aligned}
&\boldsymbol{\sigma}_\Gamma = \partial_{\boldsymbol{e}_\Gamma}\psi_\Gamma,\ s_\Gamma = -\partial_{\theta_\Gamma}\psi_\Gamma,\ \boldsymbol{d}_\Gamma = -\partial_{\boldsymbol{e}_\Gamma}\psi_\Gamma,\ \mu_{\Gamma,\alpha} = \partial_{c_{\Gamma,\alpha}}\psi_\Gamma, \quad \alpha = 1, 2, \ldots, M \\
&\boldsymbol{t}_\Gamma^{\mathrm{C}} = \partial_{\boldsymbol{u}_\Gamma^{\mathrm{C}}}\psi_\Gamma,\ \boldsymbol{t}_\Gamma^{\mathrm{D}} = \partial_{\boldsymbol{u}_\Gamma^{\mathrm{D}}}\psi_\Gamma,\ d_\Gamma^{\mathrm{C}} = \partial_{\varphi_\Gamma^{\mathrm{C}}}\psi_\Gamma,\ d_\Gamma^{\mathrm{D}} = \partial_{\varphi_\Gamma^{\mathrm{D}}}\psi_\Gamma,
\end{aligned} \tag{71}$$

together with the condition

$$\mathcal{D}_{\Gamma,\mathrm{en}} = -\underline{Z}_\Gamma \star \partial_t\underline{z}_\Gamma \geq 0, \quad \text{with} \quad \underline{Z}_\Gamma := \partial_{\underline{z}_\Gamma}\psi_\Gamma. \tag{72}$$

Finally, we note that, in general, all energetic "fluxes" depend on all the independent thermodynamic variables $\boldsymbol{\epsilon}_\Gamma, \theta_\Gamma, \underline{c}_\Gamma, \boldsymbol{u}_\Gamma^{\mathrm{C}}, \boldsymbol{u}_\Gamma^{\mathrm{D}}, \underline{z}_\Gamma$.

4.3. Energy equation revisited

The energy balance in (54) is conveniently reformulated in terms of the free energy density ψ (rather than the internal energy e) using the Legendre transformation (63). We then obtain

$$\theta\partial_t s + \boldsymbol{q}^{\mathrm{eff}}\cdot\boldsymbol{\nabla} - D^{\mathrm{eff}} = 0 \quad \text{in } \Omega^- \cup \Omega^+, \tag{73}$$

where we introduced the "effective" dissipation $\mathcal{D}^{\mathrm{eff}}$, defined as

$$\mathcal{D}^{\mathrm{eff}} = -\sum_\alpha \boldsymbol{j}_\alpha\cdot[\boldsymbol{\nabla}\mu'_\alpha] - \sum_\alpha r_\alpha\mu_\alpha + \boldsymbol{i}_{\mathrm{el}}\cdot\boldsymbol{e} + \mathcal{D}_{\mathrm{en}}. \tag{74}$$

Similarly, the energy Eq. (55) for the interface can be rewritten as

$$\theta_\Gamma\partial_t s_\Gamma + \boldsymbol{q}_\Gamma^{\mathrm{eff}}\cdot\boldsymbol{\nabla}_\Gamma + q_\Gamma^{\mathrm{eff,D}} - \mathcal{D}_\Gamma^{\mathrm{eff}} = 0 \quad \text{on } \Gamma, \tag{75}$$

where we introduced the "effective" dissipation $\mathcal{D}_\Gamma^{\mathrm{eff}}$, defined as:

$$\begin{aligned}
\mathcal{D}_\Gamma^{\mathrm{eff}} = &-\sum_\alpha \boldsymbol{j}_{\Gamma,\alpha}\cdot[\boldsymbol{\nabla}_\Gamma\mu'_{\Gamma,\alpha}] - \sum_\alpha r_{\Gamma,\alpha}\mu_{\Gamma,\alpha} + \boldsymbol{i}_{\Gamma,\mathrm{el}}\cdot\boldsymbol{e}_\Gamma - i_{\Gamma,\mathrm{el}}^{\mathrm{C}}\varphi_\Gamma^{\mathrm{C}} - i_{\Gamma,\mathrm{el}}^{\mathrm{D}}\varphi_\Gamma^{\mathrm{D}} \\
&- \sum_\alpha j_{\Gamma,\alpha}^{\mathrm{C}}\mu_{\Gamma,\alpha}^{\mathrm{C}} - \sum_\alpha j_{\Gamma,\alpha}^{\mathrm{D}}\mu_{\Gamma,\alpha}^{\mathrm{D}} + \mathcal{D}_{\Gamma,\mathrm{en}}.
\end{aligned} \tag{76}$$

We may note that the source terms $\mathcal{D}^{\mathrm{eff}}$ and $\mathcal{D}_\Gamma^{\mathrm{eff}}$ include contributions from the so-called Joule effect due to electronic current in the volume and interface, respectively.

5. Discussion and assessment of constraints

We now assess the consequences of the thermodynamic constraints derived in Section 4 for the actual modeling of the volume and the

[6] It would, obviously, be possible to relax this assumption and adopt an additive decomposition into energetic and dissipative parts, e.g. $\boldsymbol{\sigma} = \boldsymbol{\sigma}^\sharp + \boldsymbol{\sigma}^\flat$.

interface. The constitutive functions are first sorted into those of energetic and those of dissipative character, whereby a few representative couplings between the mechanical, chemical and electric fields are highlighted. Next, the weak forms of the governing equations are established to reveal most clearly which of the volume and interface variables call for a constitutive relation.

5.1. Preliminaries

The character of the constitutive functions assigned to "flux variables" is either energetic or dissipative, as given by the dissipation inequality:

- Bulk material variables
  - Energetic: $\boldsymbol{\sigma}, s, \boldsymbol{d}, \mu_\alpha, \underline{Z}$
  - Dissipative: $\boldsymbol{j}_\alpha, r_\alpha, \boldsymbol{i}_{\text{el}}, \boldsymbol{q}^{\text{eff}}$
- Interface variables
  - Energetic: $\boldsymbol{\sigma}_\Gamma, s_\Gamma, \boldsymbol{d}_\Gamma, \mu_{\Gamma,\alpha}, \boldsymbol{t}_\Gamma^{\text{C}}, \boldsymbol{t}_\Gamma^{\text{D}}, d_\Gamma^{\text{C}}, d_\Gamma^{\text{D}}, \underline{Z}_\Gamma$
  - Dissipative: $\boldsymbol{j}_{\Gamma,\alpha}, j_{\Gamma,\alpha}^{\text{C}}, j_{\Gamma,\alpha}^{\text{D}}, r_{\Gamma,\alpha}, \quad \boldsymbol{i}_{\Gamma,\text{el}}, i_{\Gamma,\text{el}}^{\text{C}}, i_{\Gamma,\text{el}}^{\text{D}}, \boldsymbol{q}_\Gamma^{\text{eff}}, q_\Gamma^{\text{eff,C}}, q_\Gamma^{\text{eff,D}}$

Via the proper choice of free energy densities for the volume and the interface, ψ and ψ_Γ, it is obviously possible to include a rich variety of couplings between the mechanical, chemical and electric fields. A few prominent (and classical) examples of such couplings are (i) chemo-mechanical coupling (see the application to a half-cell in Section 6) due to intercalation of the active ionic species (Li-ions in the electrode lattice), corresponding to expansion at lithiation, conversely, the chemical potential is affected by mechanical strain (or stress) giving rise to stress-assisted diffusion and migration via the mobility, (ii) electro-mechanical couplings, whereby the electric field affects the stress; conversely, dielectric permittivity values are affected by the mechanical stress. An example of a non-standard effect is electrochemical couplings, whereby the electric field affects the chemical potential and, conversely, the dielectric flux is directly influenced by the ion concentration.

5.2. Weak forms

Now, the role of the constitutive variables (energetic and dissipative) is best understood from how they appear in the pertinent weak forms for the volume and interface, respectively. These forms are introduced next, where we introduced solution spaces $\mathbb{U}$, etc. and the corresponding test spaces $\mathbb{U}^0$ etc. with the proper smoothness requirements. Typically, the solution spaces satisfy non-homogeneous Dirichlet boundary conditions, whereas functions in the corresponding test spaces take zero value on the Dirichlet boundaries.

The weak format of equilibrium in (8) and (9) for $\Omega^+ \cup \Omega^-$ and Γ, respectively, read:

$$\int_{\Omega^+\cup\Omega^-} [\delta\boldsymbol{u} \otimes \boldsymbol{\nabla}] : \boldsymbol{\sigma}(\bullet)\, \mathrm{d}V + \int_\Gamma [\![\delta\boldsymbol{u}]\!] \cdot \boldsymbol{t}_\Gamma^{\text{C}}(\bullet)\, \mathrm{d}S + \int_\Gamma \{\!\{\delta\boldsymbol{u}\}\!\} \cdot \boldsymbol{t}_\Gamma^{\text{D}}(\bullet)\, \mathrm{d}S = 0 \qquad \forall \delta\boldsymbol{u} \in \mathbb{U}^0, \tag{77a}$$

$$\int_\Gamma [\delta\boldsymbol{u}_\Gamma \otimes \boldsymbol{\nabla}_\Gamma] : \boldsymbol{\sigma}_\Gamma(\bullet)\, \mathrm{d}S - \int_\Gamma \delta\boldsymbol{u}_\Gamma \cdot \boldsymbol{t}_\Gamma^{\text{D}}(\bullet)\, \mathrm{d}S = 0 \qquad \forall \delta\boldsymbol{u}_\Gamma \in \mathbb{U}_\Gamma^0. \tag{77b}$$

The weak format of mass balance in (11) and (12) for $\Omega^+ \cup \Omega^-$ and Γ, respectively, read:

$$\int_{\Omega^+\cup\Omega^-} \delta\mu_\alpha[\partial_t c_\alpha - r_\alpha]\, \mathrm{d}V - \int_{\Omega^+\cup\Omega^-} [\boldsymbol{\nabla}\delta\mu_\alpha] \cdot \boldsymbol{j}_\alpha(\bullet)\, \mathrm{d}V - \int_\Gamma [\![\delta\mu_\alpha]\!] j_{\Gamma,\alpha}^{\text{C}}(\bullet)\, \mathrm{d}S - \int_\Gamma \{\!\{\delta\mu_\alpha\}\!\} j_{\Gamma,\alpha}^{\text{D}}(\bullet)\, \mathrm{d}S = 0 \qquad \forall \delta\mu_\alpha \in \mathbb{M}_\alpha^0,\ \alpha = 1, 2, \dots, \tag{78a}$$

$$\int_\Gamma \delta\mu_{\Gamma,\alpha}[\partial_t c_{\Gamma,\alpha} - r_{\Gamma,\alpha}]\, \mathrm{d}S - \int_\Gamma [\boldsymbol{\nabla}_\Gamma \delta\mu_{\Gamma,\alpha}] \cdot \boldsymbol{j}_{\Gamma,\alpha}(\bullet)\, \mathrm{d}S + \int_\Gamma \delta\mu_{\Gamma,\alpha} j_{\Gamma,\alpha}^{\text{D}}(\bullet)\, \mathrm{d}S = 0 \qquad \forall \delta\mu_{\Gamma,\alpha} \in \mathbb{M}_{\Gamma,\alpha}^0,\ \alpha = 1, 2, \dots. \tag{78b}$$

The weak format of the specific format of Ampere's law for an electrochemical system, as given in (29) and (30) for $\Omega^+ \cup \Omega^-$ and Γ, respectively, reads:

$$\begin{aligned}
&- \int_{\Omega^-\cup\Omega^+} \delta\varphi \sum_\alpha z'_\alpha [\partial_t c_\alpha - r_\alpha]\, \mathrm{d}V \\
&- \int_{\Omega^-\cup\Omega^+} [\boldsymbol{\nabla}\delta\varphi] \cdot [\partial_t \boldsymbol{d}(\bullet) + \boldsymbol{i}_{\text{el}}(\bullet)]\, \mathrm{d}V \\
&- \int_\Gamma [\![\delta\varphi]\!] [\partial_t d_\Gamma^{\text{C}}(\bullet) + i_{\Gamma,\text{el}}^{\text{C}}(\bullet)]\, \mathrm{d}S \\
&- \int_\Gamma \{\!\{\delta\varphi\}\!\} [\partial_t d_\Gamma^{\text{D}}(\bullet) + i_{\Gamma,\text{el}}^{\text{D}}(\bullet)]\, \mathrm{d}S = 0 \qquad \forall \delta\varphi \in \mathbb{F}^0,
\end{aligned} \tag{79a}$$

$$\begin{aligned}
&- \int_\Gamma \delta\varphi_\Gamma \sum_\alpha z'_{\Gamma,\alpha} [\partial_t c_{\Gamma,\alpha} - r_{\Gamma,\alpha}]\, \mathrm{d}S \\
&- \int_\Gamma [\boldsymbol{\nabla}_\Gamma \delta\varphi_\Gamma] \cdot [\partial_t \boldsymbol{d}_\Gamma(\bullet) + \boldsymbol{i}_{\Gamma,\text{el}}(\bullet)]\, \mathrm{d}S \\
&+ \int_\Gamma \delta\varphi_\Gamma [\partial_t d_\Gamma^{\text{D}}(\bullet) + i_{\Gamma,\text{el}}^{\text{D}}(\bullet)]\, \mathrm{d}S \\
&+ \int_\Gamma \delta\varphi_\Gamma \sum_\alpha [[\![z'_\alpha]\!] j_{\Gamma,\alpha}^{\text{C}}(\bullet) + \{\!\{\Delta z'_\alpha\}\!\} j_{\Gamma,\alpha}^{\text{D}}(\bullet)]\, \mathrm{d}S = 0 \qquad \forall \delta\varphi_\Gamma \in \mathbb{F}_\Gamma^0.
\end{aligned} \tag{79b}$$

Finally, the weak format of energy balance in (73) and (75) for $\Omega^+ \cup \Omega^-$ and Γ, respectively, read:

$$\int_{\Omega^-\cup\Omega^+} \delta\theta[\theta\partial_t s(\bullet) - \mathcal{D}^{\text{eff}}]\, \mathrm{d}V - \int_{\Omega^-\cup\Omega^+} [\boldsymbol{\nabla}\delta\theta] \cdot \boldsymbol{q}^{\text{eff}}(\bullet)\, \mathrm{d}V - \int_\Gamma [\![\delta\theta]\!] q_\Gamma^{\text{eff,C}}(\bullet)\, \mathrm{d}S - \int_\Gamma \{\!\{\delta\theta\}\!\} q_\Gamma^{\text{eff,D}}(\bullet)\, \mathrm{d}S = 0 \qquad \forall \delta\theta \in \mathbb{T}^0, \tag{80a}$$

$$\int_\Gamma \delta\theta_\Gamma[\theta_\Gamma \partial_t s_\Gamma(\bullet) - \mathcal{D}_\Gamma^{\text{eff}}]\, \mathrm{d}S - \int_\Gamma [\boldsymbol{\nabla}_\Gamma \delta\theta_\Gamma] \cdot \boldsymbol{q}_\Gamma^{\text{eff}}(\bullet)\, \mathrm{d}S + \int_\Gamma \delta\theta_\Gamma q_\Gamma^{\text{eff,D}}(\bullet)\, \mathrm{d}S = 0 \qquad \forall \delta\theta_\Gamma \in \mathbb{T}_\Gamma^0. \tag{80b}$$

5.3. Constitutive restrictions in the light of weak forms and thermodynamics

Fig. 7 shows the classification of models within ECTM with respect to kinematical and kinetic (non)coherence. In addition, it is noted that the mechanical and electric "fluxes" ($\boldsymbol{\sigma}$ and $\boldsymbol{d}$, respectively) are taken as energetic (since the dissipative parts are ignored for the sake of simplicity), whereas thermal and chemical fluxes ($\boldsymbol{q}^{\text{eff}}$ and $\boldsymbol{j}_\alpha$, respectively) are dissipative. It is illuminating to consider the special subclasses (in the left column of Fig. 7) in the light of the weak forms (77) to (80), that are introduced below:

- Mechanical problem
  - "Membrane" interface models: The special situation of continuous displacement, $[\![\boldsymbol{u}]\!] = \boldsymbol{0}$, i.e. $[\![\delta\boldsymbol{u}]\!] = \boldsymbol{0}$ in (77a), infers that a constitutive relation is required only for $\boldsymbol{t}_\Gamma^{\text{D}}$ in (77a) and (77b) (since $\boldsymbol{t}_\Gamma^{\text{C}}$ does not appear).
  - "Cohesive" interface models: The situation that $[\![\boldsymbol{u}]\!] \neq \boldsymbol{0}$, whereas the normal component of $\boldsymbol{\sigma}$ is continuous, i.e. $\boldsymbol{t}_\Gamma^{\text{D}} = \boldsymbol{0}$ in (77a) and (77b). Consequently, a constitutive relation is required only for $\boldsymbol{t}_\Gamma^{\text{C}}$ in (77a).
- Thermal problem
  - "Membrane" interface models: The special situation of continuous temperature, $[\![\theta]\!] = 0$, i.e. $[\![\delta\theta]\!] = 0$ in (80a), infers that a constitutive relation is required only for $q_\Gamma^{\text{eff,D}}$ in (80a) and (80b) (since $q_\Gamma^{\text{eff,C}}$ does not appear).

ECTM	mechanical	thermal	chemical	electrical
perfect interface model	$[\![\boldsymbol{u}]\!] = \boldsymbol{0}$ $[\![\boldsymbol{\sigma}]\!] \cdot \boldsymbol{n}_\Gamma = \boldsymbol{0}$	$[\![\theta]\!] = 0$ $[\![\boldsymbol{q}^{\text{eff}}]\!] \cdot \boldsymbol{n}_\Gamma = 0$	$[\![\mu_\alpha]\!] = 0$ $[\![\boldsymbol{j}_\alpha]\!] \cdot \boldsymbol{n}_\Gamma = 0$	$[\![\varphi]\!] = 0$ $[\![\boldsymbol{d}]\!] \cdot \boldsymbol{n}_\Gamma = 0$ $[\![\boldsymbol{i}_{\text{el}}]\!] \cdot \boldsymbol{n}_\Gamma = 0$
membrane interface model	$[\![\boldsymbol{u}]\!] = \boldsymbol{0}$ $[\![\boldsymbol{\sigma}]\!] \cdot \boldsymbol{n}_\Gamma \neq \boldsymbol{0}$	$[\![\theta]\!] = 0$ $[\![\boldsymbol{q}^{\text{eff}}]\!] \cdot \boldsymbol{n}_\Gamma \neq 0$	$[\![\mu_\alpha]\!] = 0$ $[\![\boldsymbol{j}_\alpha]\!] \cdot \boldsymbol{n}_\Gamma \neq 0$	$[\![\varphi]\!] = 0$ $[\![\boldsymbol{d}]\!] \cdot \boldsymbol{n}_\Gamma \neq 0$ $[\![\boldsymbol{i}_{\text{el}}]\!] \cdot \boldsymbol{n}_\Gamma \neq 0$
cohesive interface model	$[\![\boldsymbol{u}]\!] \neq \boldsymbol{0}$ $[\![\boldsymbol{\sigma}]\!] \cdot \boldsymbol{n}_\Gamma = \boldsymbol{0}$	$[\![\theta]\!] \neq 0$ $[\![\boldsymbol{q}^{\text{eff}}]\!] \cdot \boldsymbol{n}_\Gamma = 0$	$[\![\mu]\!] \neq 0$ $[\![\boldsymbol{j}_\alpha]\!] \cdot \boldsymbol{n}_\Gamma = 0$	$[\![\varphi]\!] \neq 0$ $[\![\boldsymbol{d}]\!] \cdot \boldsymbol{n}_\Gamma = 0$ $[\![\boldsymbol{i}_{\text{el}}]\!] \cdot \boldsymbol{n}_\Gamma = 0$
canonical interface model	$[\![\boldsymbol{u}]\!] \neq \boldsymbol{0}$ $[\![\boldsymbol{\sigma}]\!] \cdot \boldsymbol{n}_\Gamma \neq \boldsymbol{0}$	$[\![\theta]\!] \neq 0$ $[\![\boldsymbol{q}^{\text{eff}}]\!] \cdot \boldsymbol{n}_\Gamma \neq 0$	$[\![\mu]\!] \neq 0$ $[\![\boldsymbol{j}_\alpha]\!] \cdot \boldsymbol{n}_\Gamma \neq 0$	$[\![\varphi]\!] \neq 0$ $[\![\boldsymbol{d}]\!] \cdot \boldsymbol{n}_\Gamma \neq 0$ $[\![\boldsymbol{i}_{\text{el}}]\!] \cdot \boldsymbol{n}_\Gamma \neq 0$

Fig. 7. Classification of interface models in ECTM systems. The perfect interface model enforces continuity of all generalized kinematic and kinetic fields, whereas the imperfect interface models allow for discontinuity of one or more fields.
Note: The kinematic condition for the chemical field comprises diffusion-migration. In the special case of pure chemical action, the kinematic quantity is simplified to $[\![\mu_\alpha]\!]$.

  - "Cohesive" interface models: The situation that $[\![\theta]\!] \neq 0$, whereas the normal component of $\boldsymbol{q}^{\text{eff}}$ is continuous, i.e. $q_\Gamma^{\text{eff,D}} = 0$ in (80a) and (80b). Consequently, a constitutive relation is required only for $q_\Gamma^{\text{eff,C}}$ in (80a).

- Chemical problem
  - "Membrane" interface models: The special situation of continuous chemical potential, $[\![\mu_\alpha]\!] = 0$, i.e. $[\![\delta\mu_\alpha]\!] = 0$ in (78a), infers that a constitutive relation is required only for $j_{\Gamma,\alpha}^{\text{D}}$ in (78a) and (78b). In addition, since both $j_{\Gamma,\alpha}^{\text{C}}$ and $j_{\Gamma,\alpha}^{\text{D}}$ appear in (79b), a constitutive relation is still required for $j_{\Gamma,\alpha}^{\text{C}}$. It is noted that this relation must be established subject to the constraint $[\![\mu_\alpha]\!] = 0$, which can be accomplished via the use of Lagrange multipliers.
  - "Cohesive" interface models: The situation that $[\![\mu_\alpha]\!] \neq 0$, whereas the normal component of $\boldsymbol{j}_\alpha$ is continuous, i.e. $j_{\Gamma,\alpha}^{\text{D}} = 0$ in (78a), (78b) and (79b). Consequently, a constitutive relation is required for $j_{\Gamma,\alpha}^{\text{C}}$ in (78a) as well as in (79b).

- Electrical problem
  - "Membrane" interface models: The special situation of continuous electric potential, $[\![\varphi]\!] = 0$, i.e. $[\![\delta\varphi]\!] = 0$ in (79a), infers that constitutive relations are required only for d_Γ^{D} and $i_{\Gamma,\text{el}}^{\text{D}}$ in (79a) and (79b).
  - "Cohesive" interface models: The situation that $[\![\varphi]\!] \neq 0$, whereas the normal components of $\boldsymbol{d}$ and $\boldsymbol{i}_{\text{el}}$ are continuous, i.e. $d_\Gamma^{\text{D}} = 0$ and $i_{\Gamma,\text{el}}^{\text{D}} = 0$ in (79a) and (79b). Consequently, constitutive relations are required for d_Γ^{C} and $i_{\Gamma,\text{el}}^{\text{C}}$ in (79a).

6. Special cases of the canonical modeling framework

The canonical framework established in the preceding sections is now specialized to three prototype ECTM systems, illustrated in Fig. 8 : an electrode (=electronic conductor), an electrolyte (=ionic conductor), and a halfcell wafering an SEI-layer. For each system, the model assumptions are stated, and the pertinent governing equations and the constitutive constraints emerging from the dissipation inequality are extracted. A prototype model is outlined, followed by the simplification obtained when the membrane action of the interface is ignored. In order to focus on the key properties and avoid unnecessary complexity, the coupling to mechanical stresses is ignored and isothermal conditions are assumed.

6.1. Electrode (=electronic conductor) of dissimilar material with (electronic) interfaces

6.1.1. Model assumptions

As the first special case of the canonical model framework, we consider the purely electric response of an electronic conductor, consisting of two parts with dissimilar material properties that are joined along the common interface, as shown schematically in Fig. 8(left). Here, we mention two examples of vastly different cases/scales: (Das et al., 2019) (tab-to-busbar joints in conventional batteries) and (Greenhalgh et al., 2025) (contacting carbon fibers in structural batteries). The canonical framework then collapses to Gauss' and Ampere's laws in the volume and on the interface. Despite its simplicity, this case suffices to expose the role of the interface potential φ_Γ and of the associated normal fluxes, both of which reappear in the more elaborate systems considered subsequently.

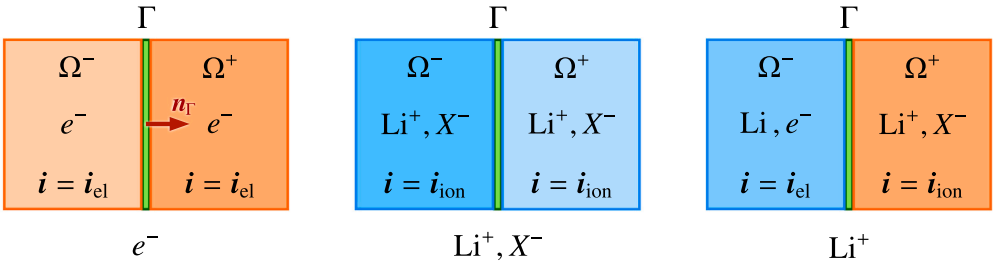


Fig. 8. Special cases of the canonical ECTM-system: (left) Electrode (=electronic conductor) of dissimilar material with (electronic) interface, (center) Electrolyte (=ionic conductor) of dissimilar material with (ionic) interface, (right) Halfcell (negative electrode and electrolyte) with electronic interface (SEI).

6.1.2. Governing equations: Gauss' and Ampere's laws

The local versions of Gauss' law read:

$$-\zeta_{\text{el}} + \boldsymbol{d}\cdot\boldsymbol{\nabla} = 0 \quad \text{in } \Omega^+\cup\Omega^-\,, \tag{81}$$

and

$$-\zeta_{\Gamma,\text{el}} + \boldsymbol{d}_\Gamma\cdot\boldsymbol{\nabla}_\Gamma + d_\Gamma^{\text{D}} = 0 \quad \text{on } \Gamma\,, \tag{82}$$

whereas the local versions of Ampere's law read:

$$[\partial_t\boldsymbol{d} + \boldsymbol{i}_{\text{el}}]\cdot\boldsymbol{\nabla} = 0 \quad \text{in } \Omega^+\cup\Omega^-\,, \tag{83}$$

and

$$[\partial_t\boldsymbol{d}_\Gamma + \boldsymbol{i}_{\Gamma,\text{el}}]\cdot\boldsymbol{\nabla}_\Gamma + \partial_t d_\Gamma^{\text{D}} + i_{\Gamma,\text{el}}^{\text{D}} = 0 \quad \text{on } \Gamma\,. \tag{84}$$

Like in the canonical situation, it appears that initial conditions are required on $(\boldsymbol{d}\cdot\boldsymbol{\nabla})(0)$, $(\boldsymbol{d}_\Gamma\cdot\boldsymbol{\nabla}_\Gamma)(0)$ and on $d_\Gamma^{\text{D}}(0)$. Without loss of generality, we shall choose homogeneous values.

Remark 7. From Gauss' law in (81) and (82), it is possible to compute the volume-specific and surface-specific free charge ζ_{el} and $\zeta_{\Gamma,\text{el}}$, respectively, as part of postprocessing. Moreover, we note that the initial conditions are equivalent to conditions on $\zeta_{\text{el}}(0)$ and $\zeta_{\Gamma,\text{el}}(0)$.

6.1.3. Constitutive constraints

As to the energetic quantities $\boldsymbol{d}$ in $\Omega^+\cup\Omega^-$ and $\boldsymbol{d}_\Gamma, d_\Gamma^{\text{C}}, d_\Gamma^{\text{D}}$ on Γ, we recall

$$\begin{aligned}&\boldsymbol{d} = -\partial_e\psi,\\ &\boldsymbol{d}_\Gamma = -\partial_{e_\Gamma}\psi_\Gamma,\ d_\Gamma^{\text{C}} = \partial_{\varphi_\Gamma^{\text{C}}}\psi_\Gamma,\ d_\Gamma^{\text{D}} = \partial_{\varphi_\Gamma^{\text{D}}}\psi_\Gamma\,.\end{aligned} \tag{85}$$

The Fick–Ohm Inequality, which was given in its generic format in (59b), (61b), now becomes

$$\mathcal{D}_{\text{el-ch}} := \boldsymbol{i}_{\text{el}}\cdot\boldsymbol{e} \geq 0\,, \tag{86}$$

and

$$\mathcal{D}_{\Gamma,\text{el-ch}} = \boldsymbol{i}_{\Gamma,\text{el}}\cdot\boldsymbol{e}_\Gamma - i_{\Gamma,\text{el}}^{\text{C}}\varphi_\Gamma^{\text{C}} - i_{\Gamma,\text{el}}^{\text{D}}\varphi_\Gamma^{\text{D}} \geq 0 \tag{87}$$

6.1.4. A prototype model — Selected remarks

Thermodynamically admissible constitutive relations for the energetic variables are derivable from (85). It is also straightforward to propose constitutive relations for the dissipative variables that comply with (86) and (87). Here, we shall only comment on the choice of out-of-plane current density quantities $i_{\Gamma,\text{el}}^{\text{C}}$ and $i_{\Gamma,\text{el}}^{\text{D}}$ in the light of the inequality (87). An obvious choice is

$$i_{\Gamma,\text{el}}^{\text{C}}(\varphi_\Gamma^{\text{C}}) = -K_\Gamma^{\text{C}}\varphi_\Gamma^{\text{C}}\,, \tag{88a}$$

$$i_{\Gamma,\text{el}}^{\text{D}}(\varphi_\Gamma^{\text{D}}) = -K_\Gamma^{\text{D}}\varphi_\Gamma^{\text{D}}\,, \tag{88b}$$

where the constitutive parameters $K_\Gamma^{\text{C}} \geq 0$ and $K_\Gamma^{\text{D}} \geq 0$ are the electronical interface conductivities, cf. Kaessmair et al. (2014).

6.1.5. Simplified interface model: Ignored membrane action

Consider the special situation that membrane action along Γ is ignored, i.e. $\boldsymbol{i}_{\Gamma,\text{el}} = \boldsymbol{0}$, $\boldsymbol{d}_\Gamma = \boldsymbol{0}$. Ampere's law for the interface then reduces to

$$\partial_t d_\Gamma^{\text{D}} + i_{\Gamma,\text{el}}^{\text{D}} = 0\,, \tag{89}$$

which represents an evolution problem in time for each spatial point $\boldsymbol{x}_\Gamma \in \Gamma$. Upon observing the constitutive relations $i_{\Gamma,\text{el}}^{\text{D}}(\varphi_\Gamma^{\text{D}})$ and $d_\Gamma^{\text{D}}(\varphi_\Gamma^{\text{C}}, \varphi_\Gamma^{\text{D}})$, we note that it is possible to solve for the interface variable φ_Γ from the problem (89) with values $[\![\varphi]\!], \{\!\{\varphi\}\!\}$ as the data.

6.2. Electrolyte (=ionic conductor) of dissimilar material with (ionic) interfaces

6.2.1. Model assumptions

As the second special case of the canonical model framework, we consider an electrolyte (separator) consisting of two parts with dissimilar material properties that are joined along the common interface, as shown in Fig. 8(center). This design is representative of solid and hybrid state batteries, e.g., Spencer Jolly et al. (2022), Hu et al. (2023).

Unlike the previous case, where the current is carried by electrons, the charge is transported by mobile ionic species. The interface, which now acts as a "soft" barrier for the ionic transport, thus calls for constitutive relations pertaining to the chemical potentials as well as to the electric potential. To be more specific as to the electrochemical activity, it is assumed that two ionic species are involved in the analysis: Charged Li^+ and X^- (anion) in $\Omega^+\cup\Omega^-$ as well as on Γ. No redox (or other reactions) are allowed/considered when ions cross the interface. The relevant governing equations for the investigated system are then conveniently obtained from the canonical modeling upon introducing the following identifications:

$$\begin{aligned}&\Omega^+\cup\Omega^- : \quad z'_{\text{Li}} = F \quad z'_{\text{X}} = -F \quad \boldsymbol{i}_{\text{el}} = \boldsymbol{0}, \zeta_{\text{el}} = 0\,,\\ &\Gamma : \quad z'_{\Gamma,\text{Li}} = F \quad z'_{\Gamma,\text{X}} = -F \quad \boldsymbol{i}_{\Gamma,\text{el}} = \boldsymbol{0}, \zeta_{\Gamma,\text{el}} = 0\,,\end{aligned} \tag{90}$$

where $z'_\alpha = Fz_\alpha$ is the specific charge (at a given location). As a consequence, we obtain $(\Delta z'_{\text{Li}})^\pm := (z'_{\text{Li}})^\pm - z'_{\Gamma,\text{Li}} = 0$ and $(\Delta z'_{\text{X}})^\pm := (z'_{\text{X}})^\pm - z'_{\Gamma,\text{X}} = 0$.

6.2.2. Governing equations: Mass balance and Gauss'–Ampere's law

The local mass balance of ions reads:

$$\partial_t c_\alpha + \boldsymbol{j}_\alpha\cdot\boldsymbol{\nabla} = 0\,, \quad \alpha = \text{Li,X}\,, \quad \text{in } \Omega^-\cup\Omega^+\,, \tag{91}$$

and

$$\partial_t c_{\Gamma,\alpha} + \boldsymbol{j}_{\Gamma,\alpha}\cdot\boldsymbol{\nabla}_\Gamma + j_{\Gamma,\alpha}^{\text{D}} = 0 \quad \alpha = \text{Li,X}\,, \quad \text{on } \Gamma\,. \tag{92}$$

Gauss'–Ampere's law reads (valence numbers: $z_{\text{Li}} = +1$, $z_{\text{X}} = -1$.):

$$\boldsymbol{d}\cdot\boldsymbol{\nabla} - F\left[c_{\text{Li}} - c_{\text{X}}\right] = 0 \quad \text{in } \Omega^-\cup\Omega^+\,, \tag{93}$$

and

$$\boldsymbol{d}_\Gamma\cdot\boldsymbol{\nabla}_\Gamma + d_\Gamma^{\text{D}} - F\left[c_{\Gamma,\text{Li}} - c_{\Gamma,\text{X}}\right] = 0 \quad \text{on } \Gamma\,. \tag{94}$$

Remark 8. Ampere's law for the volume and interface is simply identical to the time-differentiated expression in (93) and (94), respectively. □

Initial conditions are required for $c_\alpha(0)$, $c_{\Gamma,\alpha}(0)$ for $\alpha = \text{Li,X}$.

6.2.3. Constitutive constraints

As to the energetic quantities $\boldsymbol{d}, \mu_{\text{Li}}, \mu_{\text{X}}$ in $\Omega^+ \cup \Omega^-$ and $\boldsymbol{d}_\Gamma, d^{\text{C}}_\Gamma, d^{\text{D}}_\Gamma$ on Γ, we recall

$$\begin{aligned} &\boldsymbol{d} = -\partial_{\boldsymbol{e}}\psi,\ \mu_{\text{Li}} = \partial_{c_{\text{Li}}}\psi,\ \mu_{\text{X}} = \partial_{c_{\text{X}}}\psi, \\ &\boldsymbol{d}_\Gamma = -\partial_{\boldsymbol{e}_\Gamma}\psi_\Gamma,\ d^{\text{C}}_\Gamma = \partial_{\varphi^{\text{C}}_\Gamma}\psi_\Gamma,\ d^{\text{D}}_\Gamma = \partial_{\varphi^{\text{D}}_\Gamma}\psi_\Gamma\,. \end{aligned} \tag{95}$$

The Fick–Ohm inequality, which was given in its generic format in (59b), (61b), now becomes

$$\mathcal{D}_{\text{el-ch}} := -\sum_{\alpha=\text{Li,X}} \boldsymbol{j}_\alpha \cdot \boldsymbol{\nabla}\mu'_\alpha \geq 0\,, \tag{96}$$

and

$$\mathcal{D}_{\Gamma,\text{el-ch}} = -\sum_{\alpha=\text{Li,X}} \boldsymbol{j}_{\Gamma,\alpha} \cdot \left[\boldsymbol{\nabla}_\Gamma \mu'_{\Gamma,\alpha}\right] - \sum_{\alpha=\text{Li,X}} j^{\text{C}}_{\Gamma,\alpha}\mu^{\text{C}}_{\Gamma,\alpha} - \sum_{\alpha=\text{Li,X}} j^{\text{D}}_{\Gamma,\alpha}\mu^{\text{D}}_{\Gamma,\alpha} \geq 0 \tag{97}$$

We note that μ^{C}_Γ and μ^{D}_Γ now take the explicit forms

$$\mu^{\text{C}}_{\Gamma,\alpha} = [\![\mu_\alpha]\!] + z_\alpha F [\![\varphi]\!], \quad \mu^{\text{D}}_{\Gamma,\alpha} = \{\!\{\mu_\alpha\}\!\} - \mu_{\Gamma,\alpha} + z_\alpha F \left[\{\!\{\varphi\}\!\} - \varphi_\Gamma\right], \quad \alpha = \text{Li,X} \tag{98}$$

6.2.4. A prototype model — Selected remarks

Thermodynamically admissible constitutive relations for the energetic variables are derivable from (95). It is also straightforward to propose constitutive relations for the dissipative variables that comply with (96) and (97). Here, we shall only comment on the choice of out-of-plane current density quantities $j^{\text{C}}_{\Gamma,\alpha}$ and $j^{\text{D}}_{\Gamma,\alpha}$ in the light of the inequality (97). An obvious choice is

$$j^{\text{C}}_{\Gamma,\alpha}(\mu^{\text{C}}_{\Gamma,\alpha}) = -\frac{M^{\text{C}}_{\Gamma,\alpha}}{R\theta_0}\mu^{\text{C}}_{\Gamma,\alpha}, \quad \alpha = \text{Li,X}, \tag{99a}$$

$$j^{\text{D}}_{\Gamma,\alpha}(\mu^{\text{D}}_{\Gamma,\alpha}) = -\frac{M^{\text{D}}_{\Gamma,\alpha}}{R\theta_0}\mu^{\text{D}}_{\Gamma,\alpha}, \quad \alpha = \text{Li,X}, \tag{99b}$$

where the constitutive parameters $M^{\text{C}}_{\Gamma,\alpha} \geq 0$ and $M^{\text{D}}_{\Gamma,\alpha} \geq 0$ are the chemical interface mobilities.

6.2.5. Simplified interface model: Ignored membrane action

Consider the special situation that membrane action along Γ is ignored, i.e. $\boldsymbol{j}_{\Gamma,\alpha} = \boldsymbol{0}$, $\boldsymbol{d}_\Gamma = \boldsymbol{0}$. The mass-balance and Gauss'–Ampere's law for the interface then reduce to

$$\partial_t c_{\Gamma,\alpha} + j^{\text{D}}_{\Gamma,\alpha} = 0 \quad \alpha = \text{Li,X}, \tag{100a}$$

$$d^{\text{D}}_\Gamma - F\left[c_{\Gamma,\text{Li}} - c_{\Gamma,\text{X}}\right] = 0\,, \tag{100b}$$

which represents an evolution problem in time for each spatial point $\boldsymbol{x}_\Gamma \in \Gamma$. This system must be complemented by constitutive relations for the interfacial chemical potentials, expressed as $\mu_{\Gamma,\alpha} = \mu^{\text{en}}_{\Gamma,\alpha}(c_{\Gamma,\alpha})$ for $\alpha = \text{Li,X}$. Upon observing the constitutive relations $j^{\text{D}}_{\Gamma,\alpha}(\mu^{\text{D}}_{\Gamma,\alpha})$ and $d^{\text{D}}_\Gamma(\varphi^{\text{C}}_\Gamma, \varphi^{\text{D}}_\Gamma)$, we note that it is possible to solve for the interface variables $\varphi_\Gamma, \mu_{\Gamma,\text{Li}}, \mu_{\Gamma,\text{X}}, c_{\Gamma,\text{Li}}, c_{\Gamma,\text{X}}$ from the problem (100) with values $[\![\varphi]\!], \{\!\{\varphi\}\!\}, \{\!\{\mu_{\text{Li}}\}\!\}, \{\!\{\mu_{\text{X}}\}\!\}$ as the data.

6.3. Halfcell wafering an (electronic or ionic) SEI-layer

6.3.1. Model assumptions

As our last prototype problem that illustrates the generic model framework, we consider a so-called "halfcell", which is composed of negative electrode and electrolyte volume domains wafering a Solid Electrolyte Interface (SEI) layer. This system (cell), which is illustrated schematically in Fig. 8(right), is commonly present in conventional batteries, e.g. Cheng et al. (2014), An et al. (2016), Jia et al. (2024), as well as structural batteries, e.g. Greenhalgh et al. (2025). It is also a key component in electro-chemo-mechanically activated shape morphing devices (actuators and sensors), e.g. Carlstedt et al. (2023). As to the specific micro-architecture, in a conventional battery, the active material in the negative electrode usually consists of graphite particles intercalating the ions. In a structural battery and shape-morphing device, this function is brought about by carbon fibers.

Two ionic species are involved: Charged Li and X (anion) in the electrolyte occupying Ω^+, neutral Li in the negative electrode occupying Ω^-, and charged Li in the SEI represented by the interface Γ. This means implicitly that the SEI is effectively part of the electrolyte although with different properties (due to undergone electro-chemical activity), cf. Fig. 8(right). The relevant governing equations for the investigated system in this paper are then obtained from the canonical model by introducing the following identifications:

$$\begin{array}{lllll} \Omega^- : & z'_{\text{Li}} = 0 \text{ (neutral)} & & \boldsymbol{i}_{\text{el}} \neq \boldsymbol{0}, \zeta_{\text{el}} \neq 0 \\ \Omega^+ : & z'_{\text{Li}} = F & z'_{\text{X}} = -F & \boldsymbol{i}_{\text{el}} = \boldsymbol{0}, \zeta_{\text{el}} = 0 \\ \Gamma : & z'_{\Gamma,\text{Li}} = F & & \boldsymbol{i}_{\Gamma,\text{el}} = \boldsymbol{0}, \zeta_{\Gamma,\text{el}} = 0 \end{array} \tag{101}$$

As a consequence, we now obtain $(\Delta z'_{\text{Li}})^- := (z'_{\text{Li}})^- - z'_{\Gamma,\text{Li}} = -F$ and $(\Delta z'_{\text{Li}})^+ := (z'_{\text{Li}})^+ - z'_{\Gamma,\text{Li}} = 0$.

6.3.2. Governing equations: Mass balance and Gauss'–Ampere's law

The local mass balance of ions in the electrode, Ω^-, and electrolyte, Ω^+, reads:

$$\partial_t c_{\text{Li}} + \boldsymbol{j}_{\text{Li}} \cdot \boldsymbol{\nabla} = 0 \quad \text{in } \Omega^- \cup \Omega^+\,, \tag{102a}$$

$$\partial_t c_{\text{X}} + \boldsymbol{j}_{\text{X}} \cdot \boldsymbol{\nabla} = 0 \quad \text{in } \Omega^+\,, \tag{102b}$$

and on the interface Γ

$$\partial_t c_{\Gamma,\text{Li}} + \boldsymbol{j}_{\Gamma,\text{Li}} \cdot \boldsymbol{\nabla}_\Gamma + j^{\text{D}}_{\Gamma,\text{Li}} = 0 \quad \text{on } \Gamma\,. \tag{103}$$

Gauss' law reads:

$$-\zeta_{\text{el}} + \boldsymbol{d} \cdot \boldsymbol{\nabla} = 0 \quad \text{in } \Omega^-\,, \tag{104a}$$

$$\boldsymbol{d} \cdot \boldsymbol{\nabla} - F\left[c_{\text{Li}} - c_{\text{X}}\right] = 0 \quad \text{in } \Omega^+\,, \tag{104b}$$

where it was used that $\zeta_{\text{ion}} = F\left[c_{\text{Li}} - c_{\text{X}}\right]$ in Ω^+. Further,

$$-\zeta_{\Gamma,\text{el}} + \boldsymbol{d}_\Gamma \cdot \boldsymbol{\nabla}_\Gamma + d^{\text{D}}_\Gamma - F c_{\Gamma,\text{Li}} = 0 \quad \text{on } \Gamma\,. \tag{105}$$

Ampere's law reads:

$$[\partial_t \boldsymbol{d} + \boldsymbol{i}_{\text{el}}] \cdot \boldsymbol{\nabla} = 0 \quad \text{in } \Omega^-\,, \tag{106a}$$

$$\partial_t \left[\boldsymbol{d} \cdot \boldsymbol{\nabla} - F\left[c_{\text{Li}} - c_{\text{X}}\right]\right] = 0 \quad \text{in } \Omega^+\,, \tag{106b}$$

and

$$\partial_t \left[\boldsymbol{d}_\Gamma \cdot \boldsymbol{\nabla}_\Gamma + d^{\text{D}}_\Gamma - F c_{\Gamma,\text{Li}}\right] = (i^-_{\text{el}})^\perp - F(j^-_{\text{Li}})^\perp \quad \text{on } \Gamma\,. \tag{107}$$

In order to obtain (107), we used that $[\![\boldsymbol{i}_{\text{el}}]\!] \cdot \boldsymbol{n}_\Gamma = -\boldsymbol{i}^-_{\text{el}} \cdot \boldsymbol{n}_\Gamma = -(i^-_{\text{el}})^\perp$ (since $\boldsymbol{i}^+_{\text{el}} \cdot \boldsymbol{n}_\Gamma = 0$ by modeling assumption) and that $[\![\Delta z'_{\text{Li}} \boldsymbol{j}_{\text{Li}}]\!] \cdot \boldsymbol{n}_\Gamma = F\boldsymbol{j}^-_{\text{Li}} \cdot \boldsymbol{n}_\Gamma = F(j^-_{\text{Li}})^\perp$. We note that Ampere's law for this particular system does not add any new information (as compared to Gauss' law), since it is simply identical to the time-differentiated Gauss' law.

The initial conditions are conveniently chosen as $c_{\text{Li}}(0) = 0$, $c_{\text{X}}(0) = 0$ and $\zeta_{\text{el}}(0) = \zeta_{\Gamma,\text{el}}(0) = 0$. However, we shall henceforth require (as a constitutive assumption) that the free charge from electronic activity on the interface *vanishes identically at all times*, i.e. $\zeta_{\Gamma,\text{el}} = 0$. This is achieved if the RHS of Ampere's law, as given in (107), vanishes, i.e. if we introduce the *constitutive* restriction (which has profound consequences for the formulation of the *constitutive constraint*, as will be elaborated in the next Subsection):

$$(i^-_{\text{el}})^\perp = F(j^-_{\text{Li}})^\perp \quad \text{or, equivalently}, \quad (i^-_{\text{el}})^\perp = -i^{\text{D}}_{\Gamma,\text{el}} = F\left[j^{\text{C}}_{\Gamma,\text{Li}} - \frac{1}{2} j^{\text{D}}_{\Gamma,\text{Li}}\right]. \tag{108}$$

As a result, Gauss' law in (105) then simplifies to

$$(\zeta_{\Gamma,\mathrm{el}} =)\ \boldsymbol{d}_\Gamma \cdot \boldsymbol{\nabla}_\Gamma + d^{\mathrm{D}}_\Gamma - F c_{\Gamma,\mathrm{Li}} = 0 \quad \text{on } \Gamma\,. \tag{109}$$

Remark 9. The identity $(i^+_{\mathrm{el}})^\perp = 0$ (no electronic current in the electrolyte) infers the constraint $i^{\mathrm{C}}_{\Gamma,\mathrm{el}} = -\frac{1}{2} i^{\mathrm{D}}_{\Gamma,\mathrm{el}}$. For the electrolyte domain Ω^+ with only ionic activity, Ampere's law is simply identical to the time-differentiated Gauss' law. Consequently, it does not add any further information. That $\zeta_{\Gamma,\mathrm{el}} = 0$ on Γ means that there is no accumulation of electronic charge. However, since $c_{\Gamma,\mathrm{Li}}$ can change/increase, a corresponding increase of $\zeta_{\Gamma,\mathrm{ion}}$ represents the accumulation of ionic charge. We obtain

$$(-i^+_{\mathrm{ion}})^\perp + (i^-_{\mathrm{el}})^\perp = F[(-j^+_{\mathrm{Li}})^\perp + (j^-_{\mathrm{Li}})^\perp] = -F j^{\mathrm{D}}_{\Gamma,\mathrm{Li}}\,, \tag{110}$$

using Faraday's rule of electrolysis, $(i^+_{\mathrm{ion}})^\perp = F(j^+_{\mathrm{Li}})^\perp$, and combining with (108). □

6.3.3. Constitutive constraints from the dissipation inequality

As to the energetic quantities $\boldsymbol{d}, \mu_{\mathrm{Li}}, \mu_{\mathrm{X}}$ in $\Omega^+ \cup \Omega^-$ and $\boldsymbol{d}_\Gamma, d^{\mathrm{C}}_\Gamma, d^{\mathrm{D}}_\Gamma$ on Γ, we recall

$$\begin{aligned} &\boldsymbol{d} = -\partial_{\boldsymbol{e}}\psi,\ \mu_{\mathrm{Li}} = \partial_{c_{\mathrm{Li}}}\psi,\ \mu_{\mathrm{X}} = \partial_{c_{\mathrm{X}}}\psi,\\ &\boldsymbol{d}_\Gamma = -\partial_{\boldsymbol{e}_\Gamma}\psi_\Gamma,\ d^{\mathrm{C}}_\Gamma = \partial_{\varphi^{\mathrm{C}}_\Gamma}\psi_\Gamma,\ d^{\mathrm{D}}_\Gamma = \partial_{\varphi^{\mathrm{D}}_\Gamma}\psi_\Gamma\,. \end{aligned} \tag{111}$$

The Fick–Ohm Inequality, which was given in its generic format in (61b), now becomes

$$\begin{aligned} &\mathcal{D}_{\mathrm{el-ch}} := \boldsymbol{i}_{\mathrm{el}} \cdot \boldsymbol{e} - \boldsymbol{j}_{\mathrm{Li}} \cdot \boldsymbol{\nabla}\mu_{\mathrm{Li}} \geq 0 \quad \text{in } \Omega^-\\ &\mathcal{D}_{\mathrm{el-ch}} := -\boldsymbol{j}_{\mathrm{Li}} \cdot \boldsymbol{\nabla}\mu'_{\mathrm{Li}} - \boldsymbol{j}_{\mathrm{X}} \cdot \boldsymbol{\nabla}\mu'_{\mathrm{X}} \geq 0 \quad \text{in } \Omega^+\,, \end{aligned} \tag{112}$$

and

$$\mathcal{D}_{\Gamma,\text{el-ch}} = -\boldsymbol{j}_{\Gamma,\mathrm{Li}} \cdot \left[\boldsymbol{\nabla}_\Gamma \mu'_{\Gamma,\mathrm{Li}}\right] - j^{\mathrm{C}}_{\Gamma,\mathrm{Li}}\mu^{\mathrm{C}}_{\Gamma,\mathrm{Li}} - j^{\mathrm{D}}_{\Gamma,\mathrm{Li}}\mu^{\mathrm{D}}_{\Gamma,\mathrm{Li}} - (i^-_{\mathrm{el}})^\perp\left[\varphi_\Gamma - \varphi^-\right] \geq 0 \tag{113}$$

We note that μ^{C}_Γ and μ^{D}_Γ now take the explicit forms

$$\mu^{\mathrm{C}}_{\Gamma,\mathrm{Li}} = [\![\mu_{\mathrm{Li}}]\!] + F\left[\varphi^+ - \varphi_\Gamma\right], \quad \mu^{\mathrm{D}}_{\Gamma,\mathrm{Li}} = \{\!\{\mu_{\mathrm{Li}}\}\!\} - \mu_{\Gamma,\mathrm{Li}} + \frac{1}{2}F\left[\varphi^+ - \varphi_\Gamma\right] \tag{114}$$

We also note that the interfacial electrochemical potential for Li is $\mu'_{\Gamma,\mathrm{Li}} = \mu_{\Gamma,\mathrm{Li}} + F\varphi_\Gamma$. However, due to the constitutive assumption in (108), we may eliminate $(i^-_{\mathrm{el}})^\perp$ in terms of the quantities $j^{\mathrm{C}}_{\Gamma,\mathrm{Li}}$ and $j^{\mathrm{D}}_{\Gamma,\mathrm{Li}}$. Hence, (113) becomes

$$\mathcal{D}_{\Gamma,\text{el-ch}} = -\boldsymbol{j}_{\Gamma,\mathrm{Li}} \cdot \left[\boldsymbol{\nabla}_\Gamma \mu'_{\Gamma,\mathrm{Li}}\right] - j^{\mathrm{C}}_{\Gamma,\mathrm{Li}} F\eta^{\mathrm{C}} - j^{\mathrm{D}}_{\Gamma,\mathrm{Li}} F\eta^{\mathrm{D}} \geq 0 \tag{115}$$

Obviously, μ^{C}_Γ and μ^{D}_Γ are now replaced by the functions η^{C} and η^{D}, defined as

$$F\eta^{\mathrm{C}} = [\![\mu_{\mathrm{Li}}]\!] + F[\![\varphi]\!], \quad F\eta^{\mathrm{D}} = \{\!\{\mu_{\mathrm{Li}}\}\!\} - \mu_{\Gamma,\mathrm{Li}} + F\left[\{\!\{\varphi\}\!\} - \varphi_\Gamma\right] \tag{116}$$

In the electro-chemical literature η^{C} is known as the *overpotential*, whereas it appears that η^{D} has no classical role. Clearly, (115) represents a simplification of the expression in (113) and adds profound clarity to the role of the terms involved.

6.3.4. A prototype model — Selected remarks

Similarly to the model for a purely ionic conductor (discussed in the previous Subsection), we focus on the choice of out-of-plane mass transport quantities $j^{\mathrm{C}}_{\Gamma,\mathrm{Li}}$ and $j^{\mathrm{D}}_{\Gamma,\mathrm{Li}}$, which characterize redox-interfaces/surfaces between the electrode and the electrolyte. In the light of the inequality (115), it is obvious that a "naive" choice[7] is

$$j^{\mathrm{C}}_{\Gamma,\mathrm{Li}}(\eta^{\mathrm{C}}) = -\frac{F M^{\mathrm{C}}_\Gamma}{R\theta_0}\eta^{\mathrm{C}}\,, \tag{117a}$$

$$j^{\mathrm{D}}_{\Gamma,\mathrm{Li}}(\eta^{\mathrm{D}}) = -\frac{F M^{\mathrm{D}}_\Gamma}{R\theta_0}\eta^{\mathrm{D}}\,, \tag{117b}$$

where the constitutive parameters $M^{\mathrm{C}}_\Gamma \geq 0$ and $M^{\mathrm{D}}_\Gamma \geq 0$ are, once again, the chemical interface mobilities. However, a more realistic and well-accepted model is the *classical Butler–Volmer relation*. A possible model setting is then defined/constructed as follows:

$$j^{\mathrm{C}}_{\Gamma,\mathrm{Li}}(\eta^{\mathrm{C}}) = j^{\mathrm{C},0}_\Gamma\left[\exp\left(\frac{\beta F\eta^{\mathrm{C}}}{R\theta}\right) - \exp\left(-\frac{[1-\beta]F\eta^{\mathrm{C}}}{R\theta}\right)\right], \tag{118}$$

where $0 \leq \beta \leq 1$, $j^{\mathrm{C},0}_\Gamma < 0$ is a (state-dependent) parameter. We conclude that $j^{\mathrm{C}}_{\Gamma,\mathrm{Li}} = 0$ if $\eta^{\mathrm{C}} = 0$, which is the case when $[\![\varphi]\!]$ equals the "equilibrium potential" V^{eq}, i.e. when

$$[\![\varphi]\!] = V^{\mathrm{eq}}([\![\mu_{\mathrm{Li}}]\!]) \text{ with } V^{\mathrm{eq}}([\![\mu_{\mathrm{Li}}]\!]) := -\frac{1}{F}[\![\mu_{\mathrm{Li}}]\!], \tag{119}$$

that is $\eta^{\mathrm{C}} = [\![\varphi]\!] - V^{\mathrm{eq}}([\![\mu_{\mathrm{Li}}]\!])$.

Similarly, a possible (non-classical) expression for $j^{\mathrm{D}}_{\Gamma,\mathrm{Li}}$ is

$$j^{\mathrm{D}}_{\Gamma,\mathrm{Li}}(\eta^{\mathrm{D}}) = j^{\mathrm{D},0}_\Gamma\left[\exp\left(\frac{\beta F\eta^{\mathrm{D}}}{R\theta}\right) - \exp\left(-\frac{[1-\beta]F\eta^{\mathrm{D}}}{R\theta}\right)\right], \tag{120}$$

Remark 10. The classical Butler–Volmer relation in (118) does not involve the interface fields μ_Γ and φ_Γ. Further, the models in (117) represent straightforward linearizations of (118) and (120) with the identifications $j^{\mathrm{C},0}_\Gamma = -M^{\mathrm{C}}_\Gamma$ and $j^{\mathrm{D},0}_\Gamma = -M^{\mathrm{D}}_\Gamma$, respectively. □

It is a trivial task to show that $-j^{\mathrm{C}}_{\Gamma,\mathrm{Li}}\eta^{\mathrm{C}} \geq 0$ and $-j^{\mathrm{D}}_{\Gamma,\mathrm{Li}}\eta^{\mathrm{D}} \geq 0$ (as sufficient conditions towards satisfying the dissipation inequality in (115)) by the choice of $j^{\mathrm{C}}_{\Gamma,\mathrm{Li}}$ and $j^{\mathrm{D}}_{\Gamma,\mathrm{Li}}$ in (118) and (120), respectively.[8] To the authors' knowledge, (i) this issue has not been raised previously in the literature, and further, (ii) $j^{\mathrm{D}}_{\Gamma,\mathrm{Li}}$ is a novel quantity in the modeling of electro-chemical systems.

6.3.5. Simplified interface model: Ignored membrane action

Consider the special situation that membrane action along Γ is ignored, i.e. $\boldsymbol{j}_{\Gamma,\mathrm{Li}} = \boldsymbol{0}$, $\boldsymbol{d}_\Gamma = \boldsymbol{0}$. The mass-balance and Gauss'–Ampere's law for the interface then reduce to

$$\partial_t c_{\Gamma,\mathrm{Li}} + j^{\mathrm{D}}_{\Gamma,\mathrm{Li}} = 0\,, \tag{121a}$$

$$-F c_{\Gamma,\mathrm{Li}} + d^{\mathrm{D}}_\Gamma = 0\,, \tag{121b}$$

which represents an evolution problem in time for each spatial point $\boldsymbol{x}_\Gamma \in \Gamma$. This system must be complemented by constitutive relations for the interfacial chemical potential, expressed as $\mu_{\Gamma,\mathrm{Li}} = \mu^{\mathrm{en}}_{\Gamma,\mathrm{Li}}(c_{\Gamma,\mathrm{Li}})$. Upon observing the constitutive relations $j^{\mathrm{D}}_{\Gamma,\mathrm{Li}}(\eta^{\mathrm{D}})$ and $d^{\mathrm{D}}_\Gamma(\varphi^{\mathrm{C}}_\Gamma, \varphi^{\mathrm{D}}_\Gamma)$, we note that it is possible to solve for the interface variables $c_\Gamma, \varphi_\Gamma, \mu_{\Gamma,\mathrm{Li}}$ from the problem (121) with values $[\![\varphi]\!], \{\!\{\varphi\}\!\}, \{\!\{\mu_{\mathrm{Li}}\}\!\}$ as the data.

7. Conclusions and outlook

In this paper, we have systematically investigated the electro-chemo-mechanical couplings in the bulk as well as the interface. Whereas the electromagnetic power exerted on the bulk material has been included in the literature, e.g., Salvadori et al. (2015), the extension to surface effects is novel. In this respect, the developments represent the direct generalization of the recent work by Javili

[7] The relation (117a) can be considered as a linearized version of the classical Butler–Volmer relation.

[8] For $f(x) := [\exp(\beta x) - \exp(-[1-\beta]x)]x$, $x \in \mathbb{R}$ and $0 \leq \beta \leq 1$, it holds that $f(x) \geq 0$, $f(0) = 0$.

et al. (2025), as well as previous work on thermo-mechanical and chemo-mechanical interactions (however, with more restricted model assumptions).

Limitations: The analysis is confined to statics (no dynamic effects), small deformation kinematics, absence of explicit magnetic effects, although the magnetizing field is included in the establishment of the electromagnetic power input. We do not explicitly discuss the modeling of inelastic effects. Further, we do not explicitly discuss mechanical and/or chemo-mechanical degradation and fatigue, neither for the bulk material nor for the interface, although these phenomena are important for both the mechanical and electro-chemical integrity. In particular, decohesion with chemo-mechanical couplings is important for an SEI-layer. Degradation modeling can be achieved via the use of internal variables in the free energy density. The reaction terms included in the mass balance within the bulk as well in the interface are useful for describing trapping of Li-ions that will become immobile in the lattice (e.g. in CF-fibers and graphite particles).

As an outlook to future extensions, we consider it important to account for finite deformations. This is particularly significant for shape-morphing devices, such as sensors and actuators, which are intentionally subjected to large deflections/deformations. In other words, the functional capability is intimately connected to the ability to deform. This is quite different to batteries and supercapacitors, which should be protected from severe overloading and the consequent excessive deformation that may cause structural damage. Exploiting the Joule-effect, i.e. heat generated by the electric current, requires the heat equation.

CRediT authorship contribution statement

Ali Javili: Conceptualization, Methodology, Formal analysis, Writing – original draft, Writing – review & editing. **Fredrik Larsson:** Conceptualization, Methodology, Formal analysis, Writing – original draft, Writing – review & editing. **Kenneth Runesson:** Conceptualization, Methodology, Formal analysis, Writing – original draft, Writing – review & editing. **Paul Steinmann:** Conceptualization, Methodology, Formal analysis, Writing – original draft, Writing – review & editing.

Declaration of competing interest

The authors declare that they have no known competing financial interests or personal relationships that could have appeared to influence the work reported in this paper.

Acknowledgments

AJ gratefully acknowledges the support from The Scientific and Technological Research Council of Türkiye (TÜBİTAK), grant number 224M144. The support by the Swedish Research Council (VR), grant no. 2020-05057 is gratefully acknowledged.

Appendix A. Differential geometry on surfaces

Differential geometry on a curved two-dimensional manifold, a smooth surface embedded in the flat three-dimensional Euclidean space, requires careful considerations in terms of the surface coordinate system. In the sequel, we outline these as a reference. A smooth two-dimensional surface Γ embedded in the three-dimensional Euclidean space is parameterized by surface parameters θ^α with $\alpha = 1, 2$; the corresponding covariant and contravariant surface basis vectors, tangent to Γ, are $\boldsymbol{a}_\alpha$ and $\boldsymbol{a}^\alpha$, respectively; with $\partial_{\theta^\alpha}\{\bullet\}$ abbreviated by $\{\bullet\}_{,\alpha}$ that is

$$\boldsymbol{x} = \boldsymbol{x}(\theta^\alpha)\,, \quad \boldsymbol{a}_\alpha = \boldsymbol{x}_{,\alpha}\,, \quad \boldsymbol{a}^\alpha = a^{\alpha\beta}\boldsymbol{a}_\beta\,, \quad a^{\alpha\beta} = \boldsymbol{a}^\alpha\cdot\boldsymbol{a}^\beta = [a_{\alpha\beta}]^{-1}\,, \quad a_{\alpha\beta} = \boldsymbol{a}_\alpha\cdot\boldsymbol{a}_\beta\,. \tag{A.1}$$

Thus, the surface normal $\boldsymbol{n}_\Gamma$, perpendicular to Γ, follows as $\boldsymbol{n}_\Gamma = [\boldsymbol{a}_1\times\boldsymbol{a}_2]/|\boldsymbol{a}_1\times\boldsymbol{a}_2|$. For completeness, the metric tensor (first fundamental form) reads $\boldsymbol{A}_\Gamma = \boldsymbol{a}_\alpha\otimes\boldsymbol{a}^\alpha$. In the surface coordinate system, the surface gradient, surface divergence, and (negative) surface curl operators of vector fields $\{\bullet\}$ expand as

$$\{\bullet\}\otimes\boldsymbol{\nabla}_\Gamma := \{\bullet\}_{,\alpha}\otimes\boldsymbol{a}^\alpha\,, \quad \{\bullet\}\cdot\boldsymbol{\nabla}_\Gamma := \{\bullet\}_{,\alpha}\cdot\boldsymbol{a}^\alpha\,, \quad \{\bullet\}\times\boldsymbol{\nabla}_\Gamma := \{\bullet\}_{,\alpha}\times\boldsymbol{a}^\alpha\,, \tag{A.2}$$

where $\boldsymbol{\nabla}_\Gamma$ denotes the surface gradient operator. Then the symmetric curvature tensor (second fundamental form) $\boldsymbol{K}_\Gamma$ and the total curvature K_Γ, that is, twice the mean curvature, compute as $\boldsymbol{K}_\Gamma = -\boldsymbol{n}_{\Gamma,\alpha}\otimes\boldsymbol{a}^\alpha$ and $K_\Gamma = -\boldsymbol{n}_{\Gamma,\alpha}\cdot\boldsymbol{a}^\alpha$, respectively. Finally, with Christoffel symbols $A^\alpha{}_{\beta\gamma} = \boldsymbol{a}^\alpha\cdot\boldsymbol{a}_{\beta,\gamma}$, symmetric in the covariant index pair $\beta\gamma$, thus $A^\alpha{}_{\beta\gamma} = A^\alpha{}_{(\beta\gamma)}$ (where $(\beta\gamma)$ denotes symmetrization in the index pair $\beta\gamma$), and $K_{\alpha\beta} = \boldsymbol{a}_\alpha\cdot\boldsymbol{K}_\Gamma\cdot\boldsymbol{a}_\beta$, etc., the parameter derivatives of $\boldsymbol{a}_\alpha, \boldsymbol{a}^\alpha$, and $\boldsymbol{n}_\Gamma$ follow as the Gauss and Weingarten formulae

$$\boldsymbol{a}_{\alpha,\beta} = A^\gamma{}_{\alpha\beta}\,\boldsymbol{a}_\gamma + K_{\alpha\beta}\,\boldsymbol{n}_\Gamma\,, \quad \boldsymbol{a}^\alpha{}_{,\beta} = -A^\alpha{}_{\beta\gamma}\,\boldsymbol{a}^\gamma + K^\alpha{}_\beta\,\boldsymbol{n}_\Gamma\,, \quad \boldsymbol{n}_{\Gamma,\beta} = -K_{\beta\gamma}\boldsymbol{a}^\gamma\,. \tag{A.3}$$

From the coordinate expansion of $\boldsymbol{n}_{\Gamma,\alpha}$, it can then be seen that $\boldsymbol{n}_\Gamma\times\boldsymbol{\nabla}_\Gamma$ is proportional to the axial vector of $\boldsymbol{K}_\Gamma$ and thus vanishes due to the symmetry of $\boldsymbol{K}_\Gamma$. Further relations between the fourth-order Riemann curvature tensor $\boldsymbol{R}_\Gamma$ and the second-order curvature tensor $\boldsymbol{K}_\Gamma$ (resulting in Gauss' theorema egregium) as well as for the parameter derivatives of $\boldsymbol{K}_\Gamma$ (Mainardi–Codazzi formula), helpful for the detailed derivation of the subsequent results, read, with $[\mu\cdots\nu]$ denoting skew symmetrization in the index pair μ and ν, as

$$\tfrac{1}{2}R^\alpha{}_{\beta\gamma\delta} = A^\alpha{}_{\beta[\delta,\gamma]} + A^\alpha{}_{\epsilon[\gamma}\,A^\epsilon{}_{\beta\delta]} \equiv K^\alpha{}_{[\gamma}\,K_{\beta\delta]}\,, \quad K^\alpha{}_{[\beta,\gamma]} = -A^\alpha{}_{[\gamma\delta}\,K^\delta{}_{\beta]}\,. \tag{A.4}$$

Then, for normal vector fields $\boldsymbol{v}^\perp = v^\perp\boldsymbol{n}_\Gamma$ with $\boldsymbol{\nabla}_\Gamma v^\perp = v^\perp_{,\alpha}\,\boldsymbol{a}^\alpha$ the following can be proven

$$\boldsymbol{v}^\perp\otimes\boldsymbol{\nabla}_\Gamma = \boldsymbol{n}_\Gamma\otimes\boldsymbol{\nabla}_\Gamma v^\perp - v^\perp\boldsymbol{K}_\Gamma\,, \quad \boldsymbol{v}^\perp\cdot\boldsymbol{\nabla}_\Gamma = -v^\perp K_\Gamma\,, \quad \boldsymbol{v}^\perp\times\boldsymbol{\nabla}_\Gamma = \boldsymbol{n}_\Gamma\times\boldsymbol{\nabla}_\Gamma v^\perp\,. \tag{A.5}$$

Furthermore, $[\boldsymbol{v}^\perp\times\boldsymbol{\nabla}_\Gamma]\cdot\boldsymbol{\nabla}_\Gamma = 0$ holds. Likewise, for a superficial vector field $\boldsymbol{v}^\parallel = v_\alpha\,\boldsymbol{a}^\alpha$ the relations in the above allow us to prove that

$$\begin{aligned}&\boldsymbol{v}^\parallel\otimes\boldsymbol{\nabla}_\Gamma = v_{\alpha|\beta}\,\boldsymbol{a}^\alpha\otimes\boldsymbol{a}^\beta + \boldsymbol{n}_\Gamma\otimes[\boldsymbol{v}^\parallel\cdot\boldsymbol{K}_\Gamma]\,, \quad \boldsymbol{v}^\parallel\cdot\boldsymbol{\nabla}_\Gamma = v^\alpha{}_{|\alpha}\,,\\ &\boldsymbol{v}^\parallel\times\boldsymbol{\nabla}_\Gamma = v_{\alpha|\beta}\,\boldsymbol{a}^\alpha\times\boldsymbol{a}^\beta + \boldsymbol{n}_\Gamma\times[\boldsymbol{v}^\parallel\cdot\boldsymbol{K}_\Gamma]\,.\end{aligned} \tag{A.6}$$

Here, we abbreviate the covariant derivative as $v_{\alpha|\beta} = v_{\alpha,\beta} - v_\gamma\,A^\gamma{}_{\alpha\beta}$. It can also be shown that $[\boldsymbol{v}^\parallel\times\boldsymbol{\nabla}_\Gamma]\cdot\boldsymbol{\nabla}_\Gamma = 2\,\mathrm{axl}([\boldsymbol{v}^\parallel\otimes\boldsymbol{\nabla}_\Gamma]\cdot\boldsymbol{K}_\Gamma)\cdot\boldsymbol{n}_\Gamma$, where $\mathrm{axl}(\{\bullet\})$ extracts the axial vector of the skew symmetric part of $\{\bullet\}$.

For a vector field $\{\bullet\}$, we finally define the superficial part of its tensor-valued surface gradient and the vector-valued normal part of its surface curl as

$$\{\bullet\}\otimes\boldsymbol{\nabla}^\parallel_\Gamma := \boldsymbol{I}_\Gamma\cdot[\{\bullet\}\otimes\boldsymbol{\nabla}_\Gamma]\,, \quad \{\bullet\}\times\boldsymbol{\nabla}^\perp_\Gamma := \boldsymbol{I}^\perp_\Gamma\cdot[\{\bullet\}\times\boldsymbol{\nabla}_\Gamma]\,. \tag{A.7}$$

Here, $\boldsymbol{I}^\perp_\Gamma := \boldsymbol{n}_\Gamma\otimes\boldsymbol{n}_\Gamma$ denotes the surface normal projection tensor. Observe that $\{\bullet\}\cdot\boldsymbol{\nabla}^\parallel_\Gamma \equiv \{\bullet\}\cdot\boldsymbol{\nabla}_\Gamma$ and $\boldsymbol{I}^\perp_\Gamma\cdot[\{\bullet\}\times\boldsymbol{\nabla}_\Gamma] \equiv \boldsymbol{I}^\perp_\Gamma\cdot[\{\bullet\}\times\boldsymbol{\nabla}]$ hold. Note also the similarity of the symbolic notation $\{\bullet\}\otimes\boldsymbol{\nabla}^\parallel_\Gamma$ and $\{\bullet\}\times\boldsymbol{\nabla}^\perp_\Gamma$ to the corresponding notation in a volume, where the gradient and (negative) curl expand in terms of the gradient operator $\boldsymbol{\nabla}$ as $\{\bullet\}\otimes\boldsymbol{\nabla}$ and $\{\bullet\}\times\boldsymbol{\nabla}$. When applied to normal and superficial vector fields, the above differential operators eventually result in

$$\begin{aligned}&\boldsymbol{v}^\perp\otimes\boldsymbol{\nabla}^\parallel_\Gamma = -v_\perp\boldsymbol{K}_\Gamma\,, \quad \boldsymbol{v}^\perp\times\boldsymbol{\nabla}^\perp_\Gamma = \boldsymbol{0}\,,\\ &\boldsymbol{v}^\parallel\otimes\boldsymbol{\nabla}^\parallel_\Gamma = v_{\alpha|\beta}\,\boldsymbol{a}^\alpha\otimes\boldsymbol{a}^\beta\,, \quad \boldsymbol{v}^\parallel\times\boldsymbol{\nabla}^\perp_\Gamma = v_{\alpha|\beta}\,\boldsymbol{a}^\alpha\times\boldsymbol{a}^\beta\,.\end{aligned} \tag{A.8}$$

Note that $v_{[\alpha|\beta]} = v_{[\alpha,\beta]}$, thus $\boldsymbol{v}^\parallel\times\boldsymbol{\nabla}^\perp_\Gamma = v_{\alpha,\beta}\,\boldsymbol{a}^\alpha\times\boldsymbol{a}^\beta$ may likewise be expressed in terms of partial derivatives. From these one can show that for any vector field $\{\bullet\}$ a differential identity of "divergence-curl"-type $[\{\bullet\}\times\boldsymbol{\nabla}^\perp_\Gamma]\cdot\boldsymbol{\nabla}_\Gamma = 0$ holds. Furthermore, it is obvious that for any scalar

field $\{\circ\}$ a differential identity of "curl-grad"-type $[\boldsymbol{\nabla}_\Gamma\{\circ\}]\times\boldsymbol{\nabla}_\Gamma^\perp=\boldsymbol{0}$ holds.

Appendix B. Electro-magnetic relations for domains with an interface

B.1. Resolved, integrated, and averaged interphase fields

The *interface* Γ is a dimensionally reduced idealization of the three-dimensional *interphase* $\Gamma\times[-w/2,+w/2]$. When we consider the resolved situation within $\Gamma\times[-w/2,w/2]$, we denote by $\hat{\boldsymbol{a}}_\Gamma(\boldsymbol{x},\eta)$ any resolved vector-valued quantity, where $(\boldsymbol{x},\eta)\in\Gamma\times[-w/2,+w/2]$. Taking into account the limit case $w\to 0$, we conclude that $\boldsymbol{n}_\Gamma$ does not depend on η. Thus, we can decompose the resolved quantity $\hat{\boldsymbol{a}}_\Gamma$ into perpendicular and parallel contributions $\hat{\boldsymbol{a}}_\Gamma^\perp:=\boldsymbol{I}_\Gamma^\perp\cdot\hat{\boldsymbol{a}}_\Gamma=:\hat{a}_\Gamma^\perp\boldsymbol{n}_\Gamma$ and $\hat{\boldsymbol{a}}_\Gamma^\parallel:=\boldsymbol{I}_\Gamma\cdot\hat{\boldsymbol{a}}_\Gamma$ (with orthogonalities $\hat{\boldsymbol{a}}_\Gamma^\perp\cdot\boldsymbol{I}_\Gamma=\boldsymbol{0}$ and $\hat{\boldsymbol{a}}_\Gamma^\parallel\cdot\boldsymbol{I}_\Gamma^\perp=\boldsymbol{0}$), respectively; thus, we have

$$\hat{\boldsymbol{a}}_\Gamma(\boldsymbol{x},\eta)=\hat{a}_\Gamma^\perp(\boldsymbol{x},\eta)\,\boldsymbol{n}_\Gamma(\boldsymbol{x})+\hat{\boldsymbol{a}}_\Gamma^\parallel(\boldsymbol{x},\eta)\,.$$

Next, as a crucial distinction, we define (through thickness) *integrated* and (over thickness) *averaged* counterparts of the contributions $\hat{\boldsymbol{a}}_\Gamma^{\perp/\parallel}$ to the resolved quantity $\hat{\boldsymbol{a}}_\Gamma$ at the interface level Γ as

$$\boldsymbol{a}_\Gamma^{\perp/\parallel}:=\int_{-w/2}^{w/2}\hat{\boldsymbol{a}}_\Gamma^{\perp/\parallel}\,\mathrm{d}\eta\quad\text{and}\quad\bar{\boldsymbol{a}}_\Gamma^{\perp/\parallel}:=\frac{1}{w}\int_{-w/2}^{w/2}\hat{\boldsymbol{a}}_\Gamma^{\perp/\parallel}\,\mathrm{d}\eta\,.\tag{B.1}$$

Then, two situations can occur: either the resolved quantity is *finite* and can be represented by its finite, averaged counterpart (also) when $w\to 0$ (zero divided by zero l'Hospital limit), while the integrated counterpart vanishes when $w\to 0$; or the resolved quantity is *infinite* and can be represented by its finite, integrated counterpart when $w\to 0$ (infinity times zero l'Hospital limit), while the averaged counterpart is infinite when $w\to 0$. For clarification, consider the case of a thin mechanical membrane: here, the resolved membrane strain and its averaged counterpart are finite (strain-type situation), whereas the resolved membrane stress is infinite and its integrated counterpart (the stress resultant) is finite (stress-type situation). Note that the situation can generally be different for the $\hat{\boldsymbol{a}}_\Gamma^{\perp/\parallel}$ components.

B.2. Ampere's law

B.2.1. Preliminaries

Ampere's law is one of the two circulation laws expressed as Maxwell's equations. It relates the magnetic field $\boldsymbol{h}$ along an arbitrary closed space-curved loop γ in $\mathbb{R}^3$ to the so-called Maxwell current, defined as $\boldsymbol{i}_{\mathrm{Max}}:=\boldsymbol{i}+\partial_t\boldsymbol{d}$, through the curved surface ω that is enclosed by γ. In its global format, the relation reads

$$\int_\omega\boldsymbol{i}_{\mathrm{Max}}\cdot\boldsymbol{n}\,\mathrm{d}S=\oint_\gamma\boldsymbol{h}\cdot\boldsymbol{t}\,\mathrm{d}L\,,\tag{B.2}$$

where the unit normal $\boldsymbol{n}$ is directed so that the tangent vector $\boldsymbol{t}$ pertains to a positive circulation around it.

B.2.2. Ampere's law across an interface

Recall Ampere's law in integral form as given in (20)

$$\begin{aligned}&\int_{\omega^-}\boldsymbol{i}_{\mathrm{Max}}\cdot\boldsymbol{n}\,\mathrm{d}S+\int_{\mathcal{L}}\boldsymbol{i}_{\mathrm{Max},\Gamma}^\parallel\cdot\boldsymbol{n}_{\mathrm{L}}\,\mathrm{d}L+\int_{\omega^+}\boldsymbol{i}_{\mathrm{Max}}\cdot\boldsymbol{n}\,\mathrm{d}S\\&=\int_{\gamma^-}\boldsymbol{h}\cdot\boldsymbol{t}\,\mathrm{d}L+h_\Gamma^\perp\big|_A+\int_{\gamma^+}\boldsymbol{h}\cdot\boldsymbol{t}\,\mathrm{d}L-h_\Gamma^\perp\big|_B\,.\end{aligned}\tag{B.3}$$

Identifying the loops around ω^+ and ω^- as $\partial\omega^\pm=\gamma^\pm\cup\mathcal{L}$, we may restate this equation as follows

$$\begin{aligned}&\int_{\omega^-}\boldsymbol{i}_{\mathrm{Max}}\cdot\boldsymbol{n}\,\mathrm{d}S-\int_{\partial\omega^-}\boldsymbol{h}\cdot\boldsymbol{t}\,\mathrm{d}L+\int_{\omega^+}\boldsymbol{i}_{\mathrm{Max}}\cdot\boldsymbol{n}\,\mathrm{d}S-\int_{\partial\omega^+}\boldsymbol{h}\cdot\boldsymbol{t}\,\mathrm{d}L\\&+\int_{\mathcal{L}}\boldsymbol{i}_{\mathrm{Max},\Gamma}^\parallel\cdot\boldsymbol{n}_{\mathrm{L}}\,\mathrm{d}L-\int_{\mathcal{L}}[\![\boldsymbol{h}]\!]\cdot\boldsymbol{t}^-\,\mathrm{d}L+h_\Gamma^\perp\big|_B-h_\Gamma^\perp\big|_A=0\,,\end{aligned}\tag{B.4}$$

where we used $\boldsymbol{t}^+=-\boldsymbol{t}^-$ on $\mathcal{L}$. We now employ *Stokes' theorem* for converting the terms

$$\int_{\partial\omega^\pm}\boldsymbol{h}\cdot\boldsymbol{t}\,\mathrm{d}L=-\int_{\omega^\pm}[\boldsymbol{h}\times\boldsymbol{\nabla}]\cdot\boldsymbol{n}\,\mathrm{d}S\,.\tag{B.5}$$

Furthermore, the *fundamental theorem of calculus*, for a variable l running from A to B, can be expressed as

$$h_\Gamma^\perp\big|_B-h_\Gamma^\perp\big|_A=\int_{\mathcal{L}}\frac{\partial}{\partial l}h_\Gamma^\perp\,\mathrm{d}L=\int_{\mathcal{L}}\left[\boldsymbol{\nabla}_\Gamma h_\Gamma^\perp\right]\cdot\boldsymbol{t}^-\,\mathrm{d}L\,.\tag{B.6}$$

Finally, using the relation $\boldsymbol{t}^-=\boldsymbol{n}_{\mathrm{L}}\times\boldsymbol{n}_\Gamma$ for the three orthogonal unit vectors on $\mathcal{L}$, we can insert the expressions in (B.5) and (B.6) into (B.4) to obtain

$$\begin{aligned}&\int_{\omega^+\cup\omega^-}\left[\boldsymbol{i}_{\mathrm{Max}}+\boldsymbol{h}\times\boldsymbol{\nabla}\right]\cdot\boldsymbol{n}\,\mathrm{d}S\\&+\int_{\mathcal{L}}\left[\boldsymbol{i}_{\mathrm{Max},\Gamma}^\parallel+[h_\Gamma^\perp\boldsymbol{n}_\Gamma]\times\boldsymbol{\nabla}_\Gamma+[\![\boldsymbol{h}]\!]\times\boldsymbol{n}_\Gamma\right]\cdot\boldsymbol{n}_{\mathrm{L}}\,\mathrm{d}L=0\,,\end{aligned}\tag{B.7}$$

where we used $\boldsymbol{n}_\Gamma\times\boldsymbol{\nabla}_\Gamma=\boldsymbol{0}$ and re-wrote $\boldsymbol{n}_\Gamma\times[\boldsymbol{\nabla}_\Gamma h_\Gamma^\perp]=[h_\Gamma^\perp\boldsymbol{n}_\Gamma]\times\boldsymbol{\nabla}_\Gamma$ to resemble the structure of the volume format of Ampere's law. From (B.7) it is then possible to deduce the local equations. Firstly, since (B.7) must hold for any surface $\omega^\pm$, and for any normal direction $\boldsymbol{n}$, we obtain the common Ampere's law in the volume

$$\boldsymbol{i}_{\mathrm{Max}}+\boldsymbol{h}\times\boldsymbol{\nabla}=\boldsymbol{0}\quad\text{in }\Omega^-\cup\Omega^+\,.\tag{B.8}$$

Now, using the differential identity of "divergence-curl"-type, $[\boldsymbol{h}\times\boldsymbol{\nabla}]\cdot\boldsymbol{\nabla}=0$ for any twice differentiable vector field $\boldsymbol{h}$, we obtain the relation

$$\boldsymbol{i}_{\mathrm{Max}}\cdot\boldsymbol{\nabla}=0\quad\text{in }\Omega^-\cup\Omega^+\,.\tag{B.9}$$

Next, considering arbitrary curves $\mathcal{L}$ with in-plane tangential vector $\boldsymbol{n}_{\mathrm{L}}\perp\boldsymbol{n}_\Gamma$, we conclude that

$$\boldsymbol{I}_\Gamma\cdot\left[\boldsymbol{i}_{\mathrm{Max},\Gamma}^\parallel+[h_\Gamma^\perp\boldsymbol{n}_\Gamma]\times\boldsymbol{\nabla}_\Gamma+[\![\boldsymbol{h}]\!]\times\boldsymbol{n}_\Gamma\right]=\boldsymbol{0}\,.\tag{B.10}$$

Since all three terms inside the bracket in (B.10) are superficial, that is, they are indeed orthogonal to $\boldsymbol{n}_\Gamma$, the final result is

$$\boldsymbol{i}_{\mathrm{Max},\Gamma}^\parallel+[h_\Gamma^\perp\boldsymbol{n}_\Gamma]\times\boldsymbol{\nabla}_\Gamma+[\![\boldsymbol{h}]\!]\times\boldsymbol{n}_\Gamma=\boldsymbol{0}\,.\tag{B.11}$$

Note that $\boldsymbol{i}_{\mathrm{Max},\Gamma}^\parallel$ and $h_\Gamma^\perp\boldsymbol{n}_\Gamma$ are necessarily *finite* in order to make sense of (B.11) as the remaining term $[\![\boldsymbol{h}]\!]\times\boldsymbol{n}_\Gamma$ is also finite. Next, we evaluate the surface divergence of the expression in (B.11) as

$$\boldsymbol{i}_{\mathrm{Max},\Gamma}^\parallel\cdot\boldsymbol{\nabla}_\Gamma+\left[[h_\Gamma^\perp\boldsymbol{n}_\Gamma]\times\boldsymbol{\nabla}_\Gamma\right]\cdot\boldsymbol{\nabla}_\Gamma+\left[[\![\boldsymbol{h}]\!]\times\boldsymbol{n}_\Gamma\right]\cdot\boldsymbol{\nabla}_\Gamma=0\,.\tag{B.12}$$

The second term vanishes due to the surface differential identity of "divergence-curl"-type $\left[[v^\perp\boldsymbol{n}_\Gamma]\times\boldsymbol{\nabla}_\Gamma\right]\cdot\boldsymbol{\nabla}_\Gamma=0$ for any sufficiently differentiable normal vector field $v^\perp\boldsymbol{n}_\Gamma$, cf. Appendix A. Furthermore, the last term in (B.12) can be rewritten using (B.8) as

$$\begin{aligned}\left[[\![\boldsymbol{h}]\!]\times\boldsymbol{n}_\Gamma\right]\cdot\boldsymbol{\nabla}_\Gamma&=-[\![\boldsymbol{h}\times\boldsymbol{\nabla}_\Gamma]\!]\cdot\boldsymbol{n}_\Gamma+[\![\boldsymbol{h}]\!]\cdot\left[\boldsymbol{n}_\Gamma\times\boldsymbol{\nabla}_\Gamma\right]\\&=-[\![\boldsymbol{h}\times\boldsymbol{\nabla}]\!]\cdot\boldsymbol{n}_\Gamma=[\![\boldsymbol{i}_{\mathrm{Max}}]\!]\cdot\boldsymbol{n}_\Gamma\,,\end{aligned}$$

where we used $[\{\bullet\}\times\boldsymbol{\nabla}]\cdot\boldsymbol{n}_\Gamma=\left[\{\bullet\}\times\boldsymbol{\nabla}_\Gamma\right]\cdot\boldsymbol{n}_\Gamma$ and $\boldsymbol{n}_\Gamma\times\boldsymbol{\nabla}_\Gamma=\boldsymbol{0}$. Finally, we conclude from (B.12) that

$$\boldsymbol{i}_{\mathrm{Max},\Gamma}^\parallel\cdot\boldsymbol{\nabla}_\Gamma+[\![\boldsymbol{i}_{\mathrm{Max}}]\!]\cdot\boldsymbol{n}_\Gamma=0\,.\tag{B.13}$$

B.2.3. Ampere's law inside an interphase

In order to derive a relation that involves the normal component of $\boldsymbol{i}_{\mathrm{Max},\Gamma}$, we consider the special case that the loop is embedded entirely within the *interphase* with the normal $\boldsymbol{n}$ identical to the interface normal $\boldsymbol{n}_\Gamma$, see Fig. 5. More specifically, we consider the circulation law inside the resolved interphase for a given through-thickness coordinate $\eta\in[-w/2,+w/2]$. We may then state Ampere's law in integral form for the resolved fields as follows

$$\int_\omega\hat{i}_{\mathrm{Max},\Gamma}^\perp\,\mathrm{d}S=\int_\gamma\hat{\boldsymbol{h}}_\Gamma^\parallel\cdot\boldsymbol{t}\,\mathrm{d}L\,,\tag{B.14}$$

where we introduced $\hat{i}^{\perp}_{\mathrm{Max},\Gamma} := \hat{i}^{\perp}_{\Gamma} + \partial_t \hat{d}^{\perp}_{\Gamma}$. From Stokes' theorem, it follows directly that

$$\int_{\gamma} \hat{\boldsymbol{h}}^{\parallel}_{\Gamma} \cdot \boldsymbol{t}\,\mathrm{d}L = -\int_{\omega} \left[\hat{\boldsymbol{h}}^{\parallel}_{\Gamma} \times \boldsymbol{\nabla}\right] \cdot \boldsymbol{n}_{\Gamma}\,\mathrm{d}S = -\int_{\omega} \left[\hat{\boldsymbol{h}}^{\parallel}_{\Gamma} \times \boldsymbol{\nabla}_{\Gamma}\right] \cdot \boldsymbol{n}_{\Gamma}\,\mathrm{d}S\,. \tag{B.15}$$

We thus obtain that

$$\int_{\omega} \hat{i}^{\perp}_{\mathrm{Max},\Gamma} + \left[\hat{\boldsymbol{h}}^{\parallel}_{\Gamma} \times \boldsymbol{\nabla}_{\Gamma}\right] \cdot \boldsymbol{n}_{\Gamma}\,\mathrm{d}S = 0\,, \tag{B.16}$$

from which we deduce the local equation as

$$\hat{i}^{\perp}_{\mathrm{Max},\Gamma} + \left[\hat{\boldsymbol{h}}^{\parallel}_{\Gamma} \times \boldsymbol{\nabla}_{\Gamma}\right] \cdot \boldsymbol{n}_{\Gamma} = 0 \quad \text{on } \Gamma \times [-w/2, +w/2]\,. \tag{B.17}$$

Finally, we integrate (B.17) through the thickness, to obtain a relation in *integrated* quantities

$$i^{\perp}_{\mathrm{Max},\Gamma} + \left[\boldsymbol{h}^{\parallel}_{\Gamma} \times \boldsymbol{\nabla}_{\Gamma}\right] \cdot \boldsymbol{n}_{\Gamma} = 0 \quad \text{on } \Gamma\,. \tag{B.18}$$

This relation complements (B.11) in terms of establishing Ampere's law on an interface. However, it is not operational. In fact, comparing with the 3D-case (where $\boldsymbol{i}_{\mathrm{Max}}$ and $\boldsymbol{h}$ are continuous in the div and curl sense, respectively), we note that the corresponding resolved quantities appearing in (B.17) are *finite* and thus $i^{\perp}_{\Gamma}, d^{\perp}_{\Gamma}, \boldsymbol{h}^{\parallel}_{\Gamma} \to 0$ when $w \to 0$, cf. B1. Hence, (B.18) vanishes identically for the dimensionally reduced, that is, zero-thickness, interface.

B.3. Faraday's law

B.3.1. Preliminaries

Faraday's law of induction is the second of the two circulation laws represented by Maxwell's equations. It relates the electric field $\boldsymbol{e}$ along an arbitrary closed loop γ in the three-dimensional space to the rate of magnetic flux density through the loop. In the global format, the relation is given as

$$-\int_{\omega} \left[\partial_t \boldsymbol{b}\right] \cdot \boldsymbol{n}\,\mathrm{d}S = \oint_{\gamma} \boldsymbol{e} \cdot \boldsymbol{t}\,\mathrm{d}L\,, \tag{B.19}$$

where ω is an arbitrary surface enclosed by γ.

B.3.2. Faraday's law across an interface

We shall derive the local forms of Faraday's law in complete analogy with Ampere's law. Hence, in analogy to Eq. (B.3), we first state Faraday's law in integral form as

$$\begin{aligned} &-\int_{\omega^-} \partial_t \boldsymbol{b} \cdot \boldsymbol{n}\,\mathrm{d}S - \int_{\mathcal{L}} [\partial_t \boldsymbol{b}^{\parallel}_{\Gamma}] \cdot \boldsymbol{n}_{\mathrm{L}}\,\mathrm{d}L - \int_{\omega^+} \partial_t \boldsymbol{b} \cdot \boldsymbol{n}\,\mathrm{d}S \\ &\quad = \int_{\gamma^-} \boldsymbol{e} \cdot \boldsymbol{t}\,\mathrm{d}L + e^{\perp}_{\Gamma}\Big|_A + \int_{\gamma^+} \boldsymbol{e} \cdot \boldsymbol{t}\,\mathrm{d}L - e^{\perp}_{\Gamma}\Big|_B\,. \end{aligned} \tag{B.20}$$

Repeating the derivation in Appendix B.2, we obtain the localized Faraday's law in the volume

$$-\partial_t \boldsymbol{b} + \boldsymbol{e} \times \boldsymbol{\nabla} = \boldsymbol{0} \quad \text{in } \Omega^- \cup \Omega^+\,, \tag{B.21}$$

whereas the in-plane format becomes

$$-\partial_t \boldsymbol{b}^{\parallel}_{\Gamma} + [e^{\perp}_{\Gamma} \boldsymbol{n}_{\Gamma}] \times \boldsymbol{\nabla}_{\Gamma} + [\![\boldsymbol{e}]\!] \times \boldsymbol{n}_{\Gamma} = \boldsymbol{0} \quad \text{on } \Gamma\,. \tag{B.22}$$

B.3.3. Faraday's law inside an interphase

We consider again the situation in Fig. 5 showing the circulation law within the resolved *interphase* for a given through-thickness coordinate $\eta \in [-w/2, +w/2]$. Faraday's law in integral form then becomes

$$\int_{\omega} -\partial_t \hat{b}^{\perp}_{\Gamma}\,\mathrm{d}S = \int_{\gamma} \hat{\boldsymbol{e}}^{\parallel}_{\Gamma} \cdot \boldsymbol{t}\,\mathrm{d}L\,. \tag{B.23}$$

Repeating, once again, the derivation in Appendix B.2, we obtain the localized Faraday's law for the normal component, cf. (B.17),

$$-\partial_t \hat{b}^{\perp}_{\Gamma} + \left[\hat{\boldsymbol{e}}^{\parallel}_{\Gamma} \times \boldsymbol{\nabla}_{\Gamma}\right] \cdot \boldsymbol{n}_{\Gamma} = 0 \quad \text{on } \Gamma \times [-w/2, +w/2]\,. \tag{B.24}$$

We shall further analyze this relation for the special case of electro-statics (which is the only situation that is considered in this paper); see below.

B.3.4. The case of electro-statics

We shall consider the situation of vanishing rate of the magnetic flux in order to derive the relations pertinent to electro-statics. Letting $\partial_t \boldsymbol{b} \to \boldsymbol{0}$ in (B.21), we obtain the condition

$$\boldsymbol{e} \times \boldsymbol{\nabla} = \boldsymbol{0} \quad \Rightarrow \exists\, \varphi :\ \boldsymbol{e} = -\boldsymbol{\nabla}\varphi\,, \tag{B.25}$$

from the Helmholtz decomposition in the volume. Similarly, letting $\partial_t \hat{b}^{\perp}_{\Gamma} \to 0$ in (B.24), we obtain the relation

$$\begin{aligned} &\left[\hat{\boldsymbol{e}}^{\parallel}_{\Gamma}(\boldsymbol{x},\eta) \times \boldsymbol{\nabla}_{\Gamma}\right] \cdot \boldsymbol{n}_{\Gamma} = 0 \quad \Rightarrow \exists\, \hat{\varphi}_{\Gamma}(\boldsymbol{x},\eta) : \\ &\hat{\boldsymbol{e}}^{\parallel}_{\Gamma}(\boldsymbol{x},\eta) = -\boldsymbol{\nabla}_{\Gamma} \hat{\varphi}_{\Gamma}(\boldsymbol{x},\eta)\,, \quad \eta \in [-w/2, +w/2]\,, \end{aligned} \tag{B.26}$$

from the Helmholtz decomposition on a surface. Motivated by the corresponding property in the volume, we consider that the resolved electric potential $\hat{\varphi}$ in the interphase is *continuous* and thus *finite*; therefore, we have

$$\hat{\varphi}_{\Gamma}(\bullet, \pm w/2) = \varphi^{\pm}(\bullet)\,. \tag{B.27}$$

Furthermore, we define the *averaged* potential $\bar{\varphi}_{\Gamma}$ and, as the resolved $\hat{\boldsymbol{e}}^{\parallel}_{\Gamma}$ from (B.26) is also *finite*, the *averaged* parallel electric field $\bar{\boldsymbol{e}}^{\parallel}_{\Gamma} = -\boldsymbol{\nabla}_{\Gamma} \bar{\varphi}_{\Gamma}$. Finally, considering $\partial_t \boldsymbol{b}^{\parallel}_{\Gamma} \to \boldsymbol{0}$ in (B.22), we obtain the relation

$$[e^{\perp}_{\Gamma} \boldsymbol{n}_{\Gamma}] \times \boldsymbol{\nabla}_{\Gamma} + [\![\boldsymbol{e}]\!] \times \boldsymbol{n}_{\Gamma} = \boldsymbol{0}\,. \tag{B.28}$$

Due to the assumption that the resolved electric potential $\hat{\varphi}$ within the interphase is *continuous* and *finite*, we consider $e^{\perp}_{\Gamma}$ as an *integrated* quantity

$$e^{\perp}_{\Gamma} := \int_{-w/2}^{w/2} \hat{e}^{\perp}_{\Gamma}\,\mathrm{d}\eta = \int_{-w/2}^{w/2} -\frac{\partial \hat{\varphi}_{\Gamma}}{\partial \eta}\,\mathrm{d}\eta = -[\![\varphi]\!]\,. \tag{B.29}$$

Using this relation, it is easily verified that (B.28) is identically satisfied. To this end, it is recalled that $\boldsymbol{e} = -\boldsymbol{\nabla}\varphi$ and we use $-[[\![\varphi]\!]\boldsymbol{n}_{\Gamma}] \times \boldsymbol{\nabla}_{\Gamma} - \boldsymbol{\nabla}[\![\varphi]\!] \times \boldsymbol{n}_{\Gamma} = [\boldsymbol{\nabla}_{\Gamma}[\![\varphi]\!]] \times \boldsymbol{n}_{\Gamma} - [\![\varphi]\!][\boldsymbol{n}_{\Gamma} \times \boldsymbol{\nabla}_{\Gamma}] - [\boldsymbol{\nabla}_{\Gamma}[\![\varphi]\!]] \times \boldsymbol{n}_{\Gamma} = \boldsymbol{0}$, since $\boldsymbol{n}_{\Gamma} \times \boldsymbol{\nabla}_{\Gamma} = \boldsymbol{0}$.

Remark 11. In the case of continuity of the electric potential ($[\![\varphi]\!] = 0$), the perpendicular interface electric field $e^{\perp}_{\Gamma}$ vanishes and (B.28) reduces to the common tangential continuity $[\![\boldsymbol{e}]\!] \times \boldsymbol{n}_{\Gamma} = \boldsymbol{0}$ for the bulk electric field $\boldsymbol{e}$ across any discontinuity surface. □

B.4. The concept of "effective" electromagnetic interface quantities — A summary

In summary, the above analysis of the circulation laws, accounting for a finite-thickness *interphase* $\Gamma \times [-w/2, +w/2]$ and its zero-thickness *interface* limit Γ, renders the following conclusions for the resulting "effective" quantities on Γ:

- The *integrated* parallel magnetic field $\boldsymbol{h}^{\parallel}_{\Gamma}$ vanishes, while the "effective" perpendicular field $h^{\perp}_{\Gamma}$ is finite.
- The *integrated* perpendicular Maxwell current $i^{\perp}_{\Gamma}$ vanishes, while the "effective" parallel field $\boldsymbol{i}^{\parallel}_{\Gamma}$ is finite.
- The *integrated* perpendicular electric field $e^{\perp}_{\Gamma}$ is represented by the discontinuity in electrical potential, while the averaged parallel field $\bar{\boldsymbol{e}}^{\parallel}_{\Gamma}$ is finite.

Henceforth, we set the "effective" parallel electric field to its *averaged* counterpart, that is, $\boldsymbol{e}^{\parallel}_{\Gamma} := \bar{\boldsymbol{e}}^{\parallel}_{\Gamma}$.

In conclusion, for an electromagnetic zero-thickness *interface* model, the corresponding interface magnetic and electric fields on Γ are assumed to be purely normal and parallel, respectively, and the interface Maxwell current is assumed to be purely parallel. In passing, we note that the "effective" electro-magnetic quantities on Γ resulting from the above detailed analysis of the circulation laws are in line with those hypothesized based on continuity arguments in our earlier works on

surface electro- and magneto-statics, that is, a purely parallel surface electric field in Chatzigeorgiou et al. (2014), and a purely normal surface magnetic field in Chatzigeorgiou et al. (2015).

B.5. Poynting vectors — Electromagnetic power

B.5.1. Poynting vectors in the volume and interface

The electromagnetic power flux is described through the Poynting vector. In the volume, we define

$$\boldsymbol{s} := \boldsymbol{e} \times \boldsymbol{h} = -[\boldsymbol{\nabla}\varphi] \times \boldsymbol{h} \,. \tag{B.30}$$

On the interface, we describe the flux by integrating the consistently resolved fields. Upon noting the decompositions $\hat{\boldsymbol{e}}_\Gamma = \hat{\boldsymbol{e}}_\Gamma^{\parallel} + \hat{e}_\Gamma^{\perp}\boldsymbol{n}_\Gamma$ and $\hat{\boldsymbol{h}}_\Gamma = \hat{\boldsymbol{h}}_\Gamma^{\parallel} + \hat{h}_\Gamma^{\perp}\boldsymbol{n}_\Gamma$, and observing that $\boldsymbol{n}_\Gamma \times \boldsymbol{n}_\Gamma = \boldsymbol{0}$, we define

$$\boldsymbol{s}_\Gamma := \int_{-w/2}^{w/2} \hat{\boldsymbol{e}}_\Gamma \times \hat{\boldsymbol{h}}_\Gamma \,\mathrm{d}\eta = \int_{-w/2}^{w/2} \left[\hat{e}_\Gamma^{\perp}\boldsymbol{n}_\Gamma \times \hat{\boldsymbol{h}}_\Gamma^{\parallel} + \hat{\boldsymbol{e}}_\Gamma^{\parallel} \times \hat{h}_\Gamma^{\perp}\boldsymbol{n}_\Gamma + \hat{\boldsymbol{e}}_\Gamma^{\parallel} \times \hat{\boldsymbol{h}}_\Gamma^{\parallel}\right] \mathrm{d}\eta \,. \tag{B.31}$$

We next note the following:

- Since $\hat{\boldsymbol{e}}_\Gamma^{\parallel}$ and $\hat{\boldsymbol{h}}_\Gamma^{\parallel}$ are finite, the last term in (B.31) vanishes for $w \to 0$ and, therefore, can be ignored immediately.
- From electrostatics it is recalled that $\hat{e}_\Gamma^{\perp} = -\frac{\partial \hat{\varphi}_\Gamma}{\partial \eta}$ and $\hat{\boldsymbol{e}}_\Gamma^{\parallel} = -\boldsymbol{\nabla}_\Gamma \hat{\varphi}_\Gamma$.

Together, (B.31) simplifies to

$$\boldsymbol{s}_\Gamma = -\int_{-w/2}^{w/2} \left[\frac{\partial \hat{\varphi}_\Gamma}{\partial \eta}\boldsymbol{n}_\Gamma \times \hat{\boldsymbol{h}}_\Gamma^{\parallel} + [\boldsymbol{\nabla}_\Gamma \hat{\varphi}_\Gamma] \times [\hat{h}_\Gamma^{\perp}\boldsymbol{n}_\Gamma]\right] \mathrm{d}\eta \,. \tag{B.32}$$

Next, integration by parts results in

$$-\int_{-w/2}^{w/2} \frac{\partial \hat{\varphi}_\Gamma}{\partial \eta}\boldsymbol{n}_\Gamma \times \hat{\boldsymbol{h}}_\Gamma^{\parallel} \,\mathrm{d}\eta = -\left[\hat{\varphi}_\Gamma \boldsymbol{n}_\Gamma \times \hat{\boldsymbol{h}}_\Gamma^{\parallel}\right]_{-w/2}^{+w/2} + \int_{-w/2}^{w/2} \hat{\varphi}_\Gamma \frac{\partial}{\partial \eta}\left[\boldsymbol{n}_\Gamma \times \hat{\boldsymbol{h}}_\Gamma^{\parallel}\right] \mathrm{d}\eta \,. \tag{B.33}$$

Now, we introduce additional reasonable model assumptions:

- $\boldsymbol{n}_\Gamma \times \hat{\boldsymbol{h}}_\Gamma^{\parallel}$ is continuous and linear across the interface. As a consequence, we have that

$$\boldsymbol{n}_\Gamma \times \hat{\boldsymbol{h}}_\Gamma^{\parallel}(\bullet, \pm\tfrac{w}{2}) = \boldsymbol{n}_\Gamma \times [\boldsymbol{I}_\Gamma \cdot \boldsymbol{h}^{\pm}(\bullet)] = \boldsymbol{n}_\Gamma \times \boldsymbol{h}^{\pm}(\bullet) \quad \text{and} \quad \frac{\partial}{\partial \eta}\left[\boldsymbol{n}_\Gamma \times \hat{\boldsymbol{h}}_\Gamma^{\parallel}\right] = \frac{1}{w}\boldsymbol{n}_\Gamma \times [\![\boldsymbol{h}]\!] \,.$$

- $\hat{h}_\Gamma^{\perp}$ is uniform across the interface $\rightsquigarrow \hat{h}_\Gamma^{\perp} = \frac{1}{w} h_\Gamma^{\perp}$.

As result, we obtain from (B.32) with (B.33)

$$\begin{aligned} \boldsymbol{s}_\Gamma &= -[\![\bar{\varphi}_\Gamma \boldsymbol{n}_\Gamma \times \boldsymbol{h}]\!] + \bar{\varphi}_\Gamma \boldsymbol{n}_\Gamma \times [\![\boldsymbol{h}]\!] - [\boldsymbol{\nabla}_\Gamma \bar{\varphi}_\Gamma] \times [h_\Gamma^{\perp}\boldsymbol{n}_\Gamma] \\ &= -[\boldsymbol{\nabla}_\Gamma \bar{\varphi}_\Gamma] \times [h_\Gamma^{\perp}\boldsymbol{n}_\Gamma] + \{\!\{\boldsymbol{h}\}\!\} \times \boldsymbol{n}_\Gamma [\![\varphi]\!] + [\![\boldsymbol{h}]\!] \times \boldsymbol{n}_\Gamma [\{\!\{\varphi\}\!\} - \bar{\varphi}_\Gamma] \,. \end{aligned} \tag{B.34}$$

We note that only the average value $\bar{\varphi}_\Gamma$, and not the resolved quantity $\hat{\varphi}_\Gamma$, appears in (B.34). Therefore, in the main text we drop the overbar in its counterpart (36b) without risking any confusion. Furthermore, (36b) adopts the simplified notation $\boldsymbol{e}_\Gamma := -\boldsymbol{\nabla}_\Gamma \varphi_\Gamma$.

Remark 12. Since, for any vector $\boldsymbol{a}$, it holds that $[\boldsymbol{a} \times \boldsymbol{n}_\Gamma] \cdot \boldsymbol{n}_\Gamma = 0$, we conclude from (B.34) that $\boldsymbol{s}_\Gamma \cdot \boldsymbol{n}_\Gamma = 0$, i.e. $\boldsymbol{s}_\Gamma$ is superficial. □

B.5.2. Electromagnetic power

The electro-magnetic power is given as

$$\mathcal{P}_{\mathrm{el}} = -\int_{\partial(\mathcal{B}^+ \cup \mathcal{B}^-)} \boldsymbol{s} \cdot \boldsymbol{n} \,\mathrm{d}S - \int_{\partial\mathcal{I}} \boldsymbol{s}_\Gamma \cdot \tilde{\boldsymbol{n}}_\Gamma \,\mathrm{d}L \,. \tag{B.35}$$

Upon introducing the expressions for $\boldsymbol{s}$ and $\boldsymbol{s}_\Gamma$, as defined in (B.30) and (B.34), we replace (B.35) by

$$\begin{aligned} \mathcal{P}_{\mathrm{el}} = &\int_{\partial(\mathcal{B}^+ \cup \mathcal{B}^-)} [\boldsymbol{\nabla}\varphi \times \boldsymbol{h}] \cdot \boldsymbol{n} \,\mathrm{d}S + \int_{\partial\mathcal{I}} \left[[\boldsymbol{\nabla}_\Gamma \bar{\varphi}_\Gamma] \times [h_\Gamma^{\perp}\boldsymbol{n}_\Gamma]\right] \cdot \tilde{\boldsymbol{n}}_\Gamma \,\mathrm{d}L \\ &- \int_{\partial\mathcal{I}} [\{\!\{\boldsymbol{h}\}\!\} \times \boldsymbol{n}_\Gamma [\![\varphi]\!]] \cdot \tilde{\boldsymbol{n}}_\Gamma \,\mathrm{d}L - \int_{\partial\mathcal{I}} [[\![\boldsymbol{h}]\!] \times \boldsymbol{n}_\Gamma [\{\!\{\varphi\}\!\} - \bar{\varphi}_\Gamma]] \cdot \tilde{\boldsymbol{n}}_\Gamma \,\mathrm{d}L \,. \end{aligned} \tag{B.36}$$

Using the divergence theorems for volume and interface in (4) and (6), respectively, we introduce the split of $\mathcal{P}_{\mathrm{el}}$

$$\mathcal{P}_{\mathrm{el}} = \mathcal{P}_{\mathrm{el}}^{\mathcal{B}} + \mathcal{P}_{\mathrm{el}}^{\mathcal{I}} \,, \tag{B.37}$$

where

$$\mathcal{P}_{\mathrm{el}}^{\mathcal{B}} = \int_{\mathcal{B}^+ \cup \mathcal{B}^-} [\boldsymbol{\nabla}\varphi \times \boldsymbol{h}] \cdot \boldsymbol{\nabla} \,\mathrm{d}V \,, \tag{B.38a}$$

$$\begin{aligned} \mathcal{P}_{\mathrm{el}}^{\mathcal{I}} = &\int_{\mathcal{I}} [[\boldsymbol{\nabla}_\Gamma \bar{\varphi}_\Gamma] \times [h_\Gamma^{\perp}\boldsymbol{n}_\Gamma]] \cdot \boldsymbol{\nabla}_\Gamma \,\mathrm{d}S + \int_{\mathcal{I}} [\![\boldsymbol{\nabla}\varphi \times \boldsymbol{h}]\!] \cdot \boldsymbol{n}_\Gamma \,\mathrm{d}S \\ &- \int_{\mathcal{I}} [[\![\boldsymbol{\nabla}\varphi]\!] \times \{\!\{\boldsymbol{h}\}\!\}] \cdot \boldsymbol{n}_\Gamma \,\mathrm{d}S - \int_{\mathcal{I}} [\{\!\{\boldsymbol{\nabla}\varphi\}\!\} \times [\![\boldsymbol{h}]\!]] \cdot \boldsymbol{n}_\Gamma \,\mathrm{d}S \\ &+ \int_{\mathcal{I}} [\![\varphi]\!] \{\!\{\boldsymbol{h} \times \boldsymbol{\nabla}\}\!\} \cdot \boldsymbol{n}_\Gamma \,\mathrm{d}S + \int_{\mathcal{I}} [\{\!\{\varphi\}\!\} - \bar{\varphi}_\Gamma] [\![\boldsymbol{h} \times \boldsymbol{\nabla}]\!] \cdot \boldsymbol{n}_\Gamma \,\mathrm{d}S \\ &+ \int_{\mathcal{I}} \boldsymbol{\nabla}_\Gamma \bar{\varphi}_\Gamma \cdot [[\![\boldsymbol{h}]\!] \times \boldsymbol{n}_\Gamma] \,\mathrm{d}S \,. \end{aligned} \tag{B.38b}$$

In order to obtain (B.38b), we used the relations

$$\begin{aligned} \left[[\boldsymbol{\nabla}_\Gamma \bar{\varphi}_\Gamma] \times [h_\Gamma^{\perp}\boldsymbol{n}_\Gamma]\right] \cdot \boldsymbol{n}_\Gamma &= h_\Gamma^{\perp} [\boldsymbol{\nabla}_\Gamma \bar{\varphi}_\Gamma] \cdot [\boldsymbol{n}_\Gamma \times \boldsymbol{n}_\Gamma] = 0 \\ [\{\!\{\boldsymbol{h}\}\!\} \times \boldsymbol{n}_\Gamma [\![\varphi]\!]] \cdot \boldsymbol{\nabla}_\Gamma &= [\boldsymbol{\nabla}_\Gamma [\![\varphi]\!] \times \{\!\{\boldsymbol{h}\}\!\}] \cdot \boldsymbol{n}_\Gamma - [\![\varphi]\!] \{\!\{\boldsymbol{h} \times \boldsymbol{\nabla}_\Gamma\}\!\} \cdot \boldsymbol{n}_\Gamma \\ &= [[\![\boldsymbol{\nabla}\varphi]\!] \times \{\!\{\boldsymbol{h}\}\!\}] \cdot \boldsymbol{n}_\Gamma - [\![\varphi]\!] \{\!\{\boldsymbol{h} \times \boldsymbol{\nabla}\}\!\} \cdot \boldsymbol{n}_\Gamma \\ [\{\!\{\boldsymbol{h}\}\!\} \times \boldsymbol{n}_\Gamma [\![\varphi]\!]] \cdot \boldsymbol{n}_\Gamma &= 0 \\ [[\![\boldsymbol{h}]\!] \times \boldsymbol{n}_\Gamma [\{\!\{\varphi\}\!\} - \bar{\varphi}_\Gamma]] \cdot \boldsymbol{\nabla}_\Gamma &= [\boldsymbol{\nabla}_\Gamma [\{\!\{\varphi\}\!\} - \bar{\varphi}_\Gamma] \times [\![\boldsymbol{h}]\!]] \\ &\quad \cdot \boldsymbol{n}_\Gamma - [\{\!\{\varphi\}\!\} - \bar{\varphi}_\Gamma] [\![\boldsymbol{h} \times \boldsymbol{\nabla}_\Gamma]\!] \cdot \boldsymbol{n}_\Gamma \\ &= [\{\!\{\boldsymbol{\nabla}\varphi\}\!\} \times [\![\boldsymbol{h}]\!]] \cdot \boldsymbol{n}_\Gamma - [\{\!\{\varphi\}\!\} - \bar{\varphi}_\Gamma] [\![\boldsymbol{h} \times \boldsymbol{\nabla}]\!] \\ &\quad \cdot \boldsymbol{n}_\Gamma - [\boldsymbol{\nabla}_\Gamma \bar{\varphi}_\Gamma] \cdot [[\![\boldsymbol{h}]\!] \times \boldsymbol{n}_\Gamma] \\ [[\![\boldsymbol{h}]\!] \times \boldsymbol{n}_\Gamma [\{\!\{\varphi\}\!\} - \bar{\varphi}_\Gamma]] \cdot \boldsymbol{n}_\Gamma &= 0 \,. \end{aligned}$$

Now, upon noting the identity

$$[\boldsymbol{\nabla}\varphi \times \boldsymbol{h}] \cdot \boldsymbol{\nabla} = \underbrace{[\boldsymbol{\nabla}\varphi \times \boldsymbol{\nabla}]}_{=\boldsymbol{0}} \cdot \boldsymbol{h} + \boldsymbol{\nabla}\varphi \cdot [\boldsymbol{h} \times \boldsymbol{\nabla}] \,,$$

we rewrite $\mathcal{P}_{\mathrm{el}}^{\mathcal{B}}$ in (B.38a) as

$$\mathcal{P}_{\mathrm{el}}^{\mathcal{B}} = \int_{\mathcal{B}^+ \cup \mathcal{B}^-} \boldsymbol{\nabla}\varphi \cdot [\boldsymbol{h} \times \boldsymbol{\nabla}] \,\mathrm{d}V \,. \tag{B.39}$$

Further, upon noting the surface identities

$$\begin{aligned} \left[[\boldsymbol{\nabla}_\Gamma \bar{\varphi}_\Gamma] \times [h_\Gamma^{\perp}\boldsymbol{n}_\Gamma]\right] \cdot \boldsymbol{\nabla}_\Gamma &= \underbrace{-h_\Gamma^{\perp} [[\boldsymbol{\nabla}_\Gamma \bar{\varphi}_\Gamma] \times \boldsymbol{\nabla}_\Gamma] \cdot \boldsymbol{n}_\Gamma}_{=0} \\ &\quad + \boldsymbol{\nabla}_\Gamma \bar{\varphi}_\Gamma \cdot [[h_\Gamma^{\perp}\boldsymbol{n}_\Gamma] \times \boldsymbol{\nabla}_\Gamma] = \boldsymbol{\nabla}_\Gamma \bar{\varphi}_\Gamma \cdot [[h_\Gamma^{\perp}\boldsymbol{n}_\Gamma] \times \boldsymbol{\nabla}_\Gamma] \\ [\![\boldsymbol{\nabla}\varphi \times \boldsymbol{h}]\!] \cdot \boldsymbol{n}_\Gamma &= [\{\!\{\boldsymbol{\nabla}\varphi\}\!\} \times [\![\boldsymbol{h}]\!]] \cdot \boldsymbol{n}_\Gamma + [[\![\boldsymbol{\nabla}\varphi]\!] \times \{\!\{\boldsymbol{h}\}\!\}] \cdot \boldsymbol{n}_\Gamma \,, \end{aligned}$$

we conclude that $\mathcal{P}_{\mathrm{el}}^{\mathcal{I}}$ in (B.38b) becomes

$$\begin{aligned} \mathcal{P}_{\mathrm{el}}^{\mathcal{I}} = &\int_{\mathcal{I}} \boldsymbol{\nabla}_\Gamma \bar{\varphi}_\Gamma \cdot [[h_\Gamma^{\perp}\boldsymbol{n}_\Gamma] \times \boldsymbol{\nabla}_\Gamma] \,\mathrm{d}S + \int_{\mathcal{I}} \boldsymbol{\nabla}_\Gamma \bar{\varphi}_\Gamma \cdot [[\![\boldsymbol{h}]\!] \times \boldsymbol{n}_\Gamma] \,\mathrm{d}S \\ &+ \int_{\mathcal{I}} [\![\varphi]\!] \{\!\{\boldsymbol{h} \times \boldsymbol{\nabla}\}\!\} \cdot \boldsymbol{n}_\Gamma \,\mathrm{d}S + \int_{\mathcal{I}} [\{\!\{\varphi\}\!\} - \bar{\varphi}_\Gamma] [\![\boldsymbol{h} \times \boldsymbol{\nabla}]\!] \cdot \boldsymbol{n}_\Gamma \,\mathrm{d}S \,. \end{aligned} \tag{B.40}$$

Finally, noting the identities involving $\boldsymbol{i}_{\mathrm{Max}}$ in (B.8) and $\boldsymbol{i}_{\mathrm{Max},\Gamma}^{\parallel}$ in (B.11), respectively, we obtain

$$\begin{aligned} \mathcal{P}_{\mathrm{el}}^{\mathcal{B}} &= -\int_{\mathcal{B}} \boldsymbol{i}_{\mathrm{Max}} \cdot \boldsymbol{\nabla}\varphi \,\mathrm{d}V \\ \mathcal{P}_{\mathrm{el}}^{\mathcal{I}} &= -\int_{\mathcal{I}} \boldsymbol{i}_{\mathrm{Max},\Gamma}^{\parallel} \cdot \boldsymbol{\nabla}_\Gamma \bar{\varphi}_\Gamma \,\mathrm{d}S - \int_{\mathcal{I}} \{\!\{\boldsymbol{i}_{\mathrm{Max}}\}\!\} \cdot \boldsymbol{n}_\Gamma [\![\varphi]\!] \,\mathrm{d}S \\ &\quad - \int_{\mathcal{I}} [\![\boldsymbol{i}_{\mathrm{Max}}]\!] \cdot \boldsymbol{n}_\Gamma [\{\!\{\varphi\}\!\} - \bar{\varphi}_\Gamma] \,\mathrm{d}S \,. \end{aligned} \tag{B.41}$$

This result is expressed in (37c), with the simplified notation $\boldsymbol{i}_{\mathrm{Max},\Gamma}^{\parallel} = \boldsymbol{i}_{\mathrm{Max},\Gamma}$, $\varphi_\Gamma := \bar{\varphi}_\Gamma$ and $\boldsymbol{e}_\Gamma := -\boldsymbol{\nabla}_\Gamma \varphi_\Gamma$.

References

An, S.J., Li, J., Daniel, C., Mohanty, D., Nagpure, S., Wood III, D.L., 2016. The state of understanding of the lithium-ion-battery graphite solid electrolyte interphase (SEI) and its relationship to formation cycling. Carbon 105, 52–76.

Anand, L., 2012. A Cahn–Hilliard-type theory for diffusion with large deformations. J. Mech. Phys. Solids 60, 1983–2002.

Barenblatt, G., 1959. The formation of equilibrium cracks during brittle fracture. General ideas and hypotheses. Axially-symmetric cracks. J. Appl. Math. Mech. 23 (3), 622–636.

Bigoni, D., Bordignon, N., Piccolroaz, A., Stupkiewicz, S., 2018. Bifurcation of elastic solids with sliding interfaces. Proc. R. Soc. A: Math. Phys. Eng. Sci. 474 (2209), 20170681.

van den Bosch, M., Schreurs, P., Geers, M., 2006. An improved description of the exponential xu and needleman cohesive zone law for mixed-mode decohesion. Eng. Fract. Mech. 73 (9), 1220–1234.

Brassart, L., Inglis, H., Delannay, L., Doghri, I., Geubelle, P., 2009. An extended Mori–Tanaka homogenization scheme for finite strain modeling of debonding in particle-reinforced elastomers. Comput. Mater. Sci. 45 (3), 611–616.

Cahn, J.W., Hilliard, J.E., 1958. Free energy of a nonuniform system. I. Interfacial free energy. J. Chem. Phys. 28, 258–267.

Carlstedt, D., Runesson, K., Larsson, F., Jänicke, R., Asp, L.E., 2023. Variationally consistent modeling of a sensor-actuator based on shape-morphing from electro-chemical–mechanical interactions. J. Mech. Phys. Solids 179, 105371.

Chatzigeorgiou, G., Javili, A., Steinmann, P., 2014. Surface electrostatics: theory and computations. Proc. Math. Phys. Eng. Sciences/the R. Soc. 470 (2164), 20130628.

Chatzigeorgiou, G., Javili, A., Steinmann, P., 2015. Surface magnetoelasticity theory. Arch. Appl. Mech. 85 (9), 1265–1288.

Chen, W.-X., et al., 2024. Cohesive phase-field simulations of fracture in NMC cathodes. J. Power Sources 596, 234054.

Cheng, L., Crumlin, E.J., Chen, W., Qiao, R., Hou, H., Lux, S.F., Zorba, V., Russo, R., Kostecki, R., Liu, Z., et al., 2014. The origin of high electrolyte–electrode interfacial resistances in lithium cells containing garnet type solid electrolytes. Phys. Chem. Chem. Phys. 16 (34), 18294–18300.

Christensen, J., Newman, J., 2006. Stress generation and fracture in lithium insertion materials. J. Solid State Electrochem. 10, 293–319.

Daher, N., Maugin, G.A., 1986. The method of virtual power in continuum mechanics application to media presenting singular surfaces and interfaces. Acta Mech. 60 (3–4), 217–240.

Das, A., Barai, A., Masters, I., Williams, D., 2019. Comparison of tab-to-busbar ultrasonic joints for electric vehicle li-ion battery applications. World Electr. Veh. J. 10 (3), 55.

Dell'Isola, F., Romano, A., 1987. On the derivation of thermomechanical balance equations for continuous systems with a nonmaterial interface. Internat. J. Engrg. Sci. 25 (11–12), 1459–1468.

Di Leo, C.V., et al., 2014. Phase-field theory for diffusion with elastic deformation. J. Mech. Phys. Solids 70, 1–29.

Dickinson, E.J., Wain, A.J., 2020. The Butler-Volmer equation in electrochemical theory: Origins, value, and practical application. J. Electroanal. Chem. 872, 114145.

Dugdale, D., 1960. Yielding of steel sheets containing slits. J. Mech. Phys. Solids 8 (2), 100–104.

Fagerström, M., Larsson, R., 2006. Theory and numerics for finite deformation fracture modelling using strong discontinuities. Internat. J. Numer. Methods Engrg. 66 (6), 911–948.

Firooz, S., Chatzigeorgiou, G., Steinmann, P., Javili, A., 2022. Extended general interfaces: Mori–Tanaka homogenization and average fields. Int. J. Solids Struct. 254–255, 111933.

Ge, S., Ma, Y., Wang, K., Zheng, L., Xie, X., Chen, X., Yu, H.-S., 2023. Unsaturated hydro-mechanical-electro-chemical coupling based on mixture-coupling theory: a unified model. Internat. J. Engrg. Sci. 191, 103914.

Greenhalgh, E.S., Nguyen, S., Asp, L.E., Bici, A., Bismarck, A., Fam, D., Johansson, M., Lindbergh, G., Lutkenhaus, J.L., Shaffer, M.S., et al., 2025. Characterization and reporting protocols for structural power composites: a perspective. Adv. Energy Mater. 15 (42), e04702.

Gu, S., Monteiro, E., He, Q., 2011. Coordinate-free derivation and weak formulation of a general imperfect interface model for thermal conduction in composites. Compos. Sci. Technol. 71 (9), 1209–1216.

Gurtin, M.E., Murdoch, A.I., 1975. A continuum theory of elastic material surfaces. Arch. Ration. Mech. Anal. 57 (4), 291–323.

Güzel, D., Kaiser, T., Menzel, A., 2023. A thermo-electro-mechanically coupled cohesive zone formulation for predicting interfacial damage. Eur. J. Mech. / A Solids 99, 104935.

Hashin, Z., 2001. Thin interphase/imperfect interface in conduction. J. Appl. Phys. 89 (4), 2261–2267.

Hu, Y., Li, W., Zhu, J., Hao, S.-M., Qin, X., Fan, L.-Z., Zhang, L., Zhou, W., 2023. Multi-layered electrolytes for solid-state lithium batteries. Next Energy 1 (3), 100042.

Javili, A., 2018. Variational formulation of generalized interfaces for finite deformation elasticity. Math. Mech. Solids 23 (9), 1303–1322.

Javili, A., Kaessmair, S., Steinmann, P., 2014. General imperfect interfaces. Comput. Methods Appl. Mech. Engrg. 275, 76–97.

Javili, A., Larsson, F., Runesson, K., Steinmann, P., 2025. On a canonical interface model with application to micro-heterogeneous elastic solids. Comput. Methods Appl. Mech. Engrg. 440, 117925.

Javili, A., Larsson, F., Runesson, K., Steinmann, P., 2026. Upscaling elastic interphases to canonical interface models. Comput. Methods Appl. Mech. Engrg. 451, 118694.

Javili, A., Steinmann, P., Mosler, J., 2017. Micro-to-macro transition accounting for general imperfect interfaces. Comput. Methods Appl. Mech. Engrg. 317, 274–317.

Jia, L., Zhu, J., Zhang, X., Guo, B., Du, Y., Zhuang, X., 2024. Li–solid electrolyte interfaces/interphases in all-solid-state Li batteries. Electrochem. Energy Rev. 7 (1), 12.

Kaessmair, S., Javili, A., Steinmann, P., 2014. Thermomechanics of solids with general imperfect coherent interfaces. Arch. Appl. Mech. 84 (9), 1409–1426.

Kaessmair, S., Steinmann, P., 2016. Comparative computational analysis of the Cahn–Hilliard equation with emphasis on C1-continuous methods. J. Comput. Phys. 322, 783–803.

Kaiser, T., von der Höh, N., Menzel, A., 2024. Computational multiscale modelling of material interfaces in electrical conductors. J. Mech. Phys. Solids 186, 105601.

Kamikawa, Y., et al., 2024. Electro-chemo-mechanical phase-field simulation of interfacial defects. Commun. Mater. 5, 180.

Larché, F.C., Cahn, J.W., 1973. A linear theory of thermochemical equilibrium of solids under stress. Acta Metall. 21 (8), 1051–1063.

Larché, F.C., Cahn, J.W., 1978. Equilibrium of crystalline solids under stress. Acta Metall. 26 (1), 53–60.

McBride, A., Javili, A., Steinmann, P., Bargmann, S., 2011. Geometrically nonlinear continuum thermomechanics with surface energies coupled to diffusion. J. Mech. Phys. Solids 59 (10), 2116–2133.

Moeckel, G.P., 1975. Thermodynamics of an interface. Arch. Ration. Mech. Anal. 57 (3), 255–280.

Murdoch, A.I., 1976. A thermodynamical theory of elastic material interfaces. Q. J. Mech. Appl. Math. 29 (3), 245–275.

Park, K., Paulino, G.H., 2011. Cohesive zone models: A critical review of traction–separation relationships across fracture surfaces. Appl. Mech. Rev. 64 (6), 060802.

Saeb, S., Firooz, S., Steinmann, P., Javili, A., 2021. Generalized interfaces via weighted averages for application to graded interphases at large deformations. J. Mech. Phys. Solids 149, 104234.

Salvadori, A., Grazioli, D., Geers, M., Danilov, D., Notten, P., 2015. A multiscale-compatible approach in modeling ionic transport in the electrolyte of (Lithium ion) batteries. J. Power Sources 293, 892–911.

Salvadori, A., McMeeking, R., Grazioli, D., Magri, M., 2018. A coupled model of transport-reaction-mechanics with trapping. Part I – Small strain analysis. J. Mech. Phys. Solids 114, 1–30.

Sanchez-Palencia, E., 1974. Comportements local et macroscopique d'un type de milieux physiques heterogenes. Internat. J. Engrg. Sci. 12 (4), 331–351.

Serpelloni, M., Arricca, M., Bonanno, C., Salvadori, A., 2022. Chemo-transport-mechanics in advecting membranes. Internat. J. Engrg. Sci. 181, 103746.

Spencer Jolly, D., Melvin, D.L., Stephens, I.D., Brugge, R.H., Pu, S.D., Bu, J., Ning, Z., Hartley, G.O., Adamson, P., Grant, P.S., et al., 2022. Interfaces between ceramic and polymer electrolytes: a comparison of oxide and sulfide solid electrolytes for hybrid solid-state batteries. Inorganics 10 (5), 60.

Steigmann, D.J., Ogden, R.W., 1999. Elastic surface–substrate interactions. Proc. R. Soc. A: Math. Phys. Eng. Sci. 455 (1982), 437–474.

Tang, Y., Hu, N., 2024. Chemo-mechanical phase-field modeling of dissolution-driven fracture. Comput. Methods Appl. Mech. Engrg..

Vakis, A., Yastrebov, V., Scheibert, J., Nicola, L., Dini, D., Minfray, C., Almqvist, A., Paggi, M., Lee, S., Limbert, G., Molinari, J., Anciaux, G., Aghababaei, R., Echeverri Restrepo, S., Papangelo, A., Cammarata, A., Nicolini, P., Putignano, C., Carbone, G., Stupkiewicz, S., Lengiewicz, J., Costagliola, G., Bosia, F., Guarino, R., Pugno, N., Müser, M., Ciavarella, M., 2018. Modeling and simulation in tribology across scales: An overview. Tribol. Int. 125, 169–199.

Wilmers, J., McBride, A., Bargmann, S., 2017. Interface elasticity effects in polymer-filled nanoporous metals. J. Mech. Phys. Solids 99, 163–177.

Xu, X.-P., Needleman, A., 1994. Numerical simulations of fast crack growth in brittle solids. J. Mech. Phys. Solids 42 (9), 1397–1434.

Zhang, X., Shyy, W., Sastry, A.M., 2010. Numerical simulation of intercalation-induced stress. J. Electrochem. Soc. 157, A910–A916.

Zhao, Y., Wang, R., Martínez-Pañeda, E., 2022. Phase field electro-chemo-mechanical formulation for void evolution at li interfaces. J. Mech. Phys. Solids.